UNIVERSITY OF CALIFORNIA,
IRVINE

Synthesis and Stereochemical Determination of the Peptide Antibiotic Novo29

THESIS

submitted in partial satisfaction of the requirements
for the degree of

MASTER OF SCIENCE

in Chemistry

by

Maj Krumberger

Thesis Committee:
Professor James S. Nowick, Chair
Professor Vy M. Dong
Professor Christopher Vanderwal

2022

Table of Contents

LIST OF FIGURES

LIST OF TABLES

ACKNOWLEDGEMENTS

I would like to express the deepest appreciation to my committee chair, and advisor Professor James S. Nowick, who has encouraged me along the way on the path to my master's thesis and throughout my graduate career.

I would like to thank my committee members, Professor Vy M. Dong and Professor Christopher Vanderwal, whose support on every step toward this master's thesis has been instrumental for its completion.

I would like to thank Dr. Xingyue Li who worked alongside me on this project and published some of the synthetic work that he contributed to in his Ph.D. thesis.

I thank Dr. Philip Dennison and Dr. John Kelly and the UCI Department of Chemistry NMR Spectroscopy Facility for assistance with NMR experiments. I thank Ben Katz and Dr. Felix Grun, and the UCI Mass Spectrometry facility for assistance with the mass spectrometry experiments. I thank the Berkeley Center for Structural Biology (BCSB) of the Advanced Light Source (ALS) for synchrotron data collection. The BCSB is supported in part by the NIH, NIGMS, and the Howard Hughes Medical Institute. The ALS is supported by the Director, Office of Science, Office of Basic Energy Sciences, of the U.S. Department of Energy under contract DE-AC02-05CH11231. I thank the NIH for support (AI168966, University of California, Irvine; AI136137, NovoBiotic Pharmaceuticals LLC). Initial support for the work at University of California, Irvine was provided by a subaward from NovoBiotic Pharmaceuticals LLC.

ABSTRACT OF THE THESIS

Synthesis and Stereochemical Determination of the Peptide Antibiotic Novo29

by
Maj Krumberger
Master of Science in Chemistry
University of California, Irvine, 2022
Professor James S. Nowick, Chair

This work describes the synthesis and stereochemical determination of Novo29 (clovibactin), a new peptide antibiotic that is related to teixobactin and is active against Gram-positive bacteria. Novo29 is an eight-residue depsipeptide that contains the noncanonical amino acid hydroxyasparagine of hitherto undetermined stereochemistry in a macrolactone ring. The amino acid building blocks Fmoc-(2*R*,3*R*)-hydroxyasparagine-OH and Fmoc-(2*R*,3*S*)-hydroxyasparagine-OH were synthesized from (*R*,*R*)- and (*S*,*S*)-diethyl tartrate. Novo29 and *epi*-Novo29 were then prepared by solid-phase peptide synthesis using these building blocks. Correlation with an authentic sample of Novo29 through ^{1}H NMR spectroscopy, LC-MS, and *in vitro* antibiotic activity established that Novo29 contains (2*R*,3*R*)-hydroxyasparagine. X-ray crystallography reveals that *epi*-Novo29 adopts an amphiphilic conformation, with a hydrophobic surface and a hydrophilic surface. Four sets of *epi*-Novo29 molecules pack in the crystal lattice to form a hydrophobic core. The macrolactone ring adopts a conformation in which the main-chain amide NH groups converge to create a cavity, which binds ordered water and acetate anion. The amphiphilic conformation of *epi*-Novo29 is reminiscent of the amphiphilic conformation adopted by the related antibiotic teixobactin and its derivatives, which contains a hydrophobic surface that interacts with the lipids of the bacterial cell membrane and a hydrophilic surface that interacts with the aqueous environment. Molecular modeling suggests that Novo29 can adopt an amphiphilic conformation similar to teixobactin, suggesting that Novo29 may interact with bacteria in a similar fashion to teixobactin.

Introduction

Novo29, a new antibiotic from a soil bacterium closely related to *Eleftheria terrae*, was recently reported.[1] Novo29 is an eight-residue depsipeptide comprising a macrolactone ring and a linear tail. It is active against Gram-positive bacteria, including drug-resistant human pathogens, such as MRSA and VRE. Novo29 kills bacteria by inhibiting bacterial cell-wall synthesis, with no detectable resistance occurring upon serial passaging.[2,3] Although the amino acid sequence of Novo29 was determined, the stereochemistry of the rare noncanonical amino acid hydroxyasparagine at position 5 was not able to be determined. Neither NMR spectroscopic analysis nor correlation with authentic hydroxyasparagine of known stereochemistry has thus far been feasible, leaving open the question of which hydroxyasparagine stereoisomer constituted the natural product.

Novo29 is related in structure to teixobactin, which is produced by *E. terrae*, but it is smaller, containing eight residues instead of eleven (Figure 1).[2,3] Like teixobactin, Novo29 exhibits good activity against Gram-positive bacteria and targets cell-wall precursors. Novo29 is a promising antibiotic drug candidate, because it kills drug-resistant pathogens without detectable resistance and exhibits reduced propensity to form gels upon intravenous dosing.[4] In the current study, we establish the stereochemistry of the hydroxyasparagine (hydroxyAsn) residue at position 5 and confirm the structure of Novo29 through chemical synthesis and spectroscopic and functional correlation. We also report the X-ray crystallographic structure of a hydroxyAsn epimer of Novo29 (*epi*-Novo29), which may provide insights into how Novo29 binds bacterial cell-wall precursors.

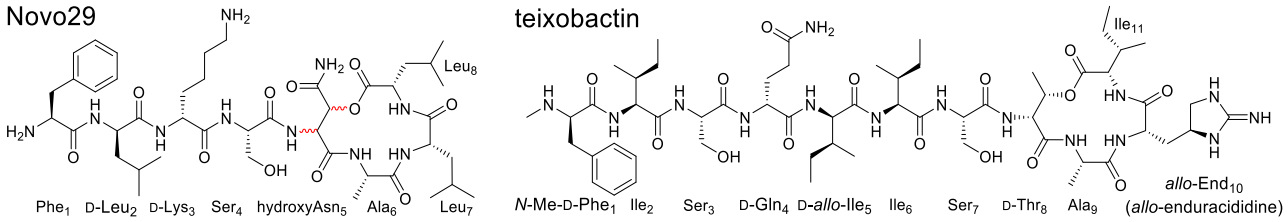

Figure 1. Structures of Novo29 and teixobactin. The unassigned stereochemistry of hydroxyAsn at position 5 of Novo29 is highlighted in red.

Results and discussion

Synthesis of Novo29 and *epi*-Novo29

We hypothesized the stereochemistry at position 5 to be (2*R*,3*R*)-hydroxyAsn, based on the similarity in structure and connectivity of D-Thr$_8$ of teixobactin, as well as the related depsipeptide antibiotic hypeptin.[5] We developed and carried out the synthesis of a suitably protected (2*R*,3*R*)-hydroxyAsn as a building block that could be readily incorporated into solid-phase peptide synthesis (SPPS). This building block is Fmoc-protected at the α-amino position; the hydroxyl and primary amide groups can tolerate SPPS without protection.[6,7] For comparison, we also synthesized the Fmoc-protected (2*R*,3*S*)-hydroxyAsn diastereomer (Figure 2).

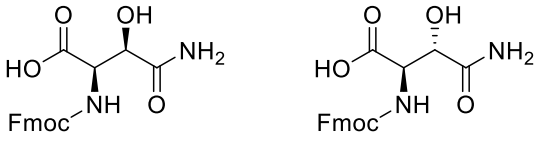

Figure 2. Structures of Fmoc-(2*R*,3*R*)-hydroxyasparagine-OH and Fmoc-(2*R*,3*S*)-hydroxyasparagine-OH.

We synthesized Fmoc-(2*R*,3*R*)-hydroxyasparagine-OH from (+)-diethyl L-tartrate as outlined in Figure 3. (2*R*,3*R*)-(+)-Diethyl L-tartrate was converted to bromo alcohol **1** by conversion to the cyclic sulfite and oxidation to the cyclic sulfate followed by ring opening with LiBr.[8] This sequence was previously established for diisopropyl and dimethyl tartrates and resulted in the formation of 80:20 and 85:15 mixtures of diastereomers.[9,10] In our hands the LiBr reaction

proceeded with the formation of the two diastereomers of bromo alcohol **1** in a 70:30 ratio favoring the desired diastereomer (Figure S1). Treatment of the mixture of diastereomers with sodium azide, to give the corresponding azido alcohols with inversion of stereochemistry, followed by reduction with H_2 and Pd/C and chromatographic separation of diastereomers afforded amino alcohol **2**.

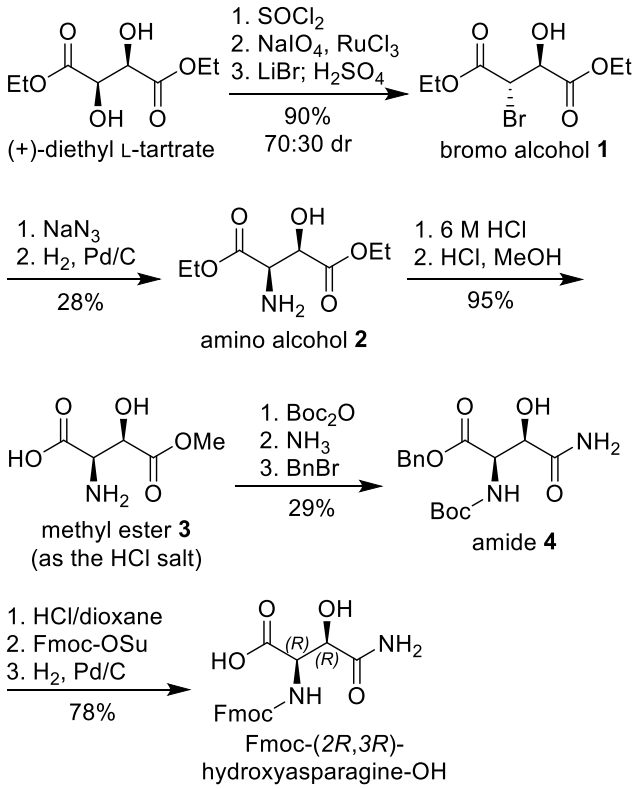

Figure 3. Synthesis of Fmoc-(2*R*,3*R*)-hydroxyasparagine-OH.

Amino alcohol **2** was converted to methyl ester **3** by hydrolysis of the ethyl ester groups in 6 M HCl followed by regioselective differentiation of the two carboxylic acid groups by Fischer esterification with HCl in CH_3OH.[11] The methyl esterification proceeds regioselectively, because the ammonium group at the 2-position deactivates the carboxylic acid group at the 1-position. Methyl ester **3** was then converted to amide **4** by Boc protection of amino group at the 2-position, ammonolysis to the amide at the 4-position, and benzyl ester protection of the carboxylic acid at the 1-position. Amide **4** was subsequently converted to Fmoc-(2*R*,3*R*)-hydroxyasparagine-OH by

removal of the Boc group with 4 M HCl in dioxane, Fmoc protection of the amino group with Fmoc-OSu, and hydrogenolysis of the benzyl ester group with H_2 and Pd/C.

We synthesized the Fmoc-(2*R*,3*S*)-hydroxyasparagine-OH diastereomer from (-)-diethyl D-tartrate in a related fashion, as outlined in Figure 4. (2*S*,3*S*)-(-)-Diethyl D-tartrate was converted to amino alcohol **5** by conversion to the cyclic sulfite with thionyl chloride, followed by ring opening with sodium azide and reduction of the azido group with H_2 and Pd/C.[12] Amino alcohol **5** was then converted to Fmoc-(2*R*,3*S*)-hydroxyasparagine-OH in a similar fashion to that described above for amino alcohol **2**.

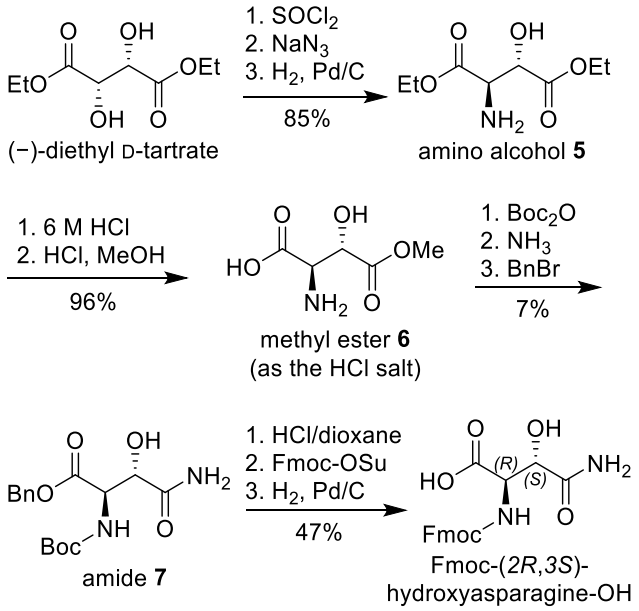

Figure 4. Synthesis of Fmoc-(2*R*,3*S*)-hydroxyasparagine-OH.

We determined the stereochemistry of Novo29 by synthesizing (2*R*,3*R*)-hydroxyAsn-Novo29 and (2*R*,3*S*)-hydroxyAsn-Novo29 and then correlating these synthetic peptides with natural Novo29 by ^{1}H NMR spectroscopy, LC-MS analysis, and MIC assays. (2*R*,3*R*)-hydroxyAsn-Novo29 and (2*R*,3*S*)-hydroxyAsn-Novo29 were synthesized by solid-phase peptide synthesis of a protected acyclic precursor followed by solution-phase cyclization, in a fashion similar to that which we have developed for the synthesis of teixobactin analogues (Figure 5).[6,13–

[17] The synthesis begins with loading Fmoc-Leu-OH (position 7) onto 2-chlorotrityl resin, followed by incorporation of residues 6 through 1. Leu_8 was esterified onto the β-hydroxy group of the (2*R*,3*R*)-hydroxyAsn or (2*R*,3*S*)-hydroxyAsn residue at position 5 by treatment with Fmoc-Leu-OH, DIC, and DMAP.[18] Fmoc deprotection of Leu_8 and cleavage of the peptide from the resin with 20% hexafluoroisopropanol (HFIP) in CH_2Cl_2 afforded the protected peptide with a free carboxylic acid group on Leu_7 and a free amino group on Leu_8. Cyclization between Leu_8 and Leu_7 was achieved with HBTU and HOBt. Global deprotection with trifluoracetic acid (TFA) and reverse-phase HPLC purification yielded (2*R*,3*R*)-hydroxyAsn-Novo29 and (2*R*,3*S*)-hydroxyAsn-Novo29 as the trifluoroacetate salts.

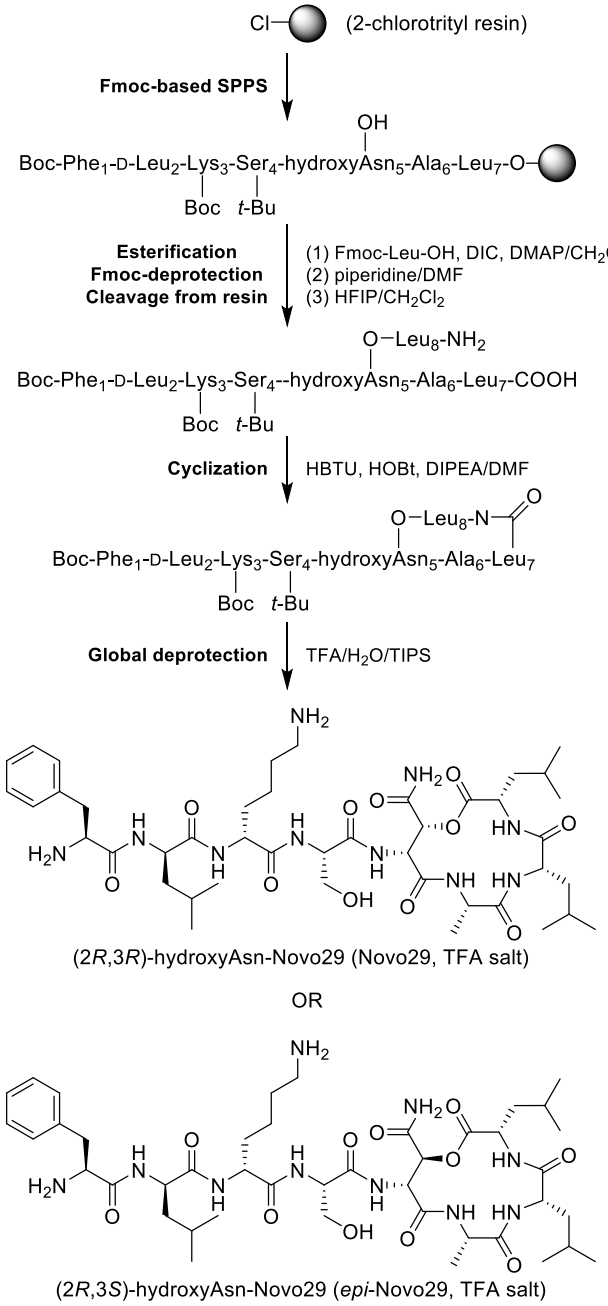

Figure 5. Synthesis of Novo29 and *epi*-Novo29.

Stereochemical determination of Novo29

The ^{1}H NMR spectrum of natural Novo29 in DMSO-d_6 matches that of (2*R*,3*R*)-hydroxyAsn-Novo29 and differs significantly from that of synthetic (2*R*,3*S*)-hydroxyAsn-Novo29 (Figure 6). Notably, the α- and β-proton resonances of the hydroxyAsn residue in natural and

(2*R*,3*R*)-hydroxyAsn-Novo29 both appear at 5.04 and 5.29 ppm, respectively, while those of (2*R*,3*S*)-hydroxyAsn-Novo29 appear at 5.14 and 5.00 ppm. From here on (2*R*,3*R*)-hydroxyAsn-Novo29 will be referred to as Novo29, and (2*R*,3*S*)-hydroxyAsn-Novo29 will be referred to as *epi*-Novo29. The amide NH region of both natural and synthetic Novo29 also match reasonably well and differ substantially from that of *epi*-Novo29. Surprisingly, the chemical shifts of the NH groups of Novo29 proved sensitive to concentration, varying by as much as 0.1 ppm over concentrations from 1–3 mM. This observation suggests that even in DMSO, Novo29 undergoes relatively strong self-association (Figure S2 and Table S1).

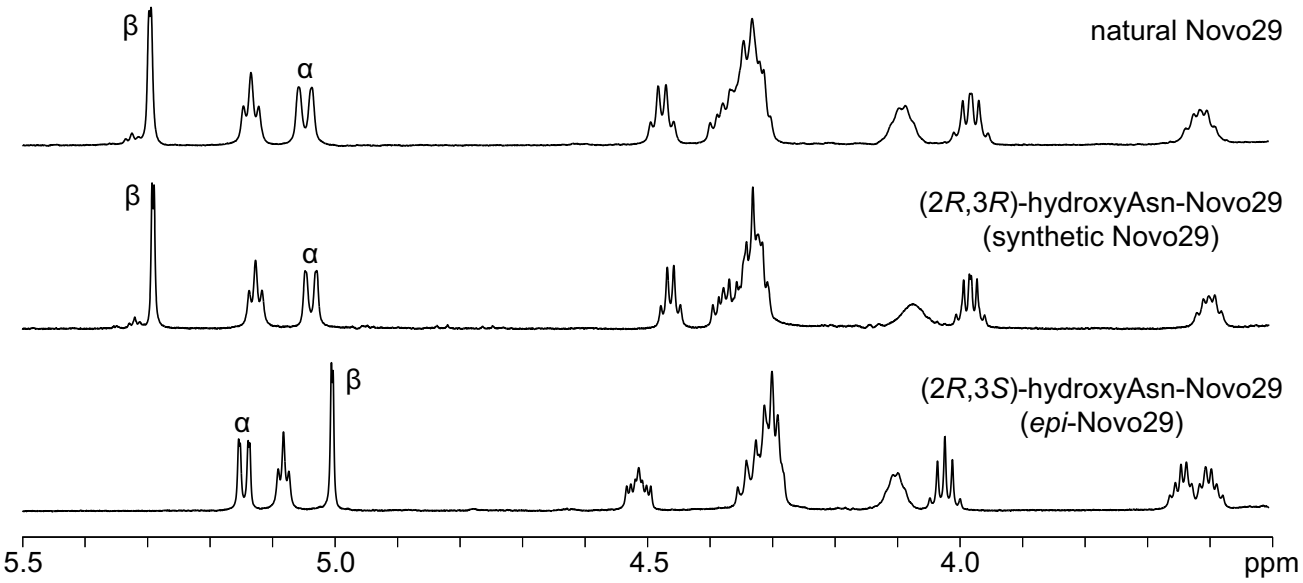

Figure 6. ^{1}H NMR spectra of natural Novo29, synthetic Novo29, and *epi*-Novo29 (3.5–5.5 ppm expansion, 500 MHz, 2 mM in DMSO-d_6). The α- and β-protons of hydroxyAsn are labeled.

To corroborate the stereochemical identity of Novo29 we compared natural Novo29 to synthetic Novo29 and *epi*-Novo29 by LC-MS. With a gradient of 3–27 % CH_3CN over 25 minutes on a C4 column, natural and synthetic Novo29 elute comparably (15.81 and 15.88 minutes, respectively), whereas *epi*-Novo29 elutes substantially later (16.57 minutes). The retention time and peak shape of Novo29 proved highly concentration dependent, with broad peaks and shorter

elution times resulting at higher concentrations, again suggesting strong self-association (Figure S3).

To further corroborate the stereochemical identity of Novo29, and to evaluate the importance of the stereochemistry of the hydroxyAsn residue, we tested the antibiotic activity of natural Novo29, synthetic Novo29, and *epi*-Novo29 using minimum inhibitory concentration (MIC) assays against two Gram-positive bacteria, *B. subtilis*, and *S. epidermidis*. We used the Gram-negative bacterium *E. coli* as a negative control. Natural Novo29 and synthetic Novo29 exhibit comparable antibiotic activity against the Gram-positive bacteria, with MIC values of 0.125 μg/mL for *B. subtilis* and 0.25 μg/mL for *S. epidermidis* (Table 1). To our surprise, both synthetic Novo29 and natural Novo29 also exhibited modest activity against *E. coli*, with MIC values of 8 μg/mL. In contrast, *epi*-Novo29 exhibited no MIC activity (>32 μg/mL) against any of the bacteria, thus indicating that the 2*R*,3*R* stereochemistry of the hydroxyAsn residue is critical to the antibiotic activity of Novo29.

Table 1. MIC values of natural Novo29, synthetic Novo29, and *epi*-Novo29 in μg/mL.

	Bacillus subtilis ATCC 6051	*Staphylococcus epidermidis* ATCC 14990	*Escherichia coli* ATCC 10798
natural Novo29	0.125	0.25	8
synthetic Novo29	0.125	0.25	8
epi-Novo29	>32	>32	>32

Crystallographic studies of *epi*-Novo29 and a molecular model of Novo29

X-ray crystallography permitted the structural elucidation of *epi*-Novo29 and may provide insights into the conformation and mechanism of action of Novo29. Both *epi*-Novo29 and Novo29 were screened for crystallization in a 96-well plate format using crystallization kits from Hampton Research (PEG/Ion, Index, and Crystal Screen). Novo29 did not form crystals

from any of the conditions tested. *epi*-Novo29 formed rod-shaped crystals from 2.8 M sodium acetate at pH 7.0. Further optimization in a 24-well plate format afforded long rectangular crystals suitable for X-ray diffraction from 2.8 M sodium acetate at pH 6.6. Diffraction data were initially collected using an X-ray diffractometer on an *epi*-Novo29 crystal that was soaked in KI to incorporate iodide ions into the lattice (PDB 8CUF). The crystallographic phases were determined using single-wavelength anomalous diffraction (SAD) phasing from the incorporated iodide ions. Higher-resolution diffraction data were subsequently collected out to 1.13 Å resolution on an unsoaked *epi*-Novo29 crystal using a synchrotron (PDB 8CUG). The crystallographic phases of the higher-resolution data were determined by molecular replacement using the KI-soaked structure as a search model. The asymmetric unit contains two molecules of *epi*-Novo29, which exhibit only minor differences in conformation.

In the X-ray crystallographic structure, *epi*-Novo29 adopts an amphiphilic conformation, with the side chains of Phe_1, D-Leu_2, Leu_7, and Leu_8 creating a hydrophobic surface and the side chains of D-Lys_3, Ser_4, and (2*R*,3*S*)-hydroxyAsn_5, as well as the *N*-terminal ammonium group, creating a hydrophilic surface (Figure 7A). An intramolecular hydrogen bond between the main-chain NH group of Ala_6 and the side chain OH group of Ser_4 helps enforce this conformation. In the lattice, *epi*-Novo29 packs so that the hydrophobic surfaces come together, with four sets of *epi*-Novo29 molecules forming a hydrophobic core (Figure 7C). The macrolactone ring of *epi*-Novo29 adopts a conformation in which the main-chain NH groups of (2*R*,3*S*)-hydroxyAsn_5, Ala_6, Leu_7, and Leu_8 converge to create a cavity, which binds ordered water and acetate anion.

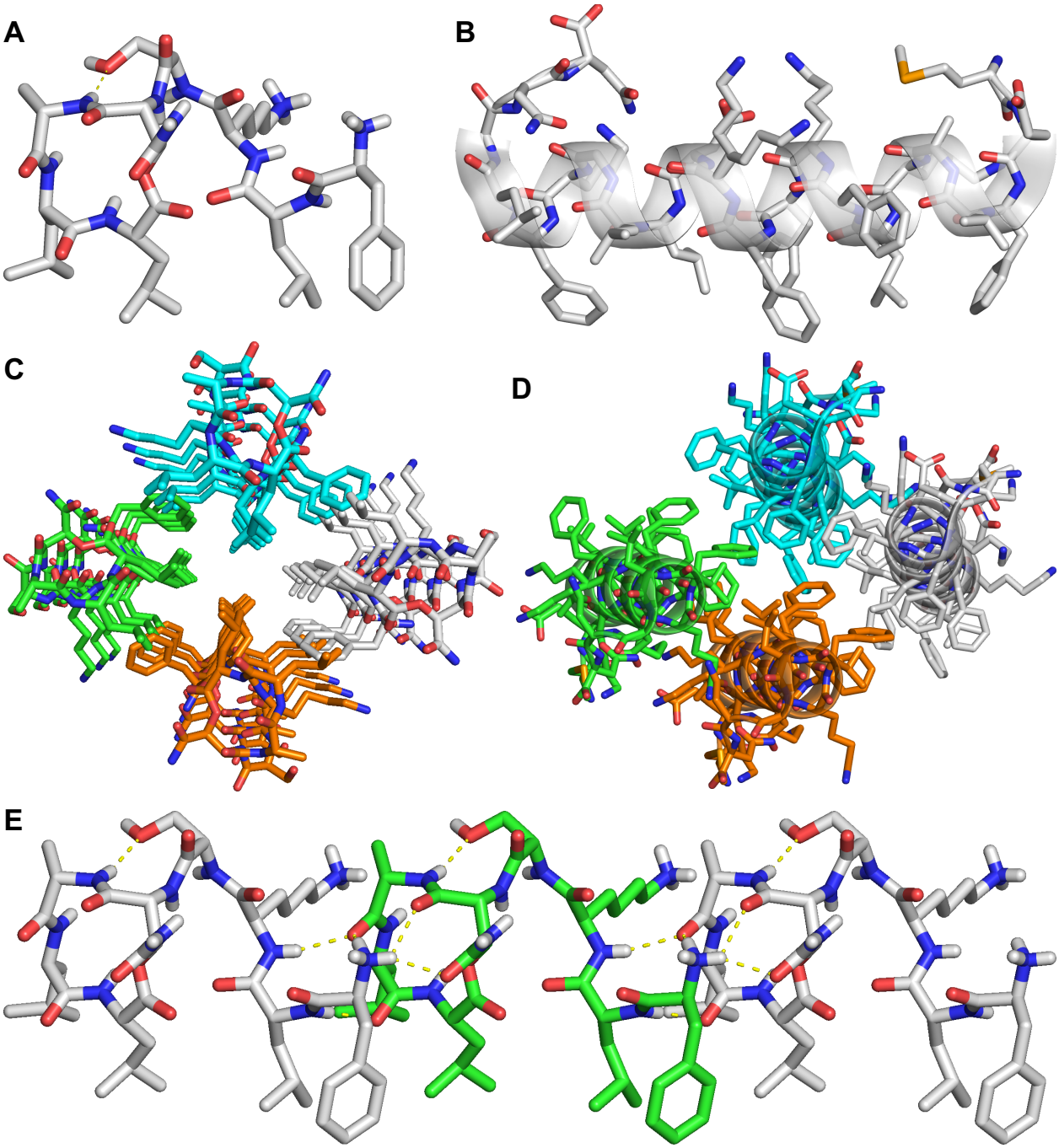

Figure 7. (A) X-ray crystallographic structure of *epi*-Novo29 (PDB 8CUG). (B) X-ray crystallographic structure of PSMα3 (PDB 5I55), illustrating the relationship of this amphiphilic 22-residue α-helical peptide to *epi*-Novo29. (C) Crystal packing of *epi*-Novo29. Molecules assemble in columns in the crystal lattice, with four columns of molecules arranged in a hydrophobic cluster through packing of Phe_1, $D\text{-}Leu_2$, Leu_7, and Leu_8. (D) Crystal packing of PSMα3, illustrating the relationship to the crystal packing of *epi*-Novo29. (E) Assembly of *epi*-Novo29 in the crystal lattice, illustrating the intermolecular hydrogen-bonding between molecules comprising the columns. Three molecules are shown.

The amphiphilic structure of *epi*-Novo29 is reminiscent of the amphiphilic structure our laboratory has previously observed for teixobactin derivatives, in which the side chains of *N*-methyl-D-Phe$_1$, Ile$_2$, D-*allo*-Ile$_5$, and Ile$_6$ create a hydrophobic surface and the side chains of Ser$_3$, D-Gln$_4$, and Ser$_7$ create a hydrophilic surface.[6,17] In teixobactin, this conformation is biologically significant, providing a hydrophobic surface that interacts with the lipids of the bacterial cell membrane and a hydrophilic surface to interact with the aqueous environment.[17,19–21] In Novo29, the amphiphilic structure likely provides similar opportunity for interaction with the bacterial cell membrane. In teixobactin, the cavity created by the macrolactone ring binds the pyrophosphate groups of lipid II and related bacterial cell-wall precursors. The macrolactone ring of Novo29 has the potential to bind the pyrophosphate groups of lipid II in a similar fashion.

The amphiphilic structure of *epi*-Novo29 is similar to that of the α-helices of phenol-soluble modulin α3 (PSMα3), a cytotoxic 22-residue peptide secreted by *S. aureus* which aggregates to form novel "cross-α" amyloid fibrils.[22] The α-helices formed by PSMα3 present phenylalanine and leucine residues on one surface, and polar residues on the other surface (Figure 7B). PSMα3 packs so that the hydrophobic surfaces come together in extended layers, in which the packing of four PSMα3 molecules resembles that of four *epi*-Novo29 molecules (Figure 7D). Although *epi*-Novo29 is much smaller than PSMα3 — 8 residues instead of 22 residues — the *epi*-Novo29 molecules daisy-chain through intermolecular hydrogen bonding to form extended structures that resemble the larger α-helices of PSMα3 (Figure 7E).

To gain additional insights into the mechanism of action of Novo29, we used the X-ray crystallographic structure of *epi*-Novo29 to create a molecular model of Novo29. Inversion of the *3S*-stereocenter of the (2*R*,3*S*)-hydroxyAsn residue of the crystal structure, followed by geometry optimization of only the side chain of the resulting (2*R*,3*R*)-hydroxyAsn residue, afforded a

crystallographically based molecular model of Novo29 (Figure 8). In this model, the molecule still adopts an amphiphilic conformation. The only difference in structure is that the side-chain amide NH group of the (2*R*,3*R*)-hydroxyAsn residue hydrogen bonds to the carbonyl group of Phe_1. This intramolecular hydrogen bond, in addition to the intramolecular hydrogen bond between the main-chain NH group of Ala_6 and the side chain OH group of Ser_4 helps enforce the amphiphilic conformation.

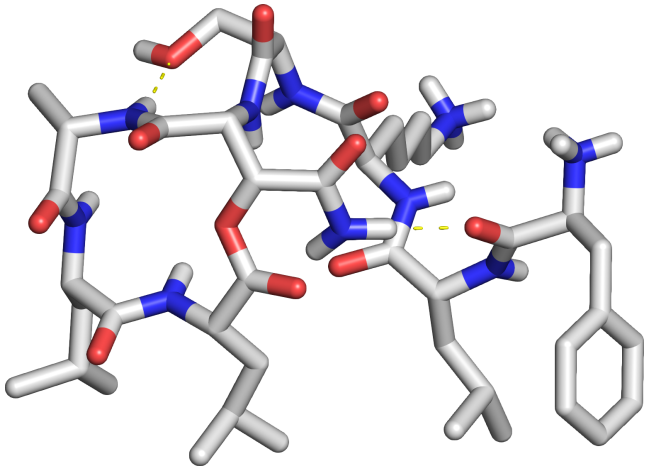

Figure 8. Molecular model of Novo29, based on the X-ray crystallographic structure of *epi*-Novo29. Intramolecular hydrogen bonds (yellow dashed lines) help enforce a preorganized conformation, in which the side chains of Phe_1, D-Leu_2, Leu_7, and Leu_8 align and can interact with the cell membrane of Gram-positive bacteria, and the macrolactone ring adopts a conformation that can bind the pyrophosphate groups of lipid II and related cell-wall precursors.

The X-ray crystallographic structure of *epi*-Novo29 and the crystallographically based molecular model of Novo29 suggest that Novo29 might be able to act upon Gram-positive bacteria in a fashion similar to teixobactin. Teixobactin adopts an amphiphilic conformation on bacteria, in which the side chains of *N*-methyl-D-Phe_1, Ile_2, D-*allo*-Ile_5, and Ile_6 insert into the cell membrane and the macrolactone ring binds the pyrophosphate groups of lipid II and related cell-wall precursors.[19] The teixobactin molecules form hydrogen-bonded dimers that further assemble on the cell membrane through β-sheet formation, causing lipid II and related cell-wall precursors to

cluster and ultimately lyse the bacteria. We envision that Novo29 also adopts an amphiphilic conformation on Gram-positive bacteria, in which the side chains of Phe_1, D-Leu_2, Leu_7, and Leu_8 insert into the cell membrane and the macrolactone ring binds the pyrophosphate groups of lipid II and related cell-wall precursors. The Novo29 molecules may further assemble through side-to-side hydrophobic interactions and end-to-end hydrogen bonding, and thus cause lipid II and related cell-wall precursors to cluster. We anticipate that the studies described in this paper will help lay the groundwork for testing this hypothesis.

Conclusion

The antibiotic Novo29 has 2*R*,3*R* stereochemistry in the hydroxyAsn residue at position 5. Novo29 and diastereomer *epi*-Novo29 are prepared by Fmoc-based solid-phase peptide synthesis followed by solution-phase cyclization. The corresponding amino acid building blocks Fmoc-(2*R*,3*R*)-hydroxyasparagine-OH and Fmoc-(2*R*,3*S*)-hydroxyasparagine-OH are prepared from (*R*,*R*)- and (*S*,*S*)-diethyl tartrate. Correlation of synthetic Novo29 and *epi*-Novo29 with natural Novo29 through NMR spectroscopy, LC-MS, and MIC assays establishes the 2*R*,3*R* stereochemistry of the hydroxyAsn residue and confirms that Novo29 is active against Gram-positive bacteria. X-ray crystallography of *epi*-Novo29 reveals an amphiphilic conformation and packing of the molecules through hydrophobic and hydrogen-bonding interactions. Molecular modeling suggests that Novo29 should be able to adopt a similar amphiphilic conformation that is further stabilized through an additional hydrogen bond between the primary amide group of the (2*R*,3*R*)-hydroxyAsn residue and the carbonyl group of the phenylalanine residue.

Notes and references

1. "Depsipeptides and uses thereof", Peoples, A. J.; Hughes, D.; Ling, L. L.; Millett. W.; Nitti, A. G.; Spoering, A.; Steadman, V. A.; Chiva, J. C.; Lazarides, L.; Jones, M. K.; Poullennes, K. G.; Lewis, K.; Epstein, S. U.S. Patent 11,203,616.

2. Novobiotic Pharmaceuticals, https://www.novobiotic.com\the-science.

3. Ling, L. L.; Schneider, T.; Peoples, A. J.; Spoering, A. L.; Engels, I.; Conlon, B. P.; Mueller, A.; Schäberle, T. F.; Hughes, D. E.; Epstein, S.; Jones, M.; Lazarides, L.; Steadman, V. A.; Cohen, D. R.; Felix, C. R.; Fetterman, K. A.; Millett, W. P.; Nitti, A. G.; Zullo, A. M.; Chen, C.; Lewis K. A new antibiotic kills pathogens without detectable resistance. *Nature* **2015**, *517*, 455–459.

4. Ling, L. L. Preclinical Development of Novo29, a New Antibiotic, *NIH RePORTER*, https://reporter.nih.gov/project-details/10111451.

5. Wirtz, D. A.; Ludwig, K. C.; Arts, M.; Marx, C. E.; Krannich, S.; Barac, P.; Kehraus, S.; Josten, M.; Henrichfreise, B.; Müller, A.; König, G. M.; Peoples, A. J.; Nitti, A. G.; Spoering, A. L.; Ling, L. L.; Lewis, K.; Crüsemann, M.; Schneider, T. Biosynthesis and Mechanism of Action of the Cell Wall Targeting Antibiotic Hypeptin. *Angew. Chem. Int. Ed.* **2021**, *60*, 13579–13586.

6. Yang, H.; Pishenko, A. V.; Li, X.; Nowick, J. S. Design, Synthesis, and Study of Lactam and Ring-Expanded Analogues of Teixobactin. *J. Org. Chem.* **2020**, *85*, 1331–1339.

7. Sieber, P.; Riniker, B. Protection of carboxamide functions by the trityl residue. Application to peptide synthesis. *Tetrahedron Lett.*, **1991**, *32*, 739–742.

8. Gao, B.; Sharpless, K. B. Vicinal diol cyclic sulfates. Like epoxides only more reactive. *J. Am. Chem. Soc.* **1988**, *110*, 7538–7539.

9. He, L.; Byun, H.S.; Bittman, R. Efficient synthesis of chiral α,β-epoxyesters via a cyclic sulfate intermediate. *Tetrahedron Lett.* **1998**, *39*, 2071–2074.

10. France, B.; Bruno, V.; Nicolas, I. Synthesis of a protected derivative of (2R,3R)-β-hydroxyaspartic acid suitable for Fmoc-based solid phase synthesis. *Tetrahedron Lett.* **2013**, *54,* 158–161.

11. Guzmán-Martinez; A.; Vannieuwenhze, M. S. An Operationally Simple and Efficient Synthesis of Orthogonally Protected L-threo-beta-Hydroxyasparagine. *Synlett* **2007**, *10*, 1513–1516.

12. Liu, L.; Wang, B.; Bi, C.; He, G.; Chen, G. Efficient preparation of β-hydroxy aspartic acid and its derivatives. *Chin. Chem. Lett.* **2018**, *29*, 1113–1115.

13. Chen, K. H.; Le, S. P.; Han, X.; Frias, J. M.; Nowick, J. S. Alanine scan reveals modifiable residues in teixobactin. *Chem. Commun.* **2017**, *53*, 11357–11359.

14. Yang, H.; Chen, K. H.; Nowick, J. S. Elucidation of the Teixobactin Pharmacophore, *ACS Chem. Biol.* **2016**, *11*, 1823–1826.

15. Yang, H.; Du Bois, D. R.; Ziller; J. W.; Nowick, J. S. X-ray crystallographic structure of a teixobactin analogue reveals key interactions of the teixobactin pharmacophore. *Chem. Commun.* **2017**, *53*, 2772–2775.

16. Morris, M. A.; Malek, M.; Hashemian, M. H.; Nguyen, B. T.; Manuse, S.; Lewis, K. L; Nowick, J. S. A Fluorescent Teixobactin Analogue. *ACS Chem. Biol.* **2020**, *15*, 1222–1231.

17. Yang, H.; Wierzbicki, M.; Du Bois D. R.; Nowick, J. S. X-ray Crystallographic Structure of a Teixobactin Derivative Reveals Amyloid-like Assembly. *J. Am. Chem. Soc.* **2018**, *140*, 14028–14032.

18. Neises, B.; Steglich, W. Simple Method for the Esterification of Carboxylic Acids. *Angew. Chem. Int. Ed. Engl.* **1978**, *17*, 522–524.

19. Shukla, R.; Lavore, F.; Maity, S.; Derks, M. G. N.; Jones, C. R.; Vermeulen, B. J. A.; Melcrová, A.; Morris, M. A.; Becker, L. M.; Wang, X.; Kumar, R.; Medeiros-Silva, J.; van Beekveld, R. A. M.;

Bonvin, A. M. J. J.; Lorent, J. H.; Lelli, M.; Nowick, J. S.; MacGillavry, H. D.; Peoples, A. J.; Spoering, A. L.; Ling, L. L.; Hughes, D. E.; Roos, W. H.; Breukink, E.; Lewis, K. and Weingarth, M. Teixobactin kills bacteria by a two-pronged attack on the cell envelope. *Nature* **2022**, *608*, 390–396.

20. Shukla, R.; Medeiros-Silva, J.; Parmar, A.; Vermeulen, B. J. A.; Das, S.; Paioni, A. L.; Jekhmane, S.; Lorent, J.; Bonvin, A. M. J. J.; Baldus, M.; Lelli, M.; Veldhuizen, E. J. A.; Breukink, E.; Singh, I.; Weingarth, M. Mode of action of teixobactins in cellular membranes. *Nat. Commun.*, **2020**, *11*, 2848.

21. Öster, C.; Walkowiak, G. P.; Hughes, D. E.; Spoering, A. L.; Peoples, A. J.; Catherwood, A. C.; Tod, J. A.; Lloyd, A. J.; Herrmann, T.; Lewis, K.; Dowson, C. G.; Lewandowski, J. R. Structural studies suggest aggregation as one of the modes of action for teixobactin. *Chem. Sci.* **2018**, *9*, 8850–8859.

22. Tayeb-Fligelman, E.; Tabachnikov, O.; Moshe, A.; Goldshmidt-Tran, O.; Sawaya, M. R.; Coquelle, N.; Colletier; J.; Landau, M. The cytotoxic Staphylococcus aureus PSMα3 reveals a cross-α amyloid-like fibril. *Science* **2017**, *355*, 831–833.

APPENDIX A: Supporting information

Table of Contents for Supporting Information

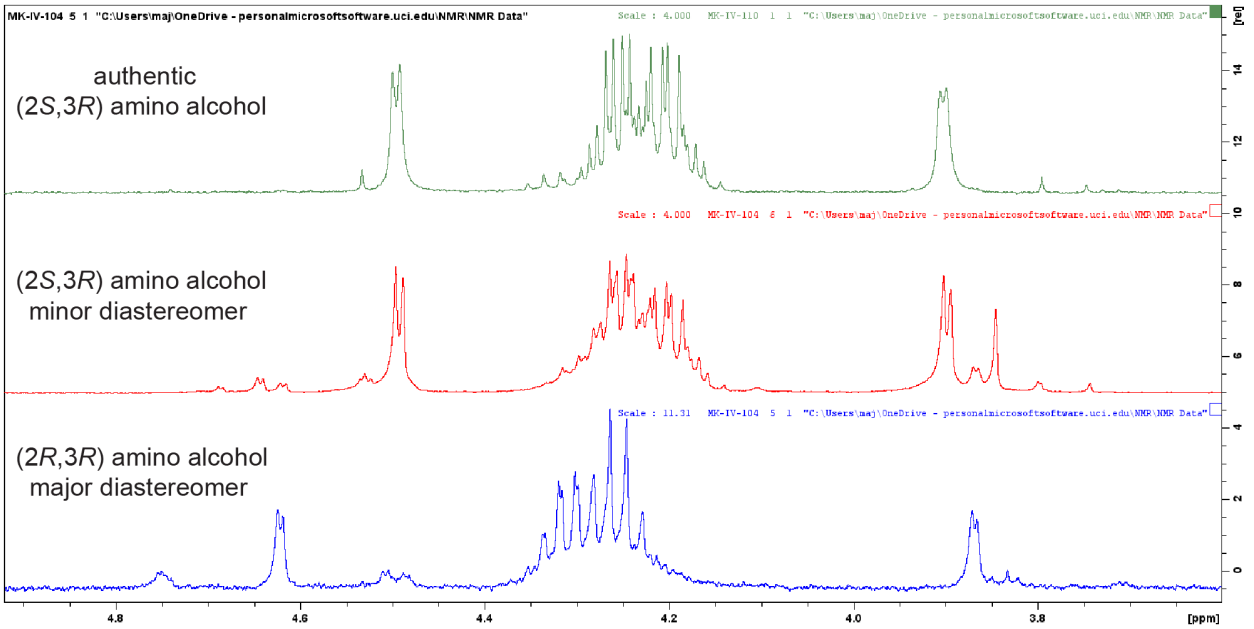

Figure S1. Establishment of (2*R*,3*R*) stereochemistry of amino alcohol **2** and the (2*S*,3*R*) stereoisomer by ^{1}H NMR spectroscopic correlation with an authentic sample of the (2*S*,3*R*) stereoisomer (the enantiomer of amino alcohol **5**) that was synthesized from (+)-diethyl L-tartrate by the route shown in Figure 4 of the main manuscript. Amino alcohol **2** was synthesized as shown in Figure 3 as a 70:30 mixture of diastereomers, which was then separated by column chromatography. Expansions of the ^{1}H NMR spectra of the major diastereomer (2*R*,3*R*, blue) and minor diastereomer (2*S*,3*R*, red) are shown. Correlation with an authentic sample of the (2*S*,3*R*) diastereomer (green) establishes that the minor diastereomer of amino alcohol **2** is (2*S*,3*R*), and thus that the major diastereomer is (2*R*,3*R*).

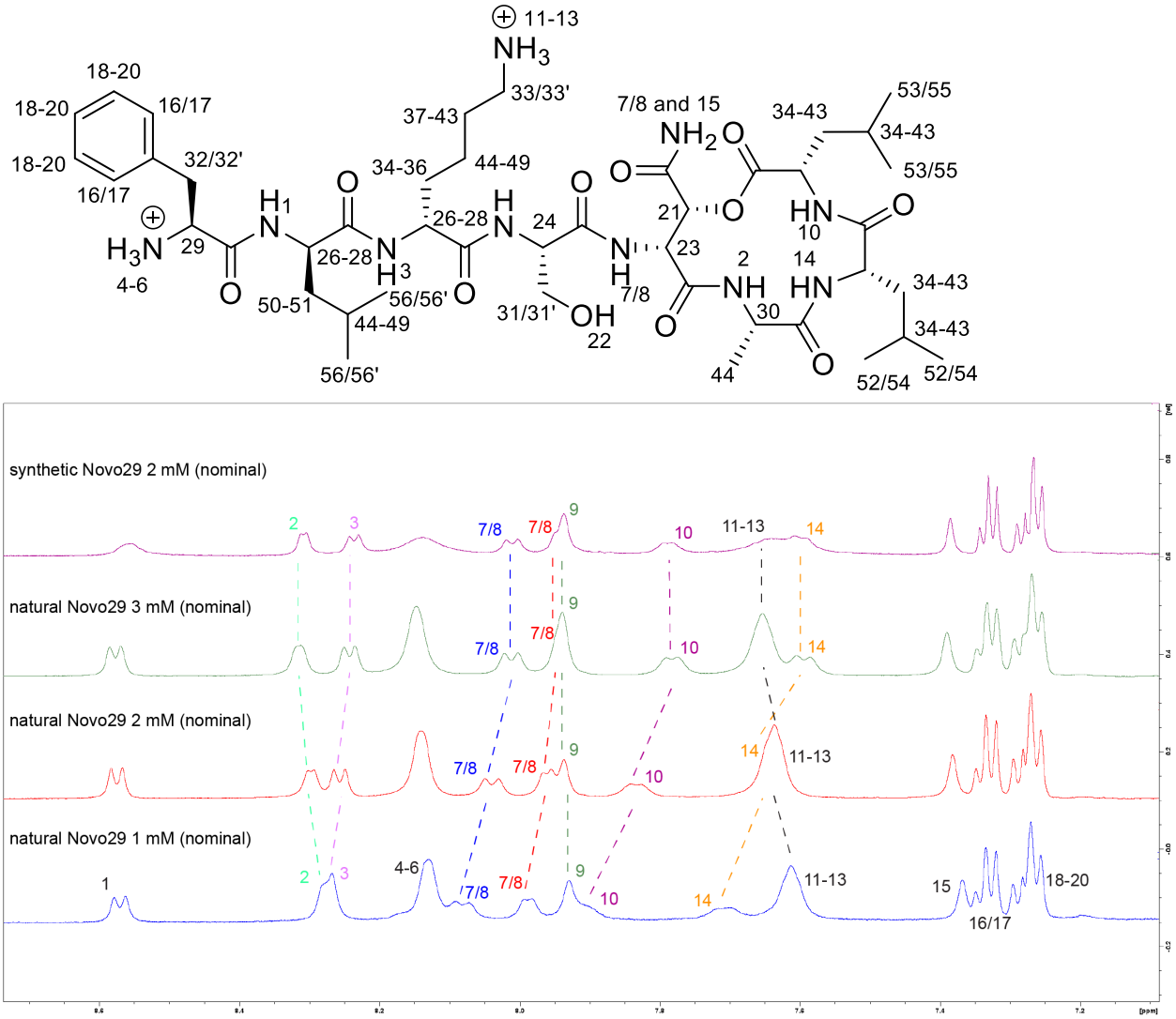

Figure S2. Comparison of the amide NH regions of the 500 MHz ^{1}H NMR spectra of samples of Novo29 in DMSO-d_6. Samples of natural Novo29 were prepared gravimetrically at nominal concentrations of 1, 2, and 3 mM. The chemical shifts of the NH resonances vary strongly with concentration. The ^{1}H NMR spectrum of a sample of synthetic Novo29 prepared gravimetrically at a nominal concentration of 2 mM matches that of the 3 mM nominal concentration sample of natural Novo29. All samples were prepared by dissolving 1–2 mg of peptide in DMSO-d_6. Discrepancies in concentration reflect errors associated with weighing out small quantities of peptide.

Table S1. Chemical shifts of the amide NH resonances of samples of Novo29.

#	natural 1 mM (nominal)	natural 2 mM (nominal)	natural 3 mM (nominal)	synthetic 2 mM (nominal)
1	8.57	8.57	8.57	8.56
2	8.28	8.29	8.31	8.30
3	8.27	8.26	8.24	8.24
4-6	8.13	8.14	8.15	8.14
7/8	8.08 & 7.98	8.04 & 7.96	8.01 & 7.95	8.01 & 7.94
9	7.99	7.96	7.94	7.94
10	7.90	7.83	7.78	7.78
11-13	7.61	7.64	7.65	7.65
14	7.71	7.65	7.60	7.60
15	7.37	7.38	7.39	7.39
16/17	7.33	7.33	7.33	7.33
18-20	7.27	7.27	7.27	7.27

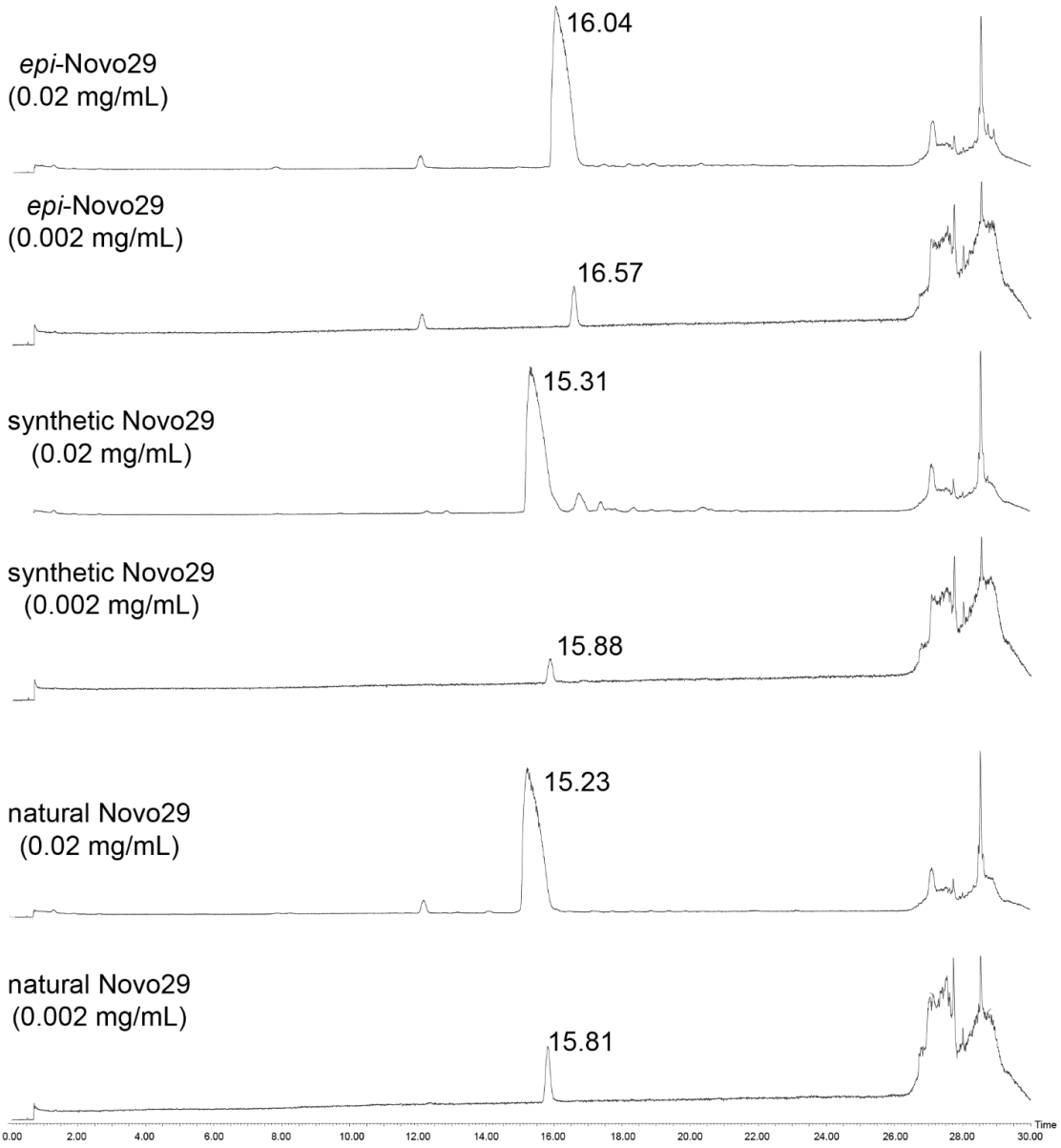

Figure S3. LC-MS of natural Novo29, synthetic Novo29, and epi-Novo29. Samples were run at (0.02 mg/mL) and (0.002 mg/mL). Traces are the total ion current (TIC) chromatograms of the samples run on a C4 column with a 3–27% CH_3CN over 25 minutes, followed by a 90% CH_3CN wash over two minutes, and a 3% CH_3CN 97% H_2O wash over one minute. The retention time and peak shape of Novo29 proved highly concentration dependent, with broad peaks and shorter elution times resulting at higher concentrations, again suggesting strong self-association.
LC/MS analysis was performed of the intact peptide sample (ACQUITY UPLC H-class system, Xevo G2-XS QTof, Waters corporation). The C4 column that was used was ACQUITY UPLC Protein BEH C4, 300 Å, 1.7 µm, 2.1 mm x 50 mm, Waters corp. The Xevo Z-spray source was operated in positive MS resolution mode, 400-4000da, with a capillary voltage of 3000V and a cone voltage of 40V (NaCsI calibration, Leu-enkephalin lock-mass). Nitrogen was used as the desolvation gas at 350C and a total flow of 800 L h–1. Retention times are given in minutes (min).

Table S2. Crystallographic properties, crystallization conditions, and data collection and model refinement statistics for *epi*-Novo29 (PDB ID 8CUG).

peptide	*epi*-Novo29 (synchrotron structure)
PDB ID	8CUG
space group	$P2_12_12_1$
a, *b*, *c* (Å)	12.105, 31.898, 37.101
α, β, λ (°)	90, 90, 90
peptides per asymmetric unit	2
crystallization conditions	2.8 M sodium acetate trihydrate pH 6.6
wavelength (Å)	1.00
resolution (Å)	24.19–1.13 (24.19–1.131)
total reflections	58890 (1401)
unique reflections	5590 (398)
multiplicity	10.5 (3.5)
completeness (%)	96.44 (69.54)
mean I/σ	22.28 (4.20)
Wilson B factor	8.32
R_{merge}	0.07324 (0.3204)
$R_{measure}$	0.07694 (0.3701)
$CC_{1/2}$	0.998 (0.938)
CC^*	0.999 (0.984)
R_{work}	0.1308 (0.2378)
R_{free}	0.1450 (0.2242)
number of non-hydrogen atoms	174
RMS_{bonds}	0.012
RMS_{angles}	1.63
Ramachandran favored (%)	100
outliers (%)	0
clashscore	3.77
average B-factor	13.49
ligands/ions	1
water molecules	42

Table S3. Crystallographic properties, crystallization conditions, and data collection and model refinement statistics for *epi*-Novo29 (PDB ID 8CUF).

peptide	*epi*-Novo29 (X-ray diffractometer structure with KI)
PDB ID	8CUF
space group	$P2_12_12_1$
a, *b*, *c* (Å)	12.1027, 31.5547, 36.9613
α, β, λ (°)	90, 90, 90
peptides per asymmetric unit	2
crystallization conditions	2.8 M sodium acetate trihydrate pH 6.6
wavelength (Å)	1.54
resolution (Å)	15.95–1.68 (1.74–1.68)
total reflections	22879 (199)
unique reflections	1741 (111)
multiplicity	13.1 (1.8)
completeness (%)	95.61 (63.07)
mean I/σ	36.10 (5.16)
Wilson B factor	8.93
R_{merge}	0.2386 (0.2593)
$R_{measure}$	0.2465 (0.3302)
$CC_{1/2}$	0.869 (0.822)
CC^*	0.964 (0.95)
R_{work}	0.1509 (0.2198)
R_{free}	0.1672 (0.0923)
number of non-hydrogen atoms	152
RMS_{bonds}	0.008
RMS_{angles}	1.08
Ramachandran favored (%)	100
outliers (%)	0
clashscore	3.75
average B-factor	9.85
ligands/ions	3
water molecules	18

Materials and Methods

General information

Chemicals and Supplies. All chemicals were used as received unless otherwise noted. Dry methylene chloride (CH_2Cl_2), tetrahydrofuran (THF), methanol (MeOH), and *N*,*N*-dimethylformamide (DMF) were obtained by passing through alumina under argon prior to use. 1,4-Dioxane (dioxane) was used without added stabilizers. Anhydrous, amine-free *N*,*N*-dimethylformamide (DMF), DIPEA, 2,4,6-collidine, and piperidine were purchased Alfa Aesar. HPLC grade acetonitrile and deionized water (18 MΩ), each containing 0.1% trifluoroacetic acid (TFA), were used for analytical and preparative reverse-phase HPLC, as well as reverse-phase chromatography using a Biotage® Isolera One flash column chromatography instrument. Commercial agents were used without purification, unless otherwise stated. (-)-Diethyl-D-tartrate was purchased from Chem-Impex. (+)-Diethyl L-tartrate, thionyl chloride ($SOCl_2$), and palladium activated on carbon (Pd/C, 10% Pd, 50 % wet with water) were purchased from Sigma Aldrich. Sodium azide (NaN_3) and benzyl bromide (BnBr) were purchased from Alfa Aesar. Hydrogen (H_2) and ammonia (NH_3) were purchased from Praxair. Sodium periodate ($NaIO_4$) and hydrochloric acid (HCl) were purchased from Fisher Chemicals. Di-*tert*-butyl dicarbonate (Boc_2O) and Fmoc *N*-hydroxysuccinimide ester (Fmoc-OSu) were purchased from GL Biochem. Ruthenium (III) chloride trihydrate ($RuCl_3 \bullet 3H_2O$) was purchased from Chem Scene. Lithium bromide (LiBr) was purchased from TCI. Amino acids, coupling agents, 2-chlorotrityl chloride resin, DIC, and triisopropylsilane were purchased from Chem-Impex.

Instrumentation. Bacteria were incubated in a Thermo Fisher Scientific MaxQ Shaker 6000. NMR spectra were recorded on a Bruker AVANCE 500 or AVANCE 600 spectrometers equipped with cryoprobes and were calibrated using residual solvent peaks ($CDCl_3$: δ_H = 7.26 ppm, δ_C = 77.16 ppm, DMSO-*d*$_6$: δ_H = 2.50 ppm, δ_C = 39.51 ppm, and CD_3OD: δ_H = 3.31 ppm, δ_C = 49.15 ppm).

Analytical reverse-phase HPLC was performed on Agilent 1260 Infinity II instrument equipped with a Phenomonex bioZen PEPTIDE 2.6 um XB-C18 column (150x4.6 mm), eluting with a gradient of acetonitrile and water (each containing 0.1% TFA) from 5-100% over 20 minutes. Peptides were purified on a Biotage Isolera One flash column chromatography instrument with a Biotage® SfarBio C18 D – Duo 300 Å 20 μm 10 g column. *epi*-Novo29 was then further purified by preparative reverse-phase HPLC on a Rainin Dynamax equipped with an Agilent Zorbax 250x 21.2 mm SB-C18 column. Both peptides were prepared and used as the trifluoroacetate (TFA) salts and were assumed to have one trifluoroacetic acid molecule per amine group on each peptide (two TFA molecules per peptide). Natural Novo29 was provided by NovoBiotic Pharmaceuticals LLC as the trifluoroacetate (TFA) salt.

Chemical synthesis of Fmoc-(2*R*,3*R*)-hydroxyAsn-OH.[1-5]

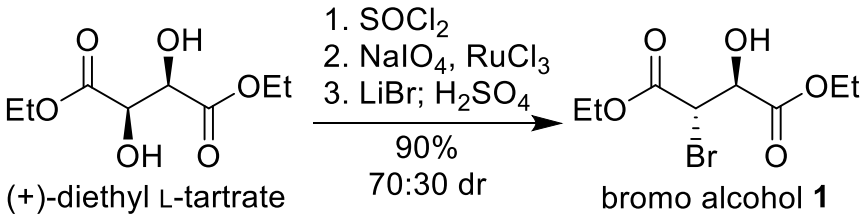

Bromo alcohol 1. A 500-mL, single-necked, round-bottom flask equipped with a magnetic stirring bar and a condenser fitted with a nitrogen inlet adapter was charged with a solution of (+)-diethyl L-tartrate (8.56 mL, 50.00 mmol, 1.0 equiv.) in 250 mL of CH_2Cl_2. (The reaction was run at ca. 0.2 M concentration of the diethyl L-tartrate.) To the solution, $SOCl_2$ (7.25 mL, 100.00 mmol, 2.0 equiv.) was added in drops over ca. 5 minutes, followed by anhydrous DMF as a catalyst (0.25 mL, 3.20 mmol, 6 mol %) The reaction mixture was heated to 35 °C and stirred for 2 hours. Then, the solution was allowed to cool to room temperature, and concentrated to dryness by rotary evaporation to afford a cyclic sulfite intermediate as a yellow oil (12.61 g, 99% yield of the unpurified product). The cyclic sulfite was used without further purification.

The cyclic sulfite intermediate (12.61 g, 50.00 mmol, 1.0 equiv.) was dissolved in 250 mL CH_2Cl_2, 125 mL CH_3CN, and 62.5 mL H_2O, and the mixture was transferred to a 500-mL, single-necked, round-bottom flask equipped with a magnetic stirring bar and a nitrogen inlet adapter. $RuCl_3 \bullet 3H_2O$ (0.327 g, 1.25 mmol, 2.5 mol %) was dissolved in 62.5 mL H_2O and added, followed by $NaIO_4$ (21.39 g, 100 mmol, 2 equiv.). The reaction mixture was stirred at 25 °C for 16 hours under N_2, and then diluted with 500 mL of Et_2O and 100 mL of H_2O. The organic layer was washed with 400 mL of saturated aqueous $NaHCO_3$, followed by 400 mL of saturated aqueous NaCl. The organic layer was concentrated to dryness by rotary evaporation to afford a cyclic sulfate intermediate as a yellow oil (12.39 g, 92 % yield of the unpurified product). The cyclic sulfate intermediate was used without further purification.

A 500-mL, three-necked, round-bottom flask equipped with a magnetic stirring bar and fitted with a nitrogen inlet adapter and two rubber septa was charged with LiBr (12.04 g, 138.60 mmol, 3 equiv.). The flask was placed under vacuum and heated to 120 °C in an oil bath for 1 hour to ensure LiBr was dry. The flask was then cooled to room temperature. The cyclic sulfate (12.39 g, 46.20 mmol, 1 equiv.) dissolved in 460 mL anhydrous THF was transferred to the flask with a capillary. (The reaction was run at ca. 0.1 M concentration of the cyclic sulfate.) The reaction mixture was stirred at 25 °C for 2 hours in a nitrogen atmosphere. The solution was concentrated to dryness by rotary evaporation. The solution was dissolved in ca. 720 mL Et_2O and 480 mL aqueous 20% H_2SO_4. The solution was stirred for 18 hours at 25 °C. The organic and aqueous layers were separated, and the aqueous layer was extracted twice with 200 mL Et_2O and dried over Na_2SO_4. The solution was concentrated to dryness by rotary evaporation to afford bromo alcohol **1** as a yellow oil (12.43 g, 99 % yield of the unpurified product). Bromo alcohol **1** was generated as a mixture of diastereomers and used without further purification. ^1H NMR (500 MHz, $CDCl_3$): δ 4.81–4.65 (m, 2 H), 4.42–4.14 (m,

4 H), 1.40–1.23 (m, 6 H), 1.28 (q, J = 7.2 Hz, 1 H). ^{13}C NMR (125 MHz, $CDCl_3$): δ 170.5, 166.8, 72.7, 71.4, 63.0, 59.9, 49.7, 47.9, 14.2. HRMS: *m/z*: $[M + Na]^+$ calcd for $C_8H_{13}BrO_5Na^+$ 290.9844, observed 290.9844.

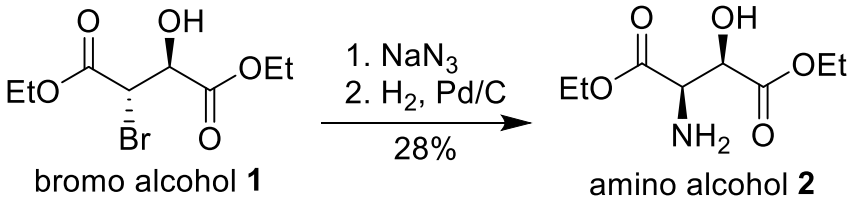

bromo alcohol **1** amino alcohol **2**

Amino alcohol 2. A 250-mL, single-necked, round-bottom flask equipped with a magnetic stirring bar, a nitrogen inlet adapter, was charged with a solution of bromo alcohol **1** (12.43 g, 46.20 mmol, 1.0 equiv.) in 180 mL of anhydrous DMF. (The reaction was run at ca. 0.25 M concentration of the bromo alcohol **1**.) NaN_3 (9.01g, 138.60 mmol, 3 equiv.) was added to the solution, and the suspension was stirred for 21 h at 25 °C. The suspension was transferred to a separatory funnel and the round bottom flask was rinsed with 300 mL H_2O. The layers were separated, and the aqueous layer was extracted with EtOAc (3 x 200 mL). The combined organic layer was dried over Na_2SO_4, filtered, and dried using rotary evaporation to yield the azide intermediate as a yellow oil (9.01 g, 84 % yield of the unpurified product). The azide intermediate was used without further purification.

A 500-mL, three-necked, round-bottom flask equipped with a magnetic stirring bar, a nitrogen inlet adapter, an inlet adapter fitted with a hydrogen balloon, and a rubber septum was charged with a solution of the crude azide intermediate (9.01 g, 38.97 mmol, 1.0 equiv.) in 100 mL of CH_3OH. (The reaction was run at 0.3 M concentration of the azide intermediate.) The flask was evacuated and back filled with nitrogen, and 10 % Pd/C (50% wet solid, 4.51 g, one half the mass of the azide intermediate) was added. A balloon containing H_2 gas was fitted to an inlet adapter and the system was evacuated and back filled with H_2 gas. The resulting suspension was stirred for 6 h, filtered through Celite, and

washed with 200 mL of additional CH_3OH. The resulting solution was concentrated by rotary evaporation to and purified by column chromatography on silica gel (elution with 5:95 CH_3OH:CH_2Cl_2) to afford amino alcohol **2** as a yellow oil (2.69 g, 33 % yield). ^{1}H NMR (500 MHz, $CDCl_3$): δ 4.48 (d, *J* = 2.7 Hz, 1 H), 4.22–4.05 (m, 4 H), δ 3.75 (d, *J* = 2.8 Hz, 1 H) 2.53 (broad s, 3 H), 1.18 (q, *J* = 7.3 Hz, 6 H). ^{13}C NMR t(125.7 MHz, $CDCl_3$): δ 172.6, 172.4, 72.0, 61.8, 61.4, 56.7, 13.96, 13.94. HRMS: *m/z*: $[M + Na]^+$ calcd for $C_8H_{15}NO_5Na^+$ 228.0848, observed 228.0843.

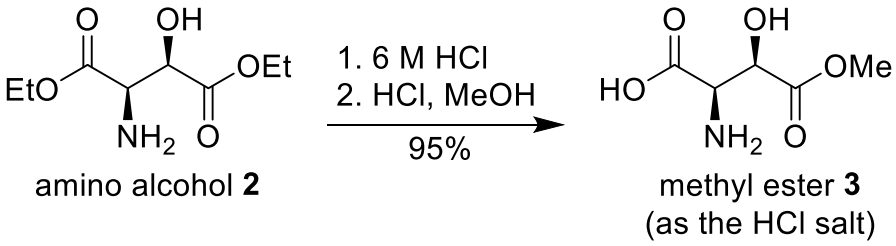

amino alcohol **2**

methyl ester **3**
(as the HCl salt)

Methyl ester 3. A 250-mL, single-necked, round-bottom flask equipped with a magnetic stirring bar and a condenser fitted with a nitrogen inlet adapter was charged with a solution of amino alcohol **2** (2.69 g, 13.11 mmol, 1.0 equiv.) in 65 ml of 6 M HCl. (The reaction was run at ca. 0.2 M concentration of the amino alcohol **2**.) The mixture was heated in an oil bath and stirred for 16 h at 100 °C, cooled to room temperature, and concentrated to dryness by rotary evaporation to afford a beige solid (2.59 g, 99 % yield of the unpurified product). The crude carboxylic acid intermediate was used in the next step without purification.

A 250-mL, single-necked, round-bottom flask equipped with a magnetic stirring bar and a condenser fitted with a nitrogen inlet adapter was charged with a solution of the crude carboxylic acid intermediate (2.45 g, 13.11 mmol, 1.0 equiv.) in 65 mL of CH_3OH. (The reaction was run at ca. 0.2 M concentration of the crude intermediate.) The mixture was cooled to 0 °C using an ice bath. A solution of 12 M HCl (2.0 mL) was then added dropwise to the flask over a few minutes. The flask was then heated in a preheated water bath at 65 °C for 30 minutes. The mixture was let to cool to room

temperature and concentrated to dryness by rotary evaporation to afford methyl ester **3** as a beige foam (2.59 g, 96 % yield of the unpurified product). Methyl ester **3** was used without further purification. ^{1}H NMR (500 MHz, CD_3OD): δ 4.65 (d, J = 3.0 Hz, 1 H), 4.16 (d, J = 3.2, 1 H), 3.71 (s, 3 H). ^{13}C NMR (125.7 MHz, CD_3OD) (major product, methyl ester **3**): δ 171.00, 168.79, 69.15, 55.19, 52.87; (minor impurity; diacid precursor impurity and dimethyl ester, partial data): δ 170.60, 167.94, 69.11, 55.28, 52.98. HRMS: *m/z*: $[M + Na]^+$ calcd for $C_5H_9NO_5Na^+$ 164.0559, observed 164.0556.

NOTE: We have found that timing is essential to the selective formation of the monomethyl ester (methyl ester **3**) from the corresponding diacid precursor. When we ran this reaction for two hours at 65 °C we observed the predominant formation of the undesired the dimethyl ester product. When we ran this reaction for 15 minutes at 65 °C we observed ca. 50% conversion to the desired methyl ester **3**, with ca. 44% diacid precursor remaining, and ca. 6% of the dimethyl ester. When we ran this reaction for 30 minutes at 65 °C we observed mostly the desired methyl ester **3** (ca. 83%), with some remaining diacid precursor (ca. 12%), and some dimethyl ester (ca. 5%).

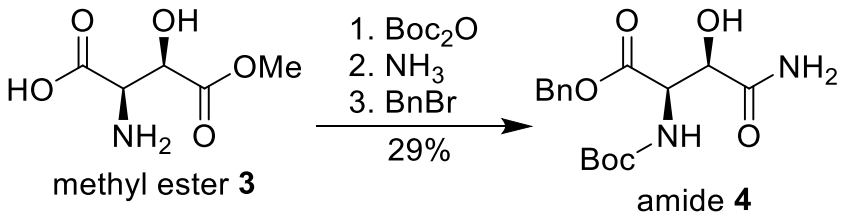

Amide 4. A 250-mL, single-necked, round-bottom flask equipped with a magnetic stirring bar and fitted with a nitrogen inlet adapter was charged with a solution of methyl ester **3** (containing the diacid precursor and dimethyl ester impurities) (2.59 g, 13.03 mmol, 1.0 equiv.) in 65 mL of 10 % w/v Na_2CO_3. The solution was cooled to 0 °C using an ice bath. While on ice, a separate solution of Boc_2O (8.53 g, 39.09 mmol, 3.0 equiv.) dissolved in 65 mL dioxane was added dropwise over 2–3 minutes. (The reaction was run at ca. 0.15 M concentration of the methyl ester **3**.) The mixture was brought to room temperature, stirred for 20 h, and concentrated to dryness using rotary evaporation. The resulting residue was dissolved in 250 mL EtOAc and transferred to a separatory funnel. The mixture was washed with 1 M HCl (3 x 250 mL). The organic layer was dried over $Na2SO_4$ and concentrated to a yellow oil. The crude product was purified by column chromatography on silica gel (elution with 10:90 CH_3OH:$CHCl_3$) to afford the Boc-protected intermediate as an oil (1.43 g, 42% yield).

A 125-mL, single-necked, high-pressure flask equipped with a magnetic stirring bar was charged with a solution of the Boc-protected intermediate (1.43 g, 5.43 mmol, 1.0 equiv.) in ca. 18 mL CH_3OH. (The reaction was run at ca. 0.3 M concentration of the Boc-protected intermediate.) A flow of NH_3 gas was applied through a syringe directly into the solution and bubbled for 20–30 min to ensure saturation with NH_3. The vessel was then capped, and the solution was stirred for 72 h at 25 °C. The solution was concentrated to dryness using rotary evaporation to afford the amide intermediate as a beige solid (1.21 g, 94% yield of the unpurified product). The crude intermediate was used in the next step without further purification.

A 100-mL, single-necked, round-bottom flask equipped with a magnetic stirring bar and fitted with a nitrogen inlet adapter was charged with a solution of the amide intermediate (1.21 g, 11.9 mmol, 1.0 equiv.) in ca. 25 mL of anhydrous DMF. (The reaction was run at ca. 0.2 M concentration of the amide intermediate.) The solution was cooled to 0 °C using an ice bath, and $NaHCO_3$ (1.07 g, 12.70 mmol, 2.5 equiv.) followed by benzyl bromide (2.42 mL, 20.4 mmol, 4.0 equiv.) was added dropwise over 10 minutes. The mixture was stirred for 2 hours at 0 °C, warmed to room temperature, and stirred for an additional 24 hours under N_2. The resulting solution was cooled again to 0 °C using an ice bath, 75 mL of H_2O was added to quench the reaction. The solution was transferred to a separatory funnel and extracted with EtOAc (3 x 50 mL). The combined organic layer was washed with 50 mL saturated aqueous NaCl, dried with Na_2SO_4, and concentrated to using rotary evaporation. The crude product was then purified by column chromatography on silica gel (elution with 5:95 CH_3OH:CH_3Cl) to afford amide **4** as white solid (1.27 g, 73% yield). ^{1}H NMR (500 MHz, $CDCl_3$): δ 7.31–7.36 (m, 5 H), 6.85 (br s, 1 H), 6.04 (br s, 1 H), 5.62 (d, *J* = 9.1 Hz, 1 H), 5.19 (s, 2 H), 5.17–5.30 (m, 2 H), 4.75 (br d, *J* = 9.1 Hz, 1 H), 4.61 (br s, 1 H), 1.39 (s, 9 H). ^{13}C NMR (125.7 MHz, $CDCl_3$): δ 173.7, 172.1, 170.2, 156.6, 135.1, 128.7, 128.5, 128.3, 81.6, 80.9, 74.8, 72.2, 68.1, 67.7, 56.4, 28.2. HRMS: *m/z*: $[M + Na]^+$ calcd for $C_{16}H_{22}N_2O_6Na^+$ 361.1375, observed 361.1371.

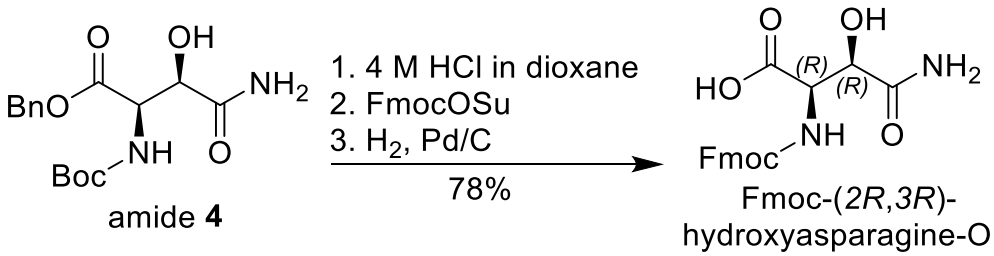

Fmoc-(2*R*,3*R*)-hydroxyasparagine-OH. A 250-mL, single-necked, round-bottom flask equipped with a magnetic stirring bar and fitted with a nitrogen inlet adapter was charged with a solution of amide **4** (1.27 g, 3.70 mmol, 1.0 equiv.) in ca. 40 mL of 4 N HCl in dioxane. (The reaction was run at ca. 0.1 M concentration of the amide **4**.) The solution was stirred for 2 hours at 25 °C and concentrated to dryness by rotary evaporation, to afford the amine intermediate as a pale-yellow solid (0.96 g, 95% yield of the unpurified product). The crude intermediate was used in the next step without further purification.

The crude amine intermediate (0.96 g, 3.50 mmol, 1.0 equiv.) was dissolved in 52 mL of 1:1 dioxane:water. (The reaction was run at ca. 0.06 M concentration of the crude amine intermediate.) The solution was cooled to 0 °C using an ice bath, and $NaHCO_3$ was added until the solution reached a pH of 6.8. Fmoc-OSu (1.42 g, 4.20 mmol, 1.2 equiv.) was then added, and the reaction mixture was stirred for 1 h on ice, warmed to room temperature, and stirred for an additional 20 hours under N_2. The resulting suspension was diluted with 120 mL EtOAc and 180 mL of saturated $NaHCO_3$ and stirred for ca. 5 min at 25 °C. The solution was transferred to a separatory funnel and the organic layer was collected; the aqueous layer was then extracted with EtOAc (2 x 80 mL). The combined organic layer was then dried with Na_2SO_4 and concentrated to by rotary evaporation to a white solid (1.61 g, 99% yield). A sample of the crude product was then purified by column chromatography on silica gel (elution with 5:95 CH_3OH:CH_3Cl) to afford the Fmoc-protected intermediate as a white solid that was used in the subsequent reaction.

A 250-mL, three-necked, round-bottom flask equipped with a magnetic stirring bar, a nitrogen inlet adapter, an inlet adapter fitted with a hydrogen balloon, and a rubber septum was charged with a solution of the Fmoc-protected intermediate (0.21 g, 0.46 mmol, 1 equiv.) from the previous step in ca. 5 mL of CH_3OH. (The reaction was run at 0.05 M concentration of the Fmoc-protected intermediate.) The flask was evacuated and back filled with nitrogen, and 10 % Pd/C (50% wet solid, 0.07 g, one half the mass of Fmoc-protected intermediate) was added. A balloon containing H_2 gas was fitted to an inlet adapter and the system was evacuated and back filled with H_2 gas. The resulting suspension was stirred for 15 minutes, filtered through Celite, and washed with additional CH_3OH. The resulting solution was concentrated by rotary evaporation to afford Fmoc-(2*R*,3*R*)-hydroxyasparagine-OH as an off-white solid (0.14 g, 83% yield of the unpurified product). ^{1}H NMR (500 MHz, CD_3SOCD_3): δ 7.89 (d, *J* = 7.7 Hz, 2 H), 7.73 (t, *J* = 8.9 Hz, 2 H), 7.47–7.26 (m, 7 H), 6.97 (br s, 1 H), 4.43 (d, *J* = 8.9 Hz, 1 H), 4.37 (s, 1 H), 4.29–4.17 (m, 3 H); (minor rotamer, ca. 15%, partial data): δ 7.64 (d, *J* = 6.8 Hz, Fmoc aromatic CH), 6.39 (d, *J* = 8.1 Hz, carbamate NH), 4.59 (d, *J* = 8.3 Hz, hydroxyAsn CH), 4.41 (s, hydroxyAsn CH), 4.19–4.06 (m, hydroxyAsn CH). ^{13}C NMR (125.7 MHz, CD_3SOCD_3): δ 173.2, 171.9, 156.1, 143.8, 143.7, 140.7, 127.7, 127.2, 127.1, 125.4, 125.4, 120.1, 71.4, 65.9, 56.9, 46.5. HRMS: *m/z*: $[M + Na]^+$ calcd for $C_{19}H_{18}N_2O_6Na^+$ 393.1063, observed 393.1060.

Chemical synthesis of Fmoc-(2*R*,3*S*)-hydroxyAsn.

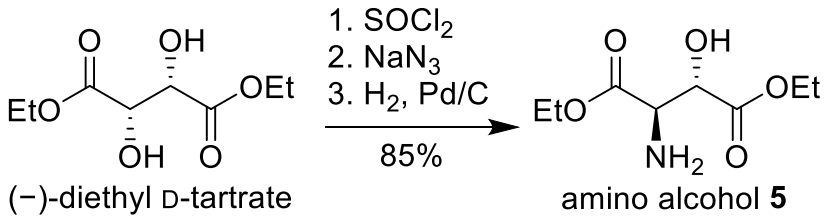

Amino alcohol 5. A 500-mL, single-necked, round-bottom flask equipped with a magnetic stirring bar and a condenser fitted with a nitrogen inlet adapter was charged with a solution of (-)-diethyl-D-tartrate (8.56 mL, 50.00 mmol, 1.0 equiv.) in 250 mL of CH_2Cl_2 (the reaction was run at ca. 0.2 M concentration of the diethyl-D-tartrate). To the solution, $SOCl_2$ (7.25 mL, 100.00 mmol, 2.0 equiv.) was added dropwise, followed by 0.25 mL cat. anhydrous DMF. The reaction mixture was heated to 35 °C and stirred for 2 hours. Then, the solution was cooled to room temperature, and concentrated to dryness by rotary evaporation to afford a cyclic sulfite intermediate as a yellow oil (12.41 g, 98% yield of the unpurified product). The cyclic sulfite was used without further purification.

A 250-mL, single-necked, round-bottom flask equipped with a magnetic stirring bar, a nitrogen inlet adapter, was charged with a solution of the cyclic sulfite intermediate (12.41 g, 49.20 mmol, 1.0 equiv.) in 100 mL of anhydrous DMF (the reaction was run at 0.5 M concentration of the bromo alcohol **1**). NaN_3 (3.99 g, 61.50 mmol, 1.25 equiv.) was added to the solution, and the suspension was stirred for 21 h at 25 °C. The suspension was transferred to a separatory funnel and the round bottom flask was rinsed with 300 mL H_2O. The layers were separated and the aqueous layer was extracted with EtOAc (3 x 200 mL). The combined organic layer was dried over Na_2SO_4, filtered, and dried using rotary evaporation to yield the azide intermediate as a yellow oil (9.96 g, 88% yield of the unpurified product). The azide intermediate was used without further purification.

A 500-mL, three-necked, round-bottom flask equipped with a magnetic stirring bar, a nitrogen inlet adapter, an inlet adapter fitted with a hydrogen balloon, and a rubber septum was charged with a

solution of the crude azide intermediate (9.96 g, 43.10 mmol, 1.0 equiv.) in 140 mL of CH_3OH (the reaction was run at 0.2 M concentration of the azide intermediate). The flask was evacuated and back filled with nitrogen, and 10 % Pd/C (50% wet solid, 4.98 g, one half the mass of the azide intermediate) was added. A balloon containing H_2 gas was fitted to an inlet adapter and the system was evacuated and back filled with H_2 gas. The resulting suspension was stirred for 6 h, filtered through Celite, and washed with 200 mL of additional CH_3OH. The resulting solution was concentrated by rotary evaporation to afford amino alcohol **5** as a yellow oil (8.84 g, 99% yield of the unpurified product). Amino alcohol **5** was used without further purification. An analytical sample was purified by column chromatography on silica gel (elution with 5:95 CH_3OH:CH_2Cl_2) for analysis. ^1H NMR (500 MHz, $CDCl_3$): δ 4.34 (d, J = 3.3 Hz, 1 H), 4.10–3.95 (m, 4 H), 3.75 (d, J = 3.3 Hz, 1 H) 3.75 (broad s, 3 H), 1.18 (m, 6 H). ^{13}C NMR (125.7 MHz, $CDCl_3$): δ 171.86, 171.82, 72.8, 61.5, 61.2, 57.5, 13.95, 13.94. HRMS: *m/z*: $[M + Na]^+$ calcd for $C_8H_{15}NO_5Na^+$ 228.0848, observed 228.0843.

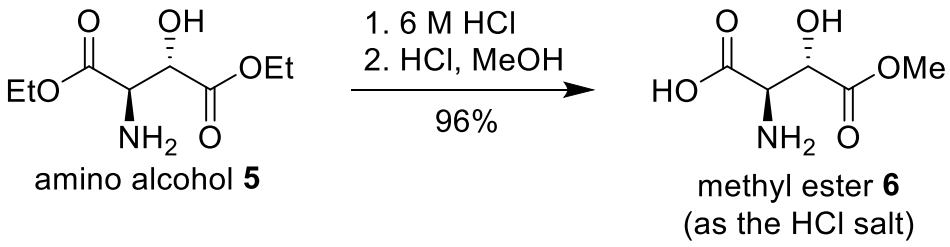

amino alcohol **5**

methyl ester **6**
(as the HCl salt)

Methyl ester 6. A 250-mL, single-necked, round-bottom flask equipped with a magnetic stirring bar and a condenser fitted with a nitrogen inlet adapter was charged with a solution of amino alcohol **5** (8.84 g, 43.10 mmol, 1.0 equiv.) in 200 mL of 6 M HCl (the reaction was run at ca. 0.2 M concentration of the amino alcohol **2**). The mixture was heated in an oil bath and stirred for 16 h at 100 °C, cooled to room temperature, and concentrated to dryness by rotary evaporation to afford a beige solid (7.99 g, 98% yield of the unpurified product). The crude carboxylic acid intermediate was used in the next step without purification.

A 250-mL, single-necked, round-bottom flask equipped with a magnetic stirring bar and a condenser fitted with a nitrogen inlet adapter was charged with a solution of the crude carboxylic acid intermediate (7.99, 43.10 mmol, 1.0 equiv.) in 240 mL of CH_3OH (the reaction was run at ca. 0.2 M concentration of the crude intermediate). The mixture was cooled to 0 °C using an ice bath. A solution of 12 M HCl (8 mL) was then added dropwise to the flask over 10 minutes. The flask was then heated in a preheated water bath at 65 °C for 15 minutes. The mixture was cooled to room temperature and concentrated to dryness by rotary evaporation to afford methyl ester **6** as a beige foam (8.60 g, 98% yield of the unpurified product). Methyl ester **6** was used without further purification. ^{1}H NMR (500 MHz, CD_3OD): (major product, methyl ester **6**, ca. 50% by integration): δ 8.65 (br s, 1 H), 4.67 (d, J = 2.6 Hz, 1 H), 4.46 (d, J = 2.6, 1 H), 3.80 (s, 3 H); (diacid precursor impurity, ca. 44% by integration): δ 4.61 (d, J = 2.5 Hz, 1 H), 4.45 (d, J = 2.5 Hz, 1 H). ^{13}C NMR (125.7 MHz, CD_3OD) (major product, methyl ester **6**): δ 170.49, 166.99, 69.92, 55.27, 51.79; (diacid precursor impurity): δ 171.51, 167.14, 68.83, 55.42. HRMS: *m/z*: $[M + H]^+$ calcd for $C_5H_9NO_5H^+$ 164.0559, observed 164.0558.

NOTE: Running the reaction for 15 minutes minimizes the formation of the dimethyl ester while still allowing a satisfactory yield of the desired monomethyl ester. Under these conditions, there is still a significant amount of the residual diacid precursor, which is observed in the ^{1}H NMR and ^{13}C NMR spectra of the unpurified product. Based on our observation for the preparation monomethyl ester **3** (above) we anticipate that 30 minutes of heating time would lead to a better yield of the desired methyl ester **6**.

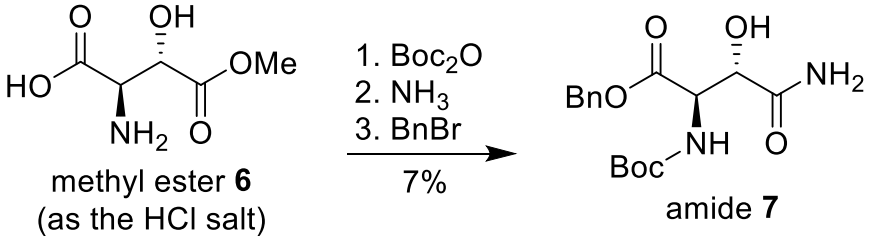

methyl ester **6**
(as the HCl salt)

amide **7**

Amide 7. A 250-mL, single-necked, round-bottom flask equipped with a magnetic stirring bar and fitted with a nitrogen inlet adapter was charged with a solution of methyl ester **6** and the diacid precursor impurity (8.60 g, 43.10 mmol, 1.0 equiv.) in 140 mL of 10 % w/v Na_2CO_3. The solution was cooled to 0 °C using an ice bath. While on ice, a separate solution of Boc_2O (7.51 g, 34.62 mmol, 3.0 equiv.) dissolved in 140 mL dioxane (to give a final concentration of 0.15 M for the methyl ester **6**) was slowly added over 2–3 minutes. The mixture was brought to room temperature, stirred for 19.5 h, and concentrated to dryness using rotary evaporation. The resulting residue was dissolved in 500 mL EtOAc and transferred to a separatory funnel. The mixture was washed with 1 M HCl (3 x 500 mL). The organic layer was dried over Na_2SO_4 and concentrated to a yellow oil. The crude product was purified by column chromatography on silica gel (elution with 10:90 CH_3OH:$CHCl_3$) to afford the Boc-protected intermediate as a yellow oil (1.65 g, 15% yield).

A 125-mL, single-necked, high-pressure flask equipped with a magnetic stirring bar was charged with a solution of the Boc-protected intermediate (1.65 g, 6.27 mmol, 1.0 equiv.) in ca. 20 mL CH_3OH (the reaction was run at ca. 0.3 M concentration of the Boc-protected intermediate). A flow of NH_3 gas was applied through a syringe directly into the solution and bubbled for 20–30 min to ensure saturation with NH_3. The vessel was then capped, and the solution was stirred for 72 h at 25 °C. The solution was concentrated to dryness using rotary evaporation to afford the amide intermediate as a beige solid (1.46 g, 98% yield of the unpurified product). The crude intermediate was used in the next step without further purification.

A 100-mL, single-necked, round-bottom flask equipped with a magnetic stirring bar and fitted with a nitrogen inlet adapter was charged with a solution of the amide intermediate (1.46 g, 3.64 mmol, 1.0 equiv.) in ca. 31 mL of anhydrous DMF (the reaction was run at ca. 0.2 M concentration of the amide intermediate). The solution was cooled to 0 °C using an ice bath, and $NaHCO_3$ (0.76 g, 9.10

mmol, 2.5 equiv.) followed by benzyl bromide (1.73 mL, 14.56 mmol, 4.0 equiv.) was added dropwise over 10 minutes. The mixture was stirred for 2 hours at 0 °C, warmed to room temperature, and stirred for an additional 24 hours under N_2. The resulting solution was cooled again to 0 °C using an ice bath, 75 mL of H_2O was added to quench the reaction. The solution was transferred to a separatory funnel and extracted with EtOAc (3 x 50 mL). The combined organic layer was washed with 50 mL saturated aqueous NaCl, dried with Na_2SO_4, and concentrated to using rotary evaporation. The crude product was then purified by column chromatography on silica gel (elution with 5:95 CH_3OH:CH_3Cl) to afford amide **4** as white solid (1.00 g, 47% yield). ^{1}H NMR (500 MHz, $CDCl_3$): δ 7.42–7.31 (m, 5 H), 6.79 (broad s, 1 H), 5.82 (broad d, *J* = 4.8 Hz, 1 H), 5.62 (broad s, 1 H), 5.54 (broad d, *J* = 6.6 Hz, 1 H), 5.31–5.18 (m, 2 H), 4.72 (broad d, *J* = 5.1 Hz, 1 H), 4.65 (broad d, *J* = 4.5 Hz, 1 H), 1.45 (s, 9 H). ^{13}C NMR (125.7 MHz, $CDCl_3$): δ 173.6, 168.1, 158.2, 135.1, 128.7, 128.7, 128.6, 81.7, 75.0, 68.2, 57.5, 28.3. HRMS: *m/z*: $[M + Na]^+$ calcd for $C_{16}H_{22}N_2O_6Na^+$ 361.1375, observed 361.1371.

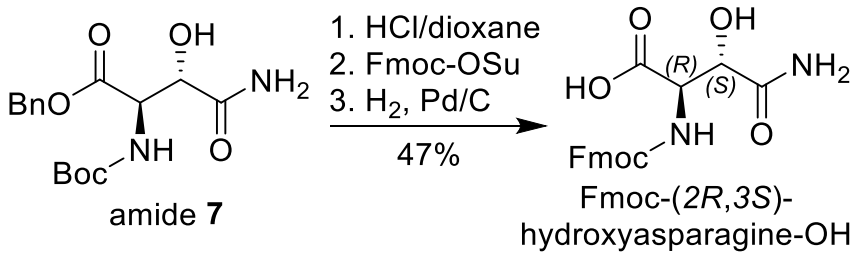

Fmoc-(2*R*,3*S*)-hydroxyasparagine-OH. A 250-mL, single-necked, round-bottom flask equipped with a magnetic stirring bar and fitted with a nitrogen inlet adapter was charged with a solution of the amide **4** (1.00 g, 2.96 mmol, 1.0 equiv.) in ca. 30 mL of 4 N HCl in dioxane. (The reaction was run at ca. 0.1 M concentration of the amide **4**.) The solution was stirred for 2 h and concentrated to dryness by rotary evaporation to a white solid (0.71 g, 99% yield of the unpurified product).

The crude intermediate (0.71 g, 2.98 mmol, 1 equiv.) was dissolved in 52 mL of 1:1 dioxane:water. (The reaction was run at ca. 0.06 M concentration of the crude intermediate). The solution was cooled to 0 °C using an ice bath, and $NaHCO_3$ was added until the solution reached a pH of 6.8. Fmoc-OSu (1.20 g, 3.55 mmol, 1.2 equiv.) was then subsequently added, and mixture was stirred for 1 h on ice, brought to room temperature, and stirred for an additional 18–20 h under N_2. The resulting suspension was diluted with 120 mL EtOAc and 180 mL of saturated $NaHCO_3$ and stirred for ca. 5 min. The solution was transferred to a separatory funnel and the organic layer was collected; the aqueous layer was then extracted with EtOAc (2 x 80 mL). The combined organic layer was then dried with Na_2SO_4 and concentrated by rotary evaporation to a white solid. The crude product was then purified by column chromatography on silica gel (elution with 5:95 CH_3OH:CH_3Cl) to afford the Fmoc-protected intermediate as a white solid (1.07 g, 79% yield).

A 250-mL, three-necked, round-bottom flask equipped with a magnetic stirring bar, a nitrogen inlet adapter, an inlet adapter fitted with a hydrogen balloon, and a rubber septum was charged with a

solution of the Fmoc-protected intermediate (1.07 g, 2.32 mmol, 1 equiv.) from the previous step in ca. 55 mL of anhydrous CH_3OH. (The reaction was run at 0.05 M concentration of the Fmoc-protected intermediate assuming 100 % conversion). The flask was evacuated and back filled with nitrogen, and ca. 10 % Pd/C (50% wet solid, one half the mass of the Fmoc-protected intermediate, 0.5 g) was added. A balloon containing H_2 gas was fitted to an inlet adapter and the system was evacuated and back filled with H_2 gas. The resulting suspension was stirred for 24 h, filtered through Celite, and washed with additional CH_3OH. The resulting solution was concentrated by rotary evaporation to afford Fmoc-(2*R*,3*S*)-hydroxyasparagine-OH as an off-white solid (0.51 g, 60% yield of the unpurified product). ^{1}H NMR (500 MHz, CD_3SOCD_3): δ 7.89 (d, *J* = 7.5 Hz, 2 H), 7.77–7.69 (m, 2 H), 7.47–7.28 (m, 7 H), 7.03 (d, *J* = 9.5 Hz, 1 H), 4.47 (dd, *J* = 9.5, 2.1 Hz, 1 H), 4.37 (d, *J* = 2.0 Hz, 1 H), 4.26–4.19 (m, 3 H); (minor rotamer, ca. 16%, partial data): δ 7.63 (d, *J* = 7.2 Hz, Fmoc aromatic CH), 6.44 (d, *J* = 9.5 Hz, carbamate NH), 4.64 (d, *J* = 9.4 Hz, hydroxyAsn CH), 4.42 (s, hydroxyAsn CH), 4.14–4.04 (m, hydroxyAsn CH). ^{13}C NMR (125.7 MHz, CD_3SOCD_3): δ 173.2, 171.9, 156.1, 143.8, 143.7, 140.7, 127.7, 127.17, 127.13, 125.43, 125.36, 120.1, 71.4, 65.9, 56.9, 46.5. HRMS: *m/z*: $[M + Na]^+$ calcd for $C_{19}H_{18}N_2O_6Na^+$ 393.1063, observed 393.1073.

Synthesis of Novo29 and *epi*-Novo29 [6]

Peptide synthesis procedure. Novo29 and *epi*-Novo29 were synthesized by manual solid-phase peptide synthesis of the corresponding linear peptide on 2-chlorotrityl resin, followed by on-resin esterification, solution-phase cyclization, deprotection, and purification. A step-by-step procedure is detailed below.

a. Loading the resin. 2-Chlorotrityl chloride resin (300 mg, 1.07 mmol/g) was added to a Bio-Rad Poly-Prep chromatography column (10 mL). Dry CH_2Cl_2 (8 mL) was used to suspend and swell

the resin for 30 min with gentle rocking. After the solution was drained from the resin, a separate solution of Fmoc-Leu-OH (75 mg, 0.7 equiv., 0.21 mmol) in 6% (v/v) 2,4,6-collidine in dry CH_2Cl_2 (8 mL) was added and the suspension was gently rocked for 5–6 h. The solution was then drained, and a mixture of CH_2Cl_2/ CH_3OH /*N*,*N*-diisopropylethylamine (DIPEA) (17:2:1, 8 mL) was added immediately. The resin was gently rocked for 1 h, to cap the unreacted 2-chlorotrityl chloride resin sites. The resin was then washed three times with dry CH_2Cl_2 and dried by passing nitrogen through the vessel. This procedure typically yields 0.15–0.20 mmol of loaded resin, as assessed by spectrophotometric analysis.

b. Manual peptide coupling. The loaded resin was suspended in dry DMF and then transferred to a solid-phase peptide synthesis vessel. Residues 6 through 1 were manually coupled using Fmoc-protected amino acid building blocks. The coupling cycle consisted of *i*. Fmoc-deprotection with of 20% (v/v) piperidine in DMF (5 mL) for 5–10 min at room temperature, *ii*. washing with dry DMF (4 x 5 mL), *iii*. coupling of the amino acid (4 equiv.) with HCTU (4 equiv.) in 20% (v/v) 2,4,6-collidine in dry DMF (5 mL) for 20–30 min, and *iv.* washing with dry DMF (4 x 5 mL). The last amino acid coupling of the linear sequence is Boc-Phe-OH, which intentionally protects the *N*-terminus from being reactive during the esterification step and cyclization steps. The resin was then transferred to a clean Bio-Rad PolyPrep chromatography column.

c. *Esterification.* In a test tube, Fmoc-Leu-OH (10 equiv.) and diisopropylcarbodiimide (10 equiv.) were dissolved in dry CH_2Cl_2 (5 mL). The resulting solution was filtered through a 0.20-μm nylon filter, and 4-dimethylaminopyridine (1 equiv.) was added to the filtrate. The resulting solution was transferred to the resin and gently agitated for 1 h. The solution was then drained, and the resin was washed with dry CH_2Cl_2 (3 x 5 mL) and DMF (3 x 5 mL).

d. *Fmoc deprotection of Leu$_8$*. The Fmoc protecting group on Leu$_8$ was removed by adding 20% (v/v) piperidine in DMF for 30 min. The solution was drained, and the resin was washed with dry DMF (3 x 5 mL) and CH_2Cl_2 (3 x 5 mL).

e. *Cleavage of the linear peptide from chlorotrityl resin*. The linear peptide was cleaved from the resin by rocking the resin in a solution of 20% (v/v) 1,1,1,3,3,3-hexafluoroispropanol (HFIP) in CH_2Cl_2 (8 mL) for 1 h. The suspension was filtered, and the filtrate was collected in a 250-mL round-bottomed flask. The resin was washed with additional cleavage solution (8 mL) for 30 min and filtered into the same 250 mL round bottom-bottomed flask. The combined filtrates were concentrated by rotary evaporation and further dried by vacuum pump to afford the crude protected linear peptide, which was cyclized without further purification.

d. *Cyclization of the linear peptide*. The crude protected linear peptide was dissolved in dry DMF (125 mL). HOAt (6 equiv.) and HATU (6 equiv.) were dissolved in 8 mL of dry DMF in a test tube to which 300 µL of diisopropylethylamine was added and the solution mixed until homogenous. The solution was then added to the round-bottom flask containing the dissolved peptide and the mixture was stirred under nitrogen at room temperature for 16–20 h. The reaction mixture was concentrated by rotary evaporation and further dried by vacuum pump to afford the crude protected cyclized peptide, which was immediately subjected to global deprotection.

e. Global deprotection of the cyclic peptide. The protected cyclic peptides were dissolved in TFA:triisopropylsilane (TIPS):H_2O (18:1:1, 10 mL) in a 1000-mL round-bottomed flask equipped with a stir bar. The solution was stirred for 1 h under nitrogen. During the 1 h deprotection, two 50-mL conical tubes containing 40 mL of dry Et_2O each were chilled on ice. After the 1 h deprotection, the peptide solution was split between the two conical tubes of Et_2O. The tubes were then centrifuged at 600x*g* for 10 min, decanted, and washed with fresh Et_2O. This process of decanting and washing

was repeated for two more times. The pelleted peptides were dried under nitrogen for 15–20 min. The deprotected cyclic peptide was then purified by reverse-phase HPLC (RP-HPLC).

f. Reverse-phase HPLC purification. The peptide was dissolved in 20% CH_3CN in H_2O (5 mL) and pre-purified on a Biotage Isolera One flash chromatography instrument equipped with a Biotage® Sfär Bio C18 D - Duo 300 Å 20 µm 25 g column. The solution of crude cyclic peptide was injected at 20% CH_3CN and eluted with a gradient of 20–50% CH_3CN. After this purification step Novo29 precipitated out of solution. The fractions containing the pure peptide were lyophilized. For *epi*-Novo29 the fractions containing the desired peptide were concentrated by rotary evaporation, diluted in 20% CH_3CN, injected on a Rainin Dynamax instrument, and eluted over a gradient of 20–40% CH_3CN over 90 min. The collected fractions were analyzed by analytical HPLC and MALDI-TOF, and the pure fractions were concentrated by rotary evaporation and lyophilized. These procedures typically yielded 5 mgs of synthetic peptides (Novo29 or *epi*-Novo29) as the TFA salts.

NMR spectroscopic studies of natural Novo29, synthetic Novo29, and *epi*-Novo29[7]

Sample Preparation. NMR spectroscopic studies of natural Novo29 and synthetic peptides were performed in DMSO-d_6. The solutions were prepared gravimetrically by dissolving a weighed portion of the peptide in the appropriate volume of solvent.

TOCSY and NOESY Data Collection. NMR spectra were recorded on a Bruker 600 MHz spectrometer with a Bruker CBBFO helium-cooled cryoprobe. TOCSY spectra were recorded with 2048 points in the *f*2 dimension and either 512 increments in the *f*1 dimension with NS = 8 and a 150-ms spin-lock mixing time. NOESY spectra were recorded with 2048 points in the *f*2 dimension and 512 increments in the *f*1 dimension with NS = 8 and a 200-ms mixing time.

TOCSY and NOESY Data Processing. NMR spectra were processed with Bruker TopSpin software. Automatic baseline correction was applied in both dimensions after phasing the spectra. 2D TOCSY and NOESY spectra were Fourier transformed to a final matrix size of 1024 x 1024 real points using a Qsine weighting function and forward linear prediction in the *f*1 dimension.

MIC assays[8]

Preparing the peptide stocks. Solutions of natural Novo29, synthetic Novo29, and *epi*-Novo29 were prepared gravimetrically by dissolving an appropriate amount of peptide in an appropriate volume of sterile DMSO to make 1 mg/mL stock solutions. The stock solutions were stored at -20 °C for subsequent experiments.

Preparation and tray setup. Bacillus subtilis (ATCC 6051), *Staphylococcus epidermidis* (ATCC 14990), and *Escherichia coli* (ATCC 10798) were cultured from glycerol stocks in Mueller-Hinton broth overnight in a shaking incubator at 37 °C. An aliquot of the 1 mg/mL antibiotic stock solutions were diluted to make a 64 μg/mL solution with Mueller-Hinton broth. A 200-μL aliquot of the 64 μg/mL solution was transferred to a 96-well plate. Two-fold serial dilutions were made with media across a 96-well plate to achieve a final volume of 100 μL in each well. These solutions had the following concentrations: 64, 32, 16, 8, 4, 2, 1, 0.5, 0.25, 0.125, and 0.0625 μg/mL. The overnight cultures of each bacterium were diluted with Mueller-Hinton broth to an OD_{600} of 0.075 as measured for 200 μL in a 96-well plate. The diluted mixture was further diluted to 1×10^6 CFU/mL with the appropriate media. A 100-μL aliquot of the 1×10^6 CFU/mL bacterial solution was added to each well in 96-well plates, resulting in final bacteria concentrations of 5×10^5 CFU/mL in each well. As 100 μL of bacteria were added to each well, natural Novo29, synthetic Novo29 and *epi*-Novo29 were also diluted to the following concentrations: 32, 16, 8, 4, 2, 1, 0.5, 0.25, 0.125, 0.0625, and 0.03125 μg/mL.

The plate was covered with a lid and incubated at 37 °C for 16 h. The optical density measurements were recorded at 600 nm and were measured using a 96-well UV/vis plate reader (MultiSkan GO, Thermo Scientific). The MIC values were taken as the lowest concentration that had no bacteria growth. Each MIC assay was run in triplicate in three independent runs to ensure reproducibility.

X-ray crystallography of *epi*-Novo29[9]

Crystallization of epi-Novo29. The hanging-drop vapor-diffusion method was used to determine initial crystallization conditions for *epi*-Novo29. Each peptide was screened in 96-well plate format using three crystallization kits (Crystal Screen, Index, and PEG/ION) from Hampton Research. A TTP LabTech Mosquito nanondisperse was used to make three 150 nL hanging drops for each well condition. The three hanging drops differed in the ratio of peptide to well solution for each condition in the 96-well plate. A 10 mg/mL solution of *epi*-Novo29 peptide in deionized water was combined with a well solution in ratios of 1:1, 1:2, and 2:1 peptide:well solution at appropriate volumes to create the three 150 nL hanging drops. Crystals of *epi*-Novo29 grew in well conditions of 2.8 M sodium acetate at pH 7.0.

Crystallization conditions for *epi*-Novo29 were optimized using a 4 x 6 matrix Hampton 24-well plate. For the *epi*-Novo29, the pH of the buffer was varied in each row (6.5, 6.6, 6.8, and 7.0). The concentration of sodium acetate in each column was varied in increments of 0.2 M (2.2, 2.4, 2.6, 2.8, 3.0, 3.2). Three hanging-drops were prepared on borosilicate glass slides by combing a 10 mg/mL solution of *epi*-Novo29 in deionized water with the well solution in the following amounts: 1 μL:1 μL, 2 μL:1 μL, and 1 μL:2 μL. Slides were inverted and pressed firmly against the silicone grease surrounding each well. Crystals were harvested with a nylon loop attached to a copper or steel pin, and flash frozen in liquid nitrogen prior to data collection. A single crystal was soaked in a mixture of potassium iodide (KI) and well solution to incorporate iodide heavy atoms into the lattice. A higher

resolution data set was subsequently collected from crystals grown in similar conditions and collected on a synchrotron X-ray source. The final optimized crystallization condition for *epi*-Novo29 is summarized in Tables S2 and S3.

Data collection, data processing, and structure determination. Diffraction data for the *epi*-Novo29 peptide were collected at the Advanced Light Source at Lawrence Berkeley National Laboratory with a synchrotron source at 1.0-Å wavelength beamline 5.0.2 up to a resolution of 1.13 Å. The dataset was indexed and integrated with XDS and scaled and merged with pointless and aimless. The crystallographic phase determination was done with Phaser. The structure was refined using phenix.refine, with manipulation of the model performed using Coot. Data collection and refinement statistics are shown Tables S2 and S3.

References

1. Gao, B.; Sharpless, K. B. Vicinal diol cyclic sulfates. Like epoxides only more reactive. *J. Am. Chem. Soc.* **1988**, *110*, 7538–7539.

2. He, L.; Byun, H.S.; Bittman, R. Efficient synthesis of chiral α,β-epoxyesters via a cyclic sulfate intermediate. *Tetrahedron Lett.* **1998**, *39*, 2071–2074.

3. France, B.; Bruno, V.; Nicolas, I. Synthesis of a protected derivative of (2R,3R)-β-hydroxyaspartic acid suitable for Fmoc-based solid phase synthesis. *Tetrahedron Lett.* **2013**, *54,* 158–161.

4. Guzmán-Martinez; A.; Vannieuwenhze, M. S. An Operationally Simple and Efficient Synthesis of Orthogonally Protected L-threo-beta-Hydroxyasparagine. *Synlett* **2007**, *10*, 1513–1516.

5. Liu, L.; Wang, B.; Bi, C.; He, G.; Chen, G. Efficient preparation of β-hydroxy aspartic acid and its derivatives. *Chin. Chem. Lett.* **2018**, *29*, 1113–1115.

6. The procedure for peptide synthesis follow closely to those that our laboratory has previously published. The procedures in this section were either adapted from or taken verbatim from: Yang, H.; Du Bois, D. R.; Ziller, J. W.; Nowick, J. S. X-ray crystallographic structure of a teixobactin analogue reveals key interactions of the teixobactin pharmacophore. *Chem. Commun*. **2017**, *53*, 2772–2775.

7. General procedures for NMR spectroscopy were either adapted from or taken verbatim from: Li, X.; Rios, S. E.; Nowick, J. S. Enantiomeric β-sheet peptides from Aβ form homochiral pleated β-sheets rather than heterochiral rippled β-sheets. *Chem. Sci.* **2022**, *13*, 7739–7746.

8. General procedures for minimum inhibitory concentration assays were either adapted from or taken verbatim from: Morris, M. A.; Malek, M.; Hashemian, M. H.; Nguyen, B. T.; Manuse, S.; Lewis, K. L; Nowick, J. S. A Fluorescent Teixobactin Analogue. *ACS Chem. Biol.* **2020**, *15*, 1222–1231.

9. General procedures for X-ray crystallography were either adapted from or taken verbatim from: Li, X.; Sabol, A. L.; Wierzbicki, M.; Salveson, P. J.; Nowick, J. S. An improved turn structure for inducing β-hairpin formation in peptides. *Angew. Chem. Int. Ed.* **2021**, *60*, 22776–22782 and Samdin, T. D.; Wierzbicki, M.; Kreutzer, A. G.; Howitz, W. J.; Valenzuela, M.; Smith, A.; Sahrai, V.; Truex, N. L.; Klun, M.; Nowick, J. S. Effects of N-terminal residues on the assembly of constrained β-hairpin peptides derived from Aβ. *J. Am. Chem. Soc.* **2020**, *142*, 11593–11601.

Characterization Data

Characterization of natural Novo29

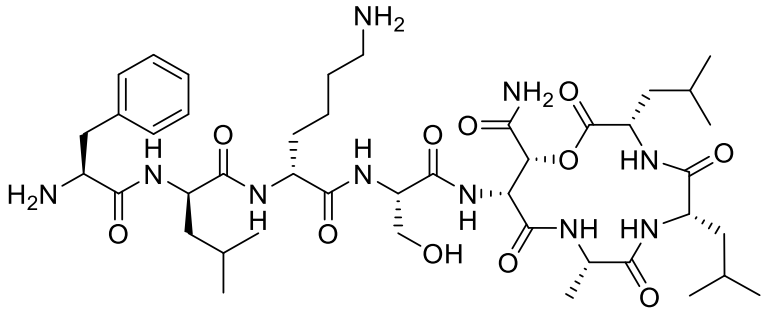

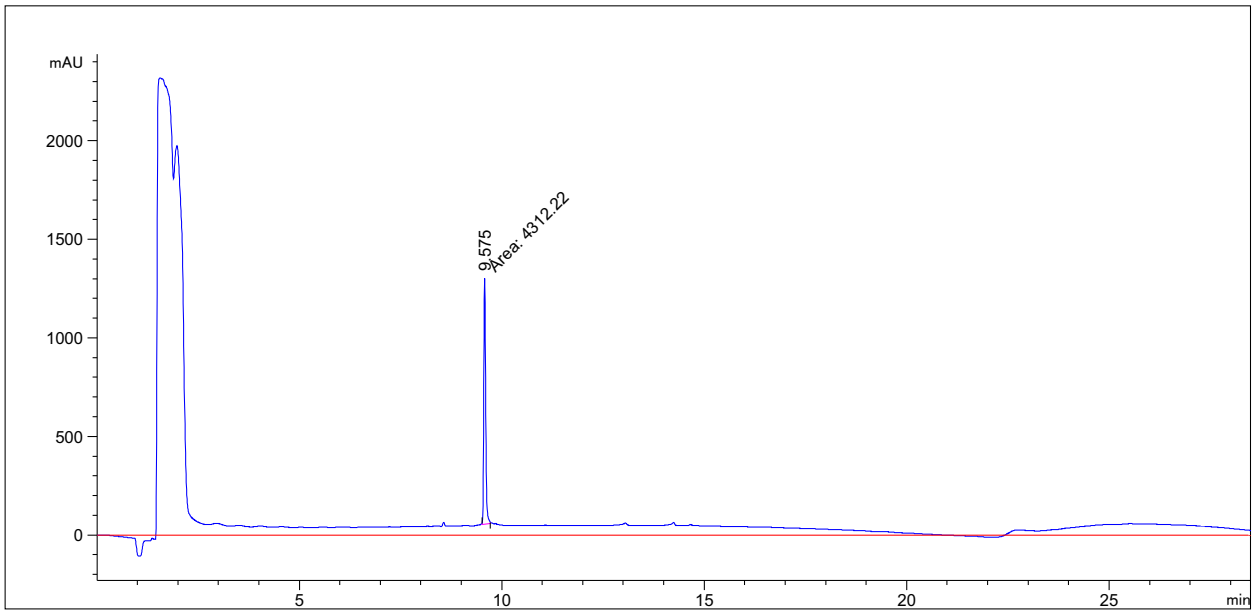

Signal 1: MWD1 A, Sig=214,4 Ref=off

Peak #	RetTime [min]	Type	Width [min]	Area [mAU*s]	Height [mAU]	Area %
1	9.575	MM	0.0569	4312.21582	1262.37280	100.0000

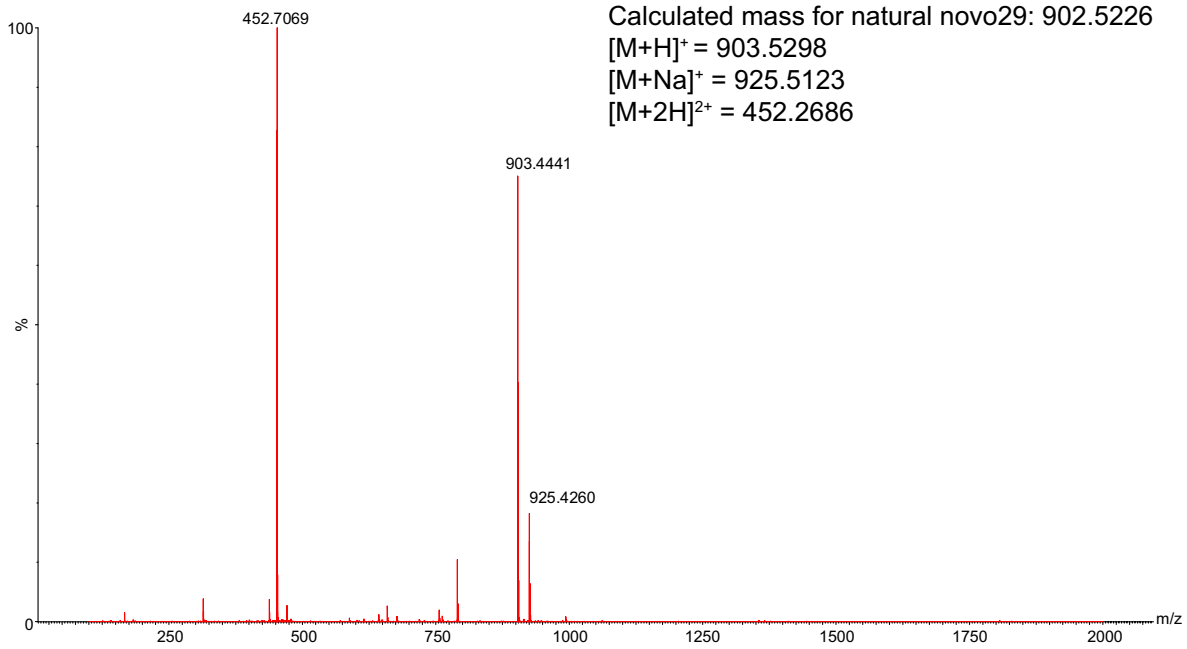
Calculated mass for natural novo29: 902.5226
[M+H]+ = 903.5298
[M+Na]+ = 925.5123
[M+2H]2+ = 452.2686
452.7069
903.4441
925.4260
100
%
0
250
500
750
1000
1250
1500
1750
2000
m/z

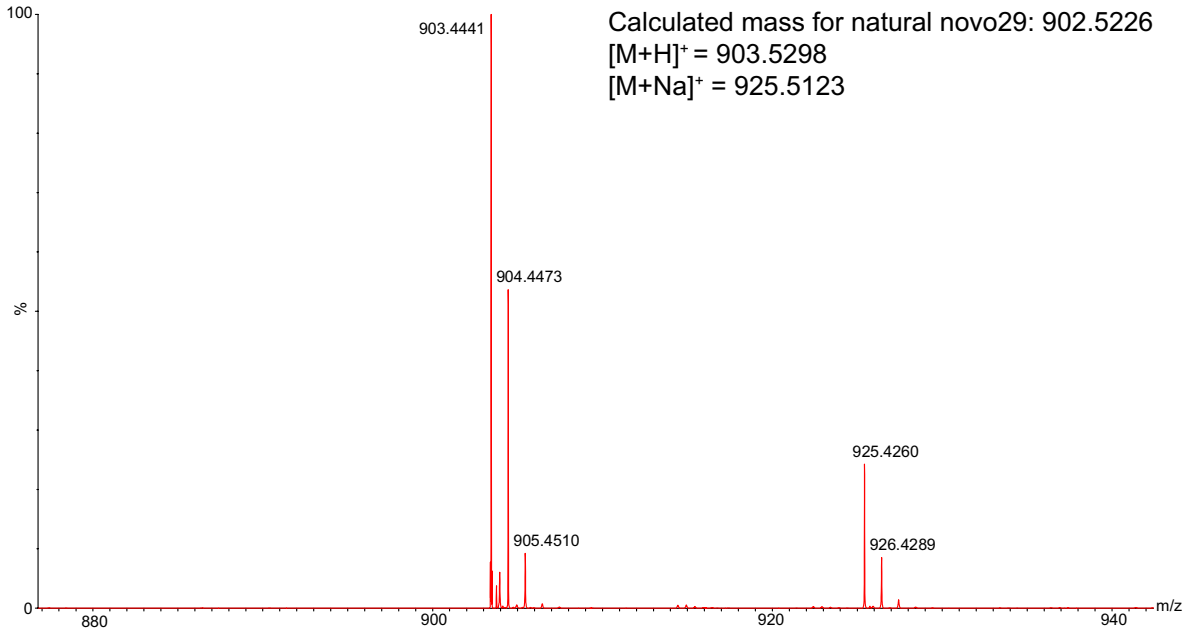
Calculated mass for natural novo29: 902.5226
[M+H]+ = 903.5298
[M+Na]+ = 925.5123
903.4441
904.4473
925.4260
905.4510
926.4289
100
%
0
880
900
920
940
m/z

Characterization of synthetic Novo29

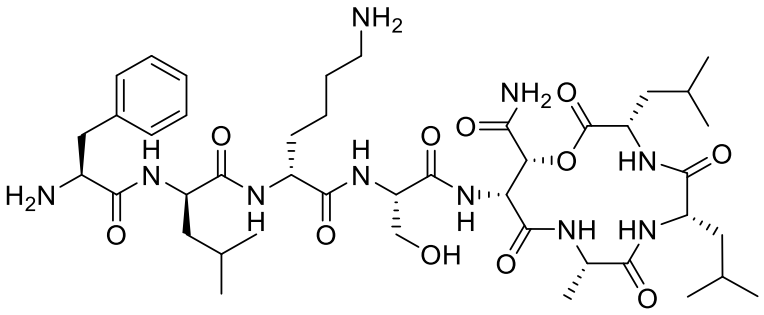

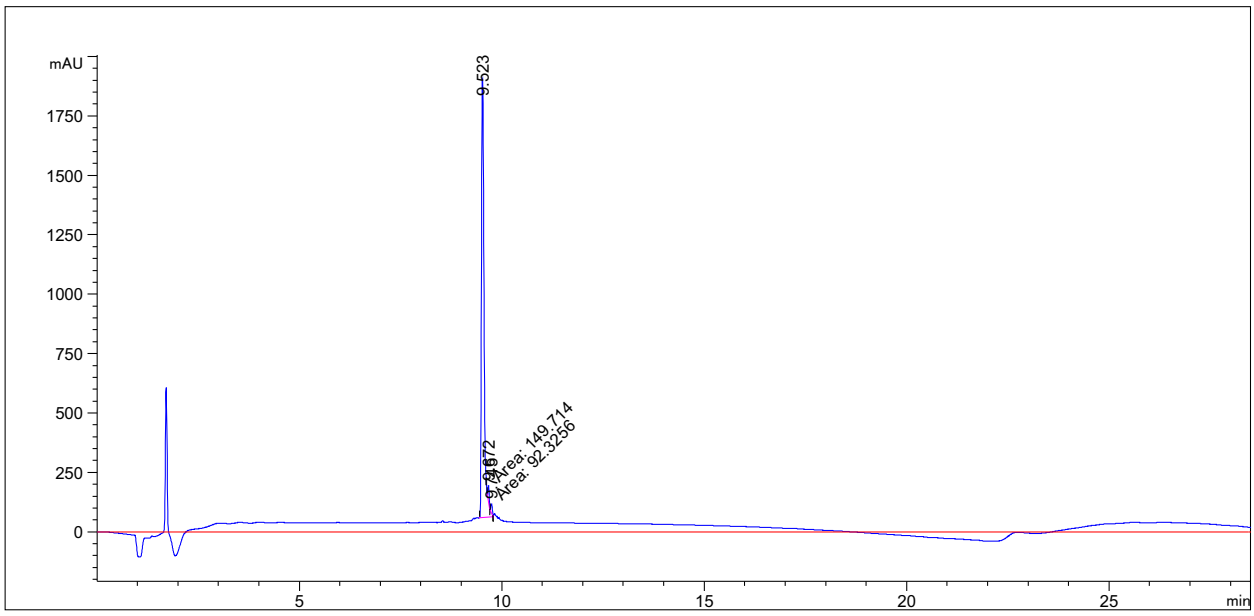

Signal 1: MWD1 A, Sig=214,4 Ref=off

Peak #	RetTime [min]	Type	Width [min]	Area [mAU*s]	Height [mAU]	Area %
1	9.523	MM R	0.0728	8129.04150	1861.80823	97.1086
2	9.672	MM T	0.0363	149.71405	68.68908	1.7885
3	9.745	MM T	0.0403	92.32558	38.15857	1.1029

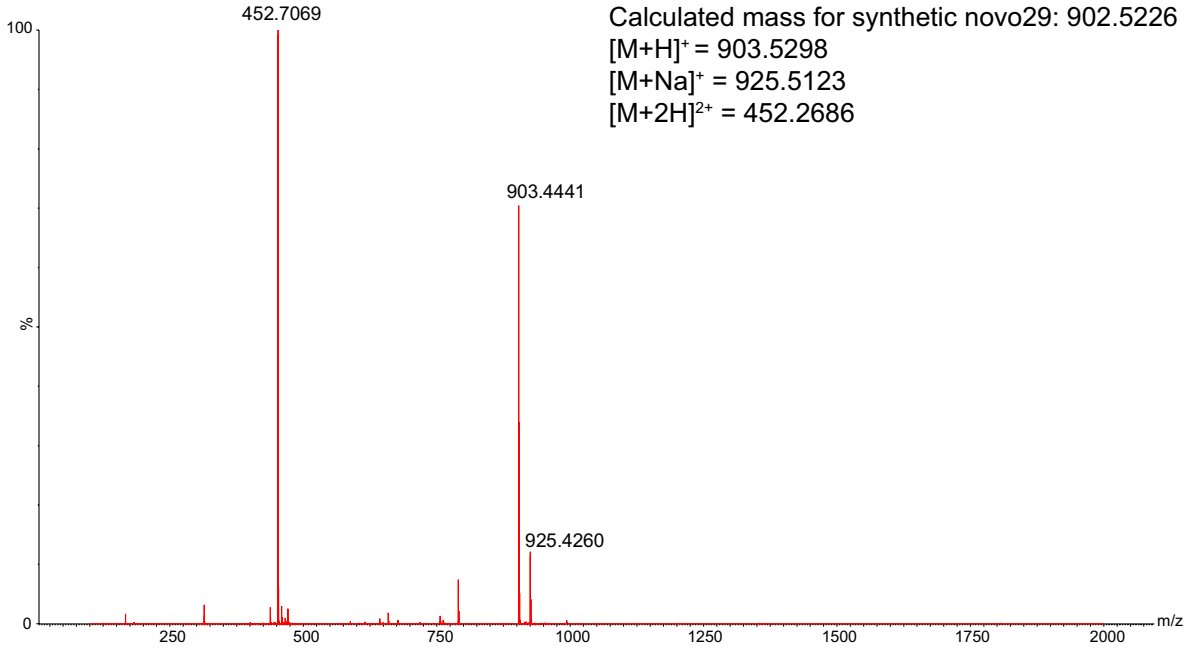
452.7069
903.4441
925.4260
100
%
0
250
500
750
1000
1250
1500
1750
2000
m/z
Calculated mass for synthetic novo29: 902.5226
[M+H]+ = 903.5298
[M+Na]+ = 925.5123
[M+2H]2+ = 452.2686

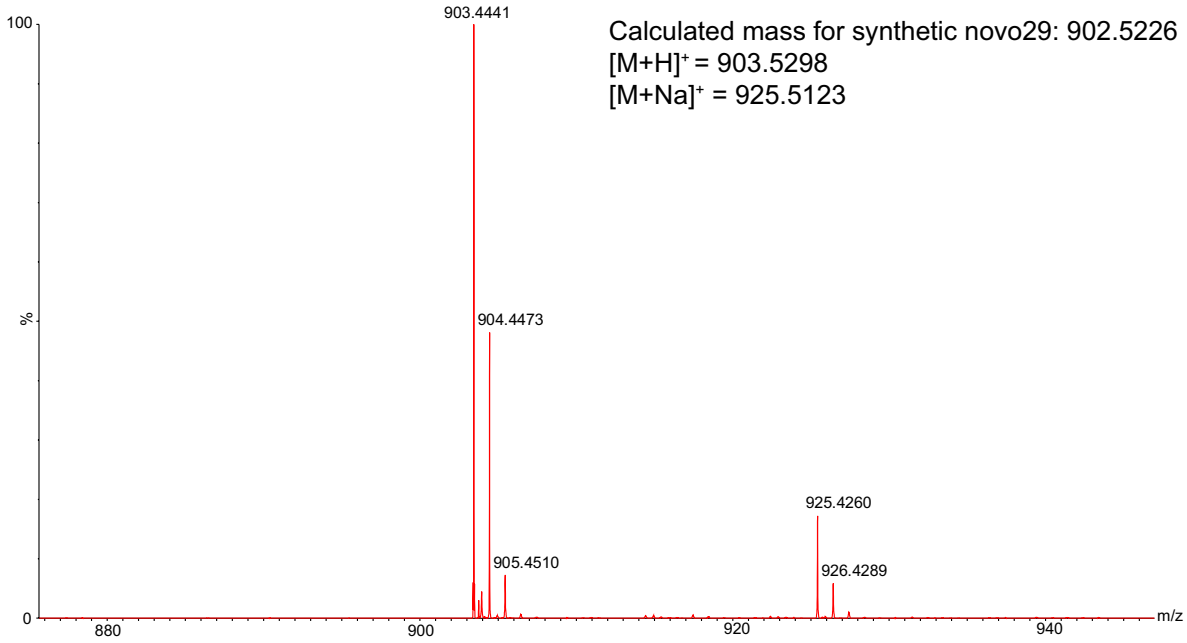
903.4441
904.4473
925.4260
905.4510
926.4289
100
%
0
880
900
920
940
m/z
Calculated mass for synthetic novo29: 902.5226
[M+H]+ = 903.5298
[M+Na]+ = 925.5123

Characterization of synthetic epi-Novo29

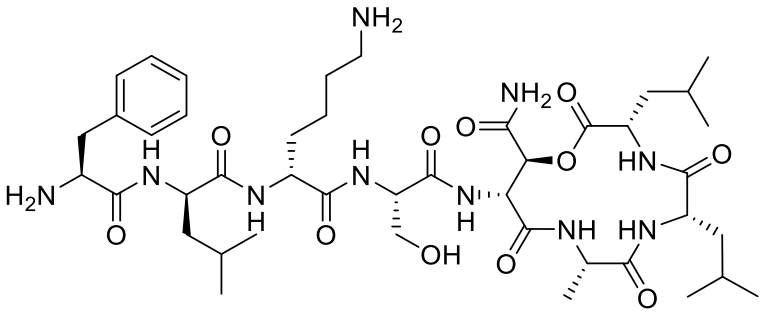

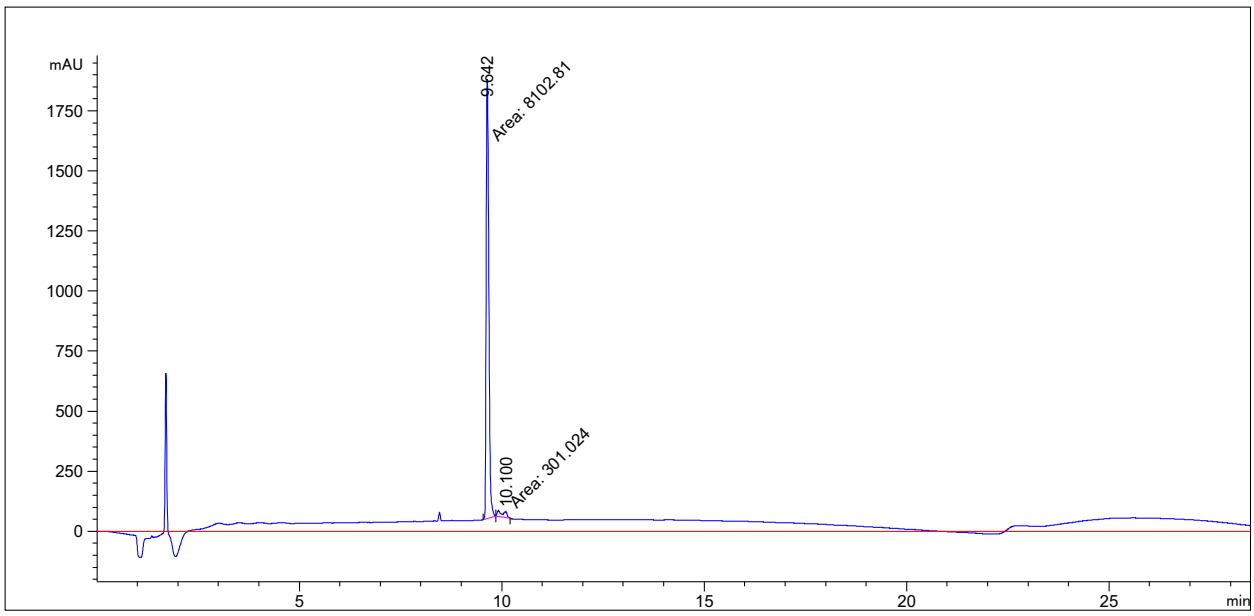

Signal 1: MWD1 A, Sig=214,4 Ref=off

Peak #	RetTime [min]	Type	Width [min]	Area [mAU*s]	Height [mAU]	Area %
1	9.642	MM	0.0735	8102.80859	1836.76953	96.4180
2	10.100	MM	0.2067	301.02429	24.26878	3.5820

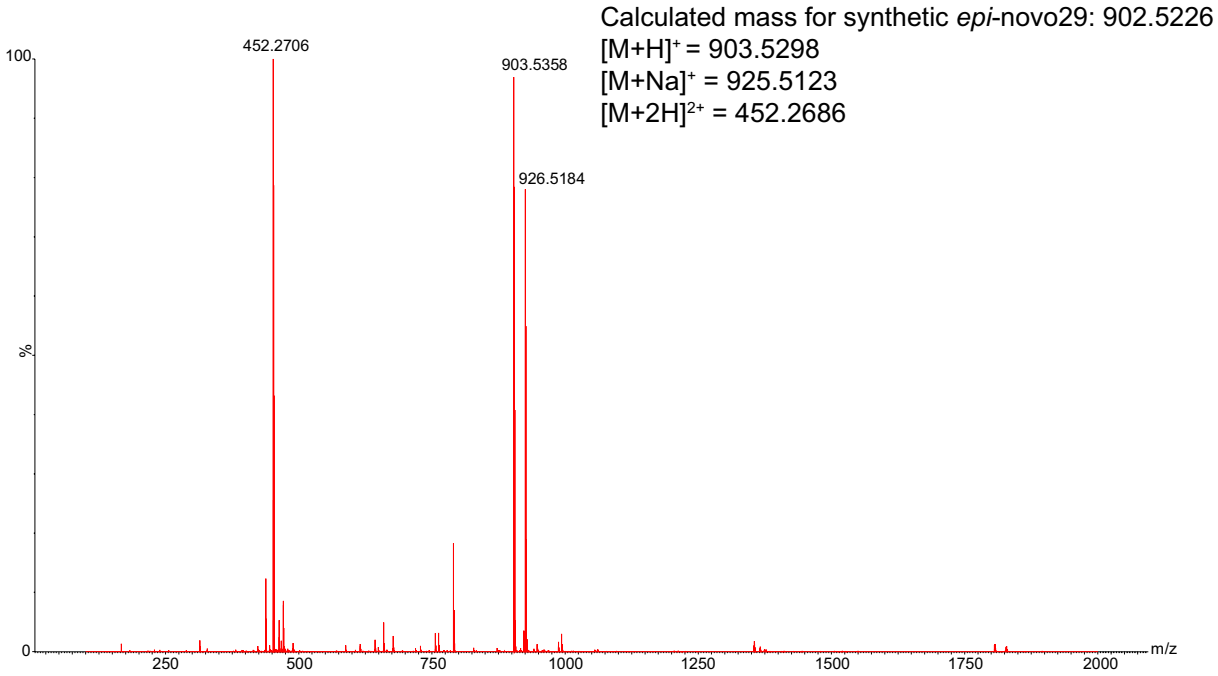
Calculated mass for synthetic *epi*-novo29: 902.5226
[M+H]+ = 903.5298
[M+Na]+ = 925.5123
[M+2H]2+ = 452.2686
452.2706
903.5358
926.5184
100
%
0
250
500
750
1000
1250
1500
1750
2000
m/z

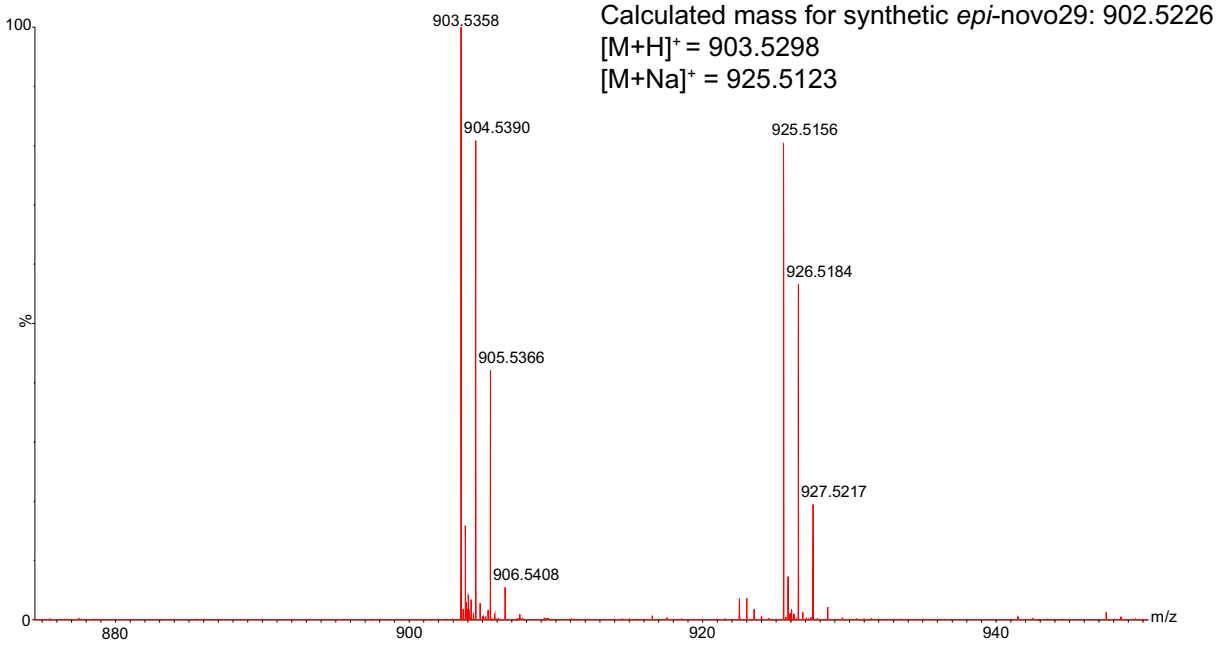
Calculated mass for synthetic *epi*-novo29: 902.5226
[M+H]+ = 903.5298
[M+Na]+ = 925.5123
903.5358
904.5390
925.5156
926.5184
905.5366
927.5217
906.5408
100
%
0
880
900
920
940
m/z

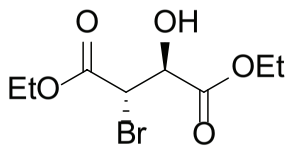

bromo alcohol **1**

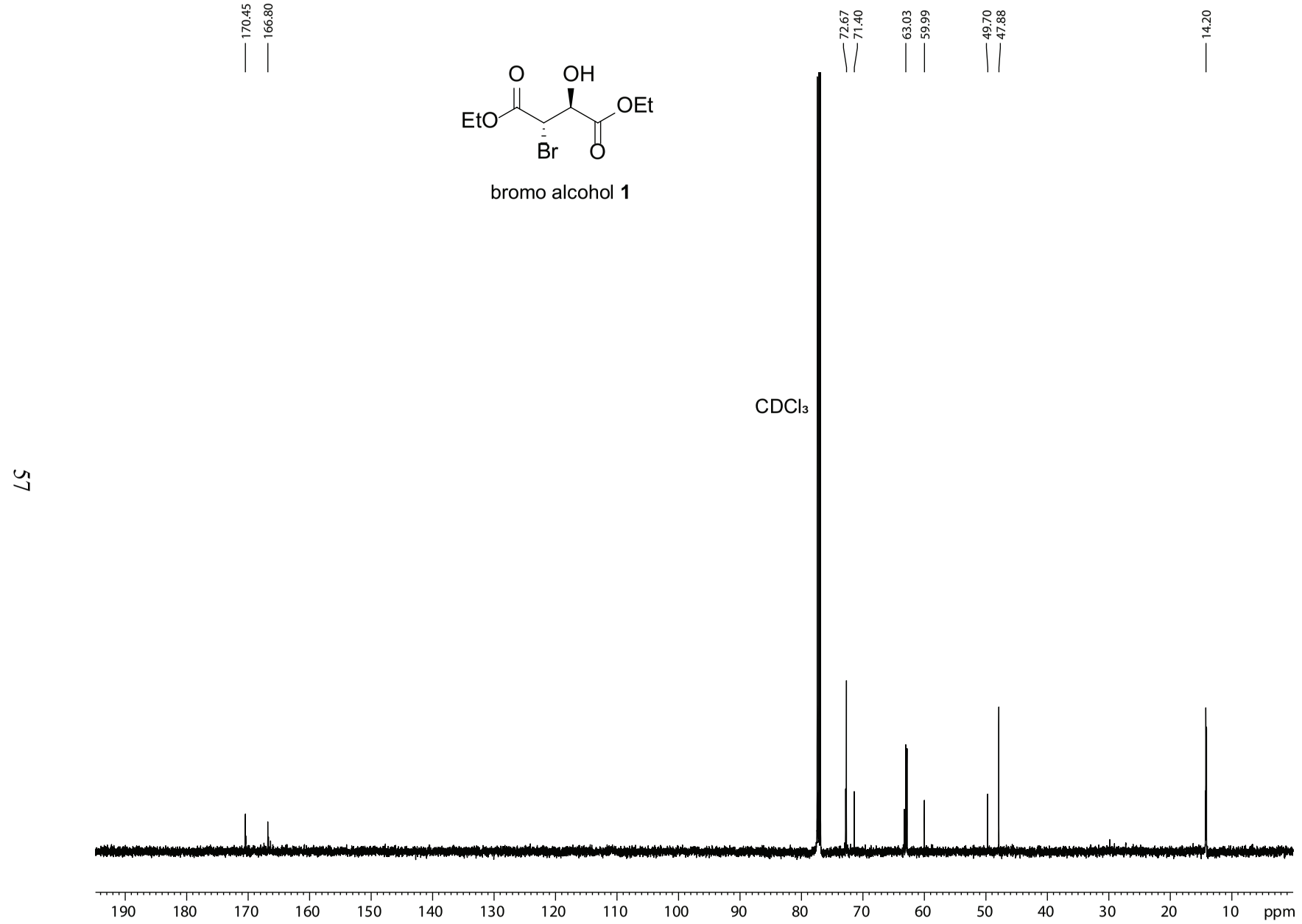
170.45
166.80
72.67
71.40
63.03
59.99
49.70
47.88
14.20
O
OH
EtO
OEt
Br
O
bromo alcohol 1
CDCl3
190
180
170
160
150
140
130
120
110
100
90
80
70
60
50
40
30
20
10
ppm

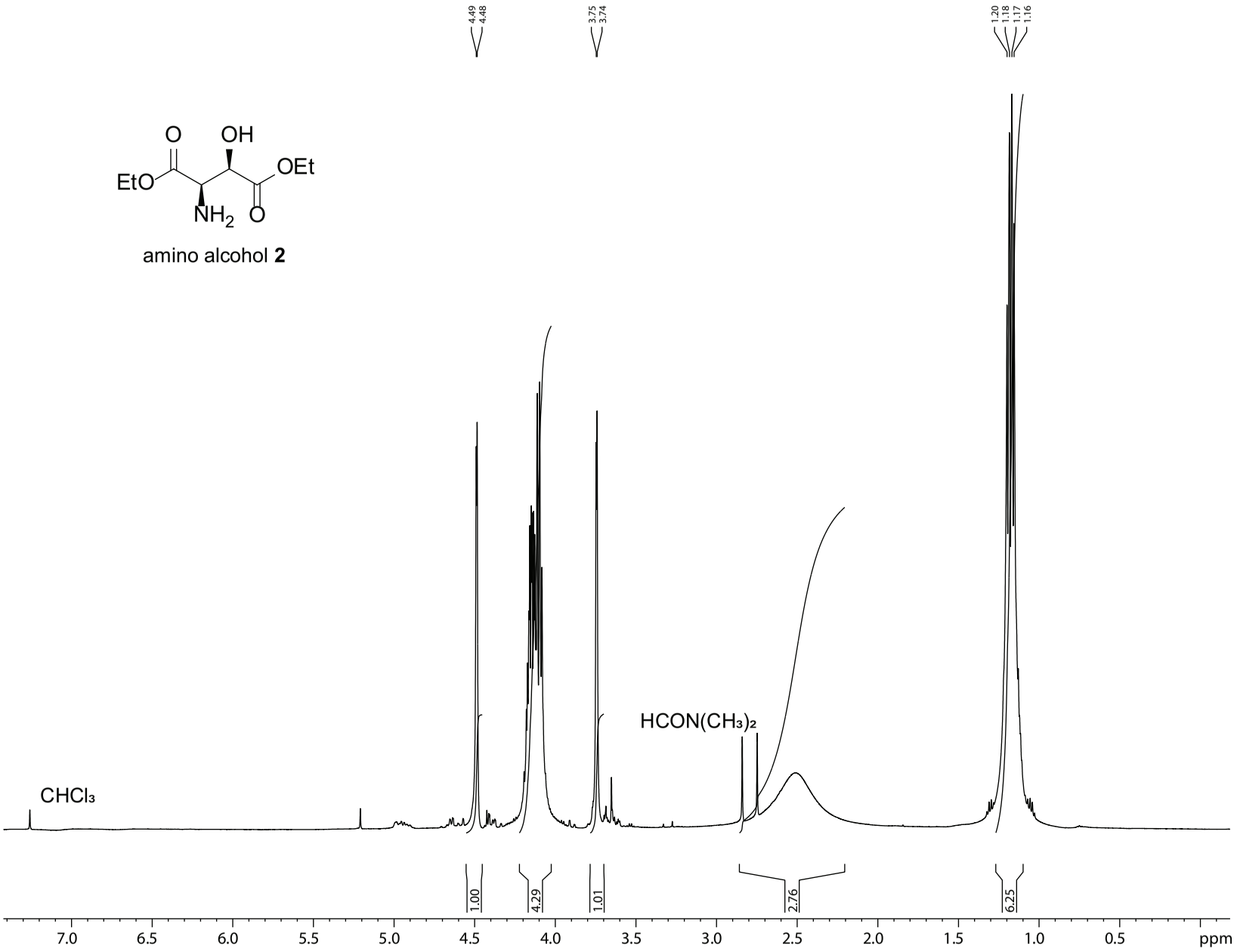
4.49
4.48
3.75
3.74
1.20
1.18
1.17
1.16
O
OH
EtO
OEt
NH2
O
amino alcohol 2
CHCl3
HCON(CH3)2
1.00
4.29
1.01
2.76
6.25
7.0
6.5
6.0
5.5
5.0
4.5
4.0
3.5
3.0
2.5
2.0
1.5
1.0
0.5
ppm

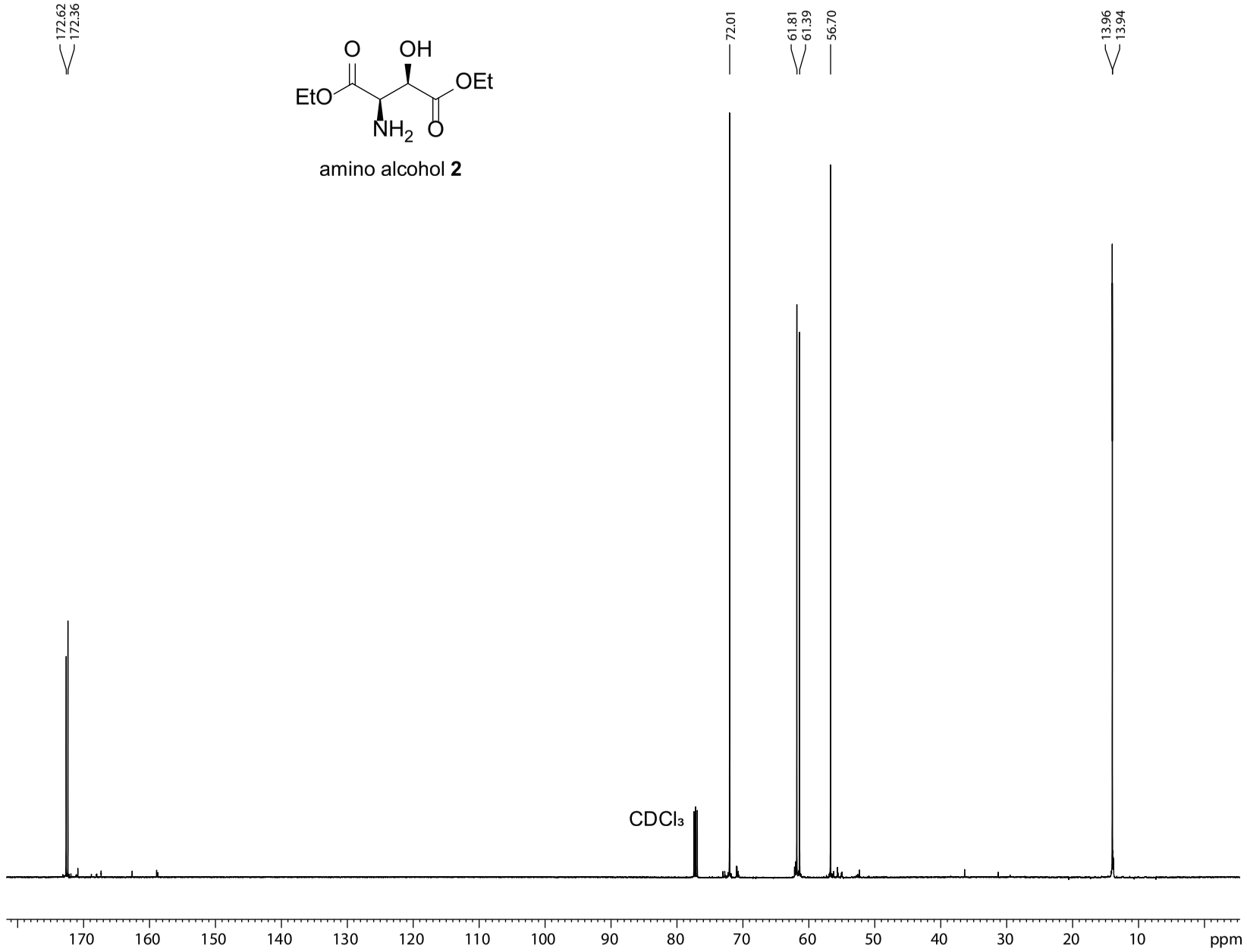
172.62
172.36
72.01
61.81
61.39
56.70
13.96
13.94
O
OH
EtO
OEt
NH2
O
amino alcohol 2
CDCl3
170
160
150
140
130
120
110
100
90
80
70
60
50
40
30
20
10
ppm

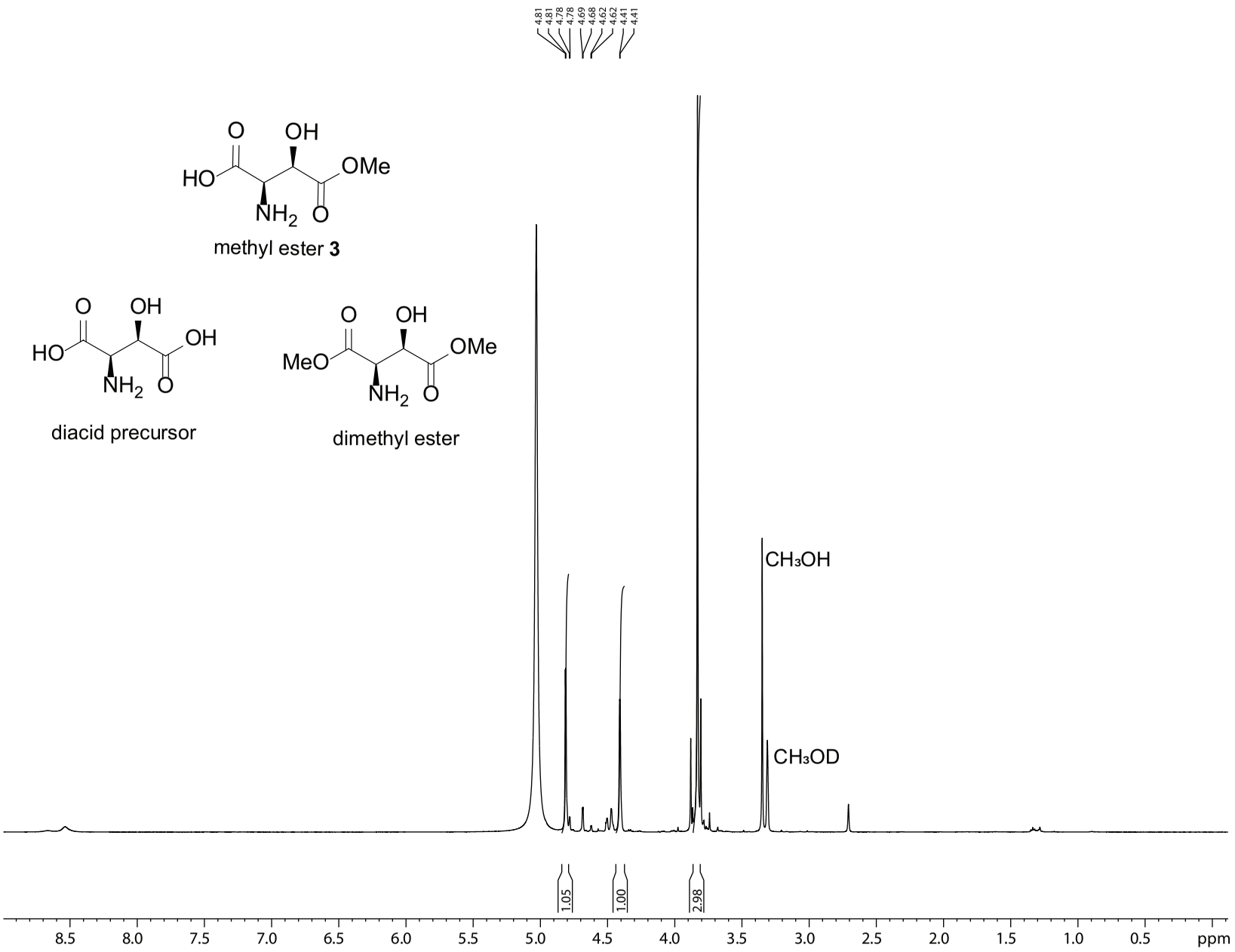
4.81
4.81
4.78
4.78
4.69
4.68
4.62
4.62
4.41
4.41
O
OH
HO
OMe
NH2
O
methyl ester 3
O
OH
HO
OH
NH2
O
diacid precursor
O
OH
MeO
OMe
NH2
O
dimethyl ester
CH3OH
CH3OD
1.05
1.00
2.98
8.5
8.0
7.5
7.0
6.5
6.0
5.5
5.0
4.5
4.0
3.5
3.0
2.5
2.0
1.5
1.0
0.5
ppm

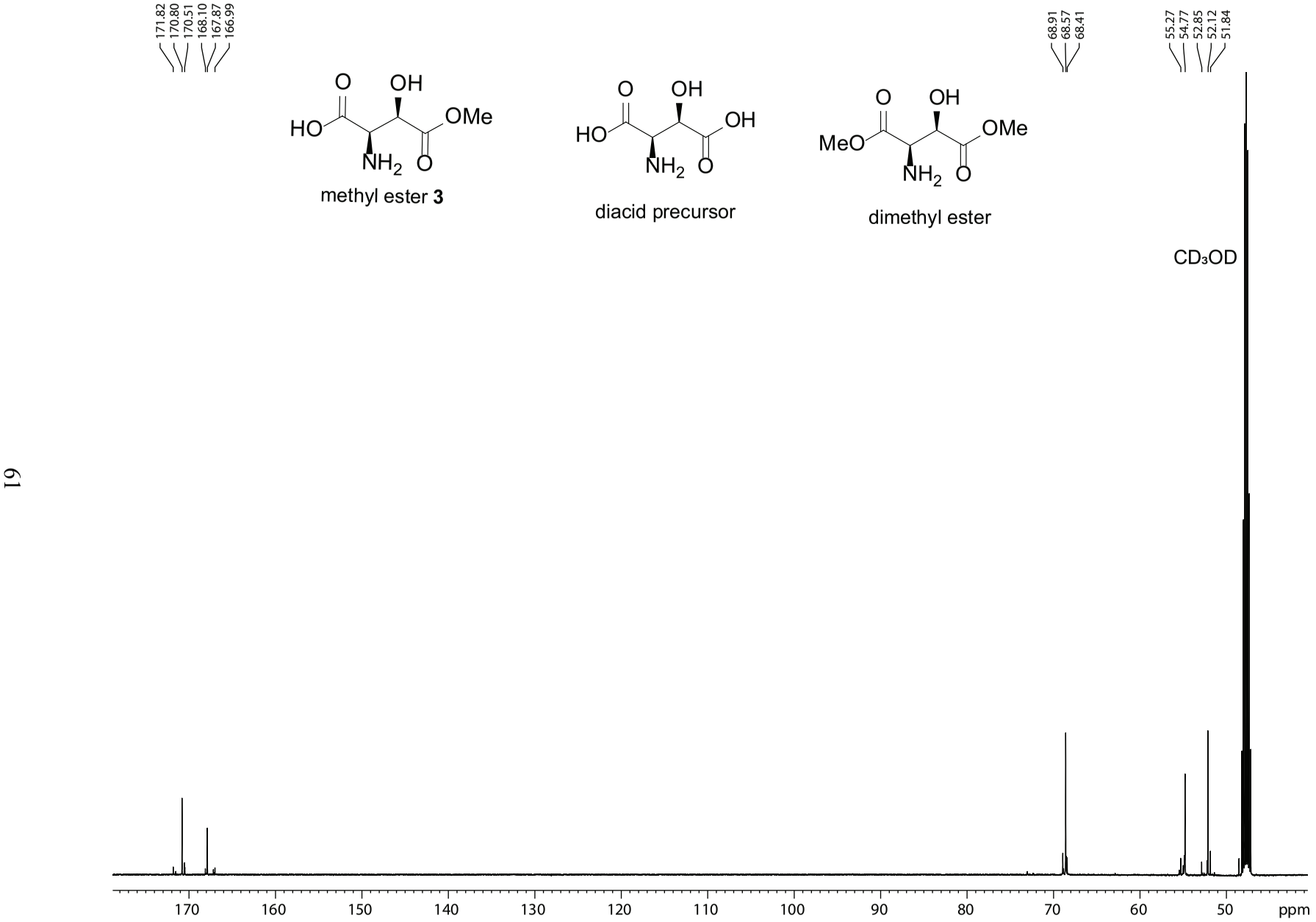
171.82
170.80
170.51
168.10
167.87
166.99
68.91
68.57
68.41
55.27
54.77
52.85
52.12
51.84
methyl ester 3
diacid precursor
dimethyl ester
CD3OD
170
160
150
140
130
120
110
100
90
80
70
60
50
ppm

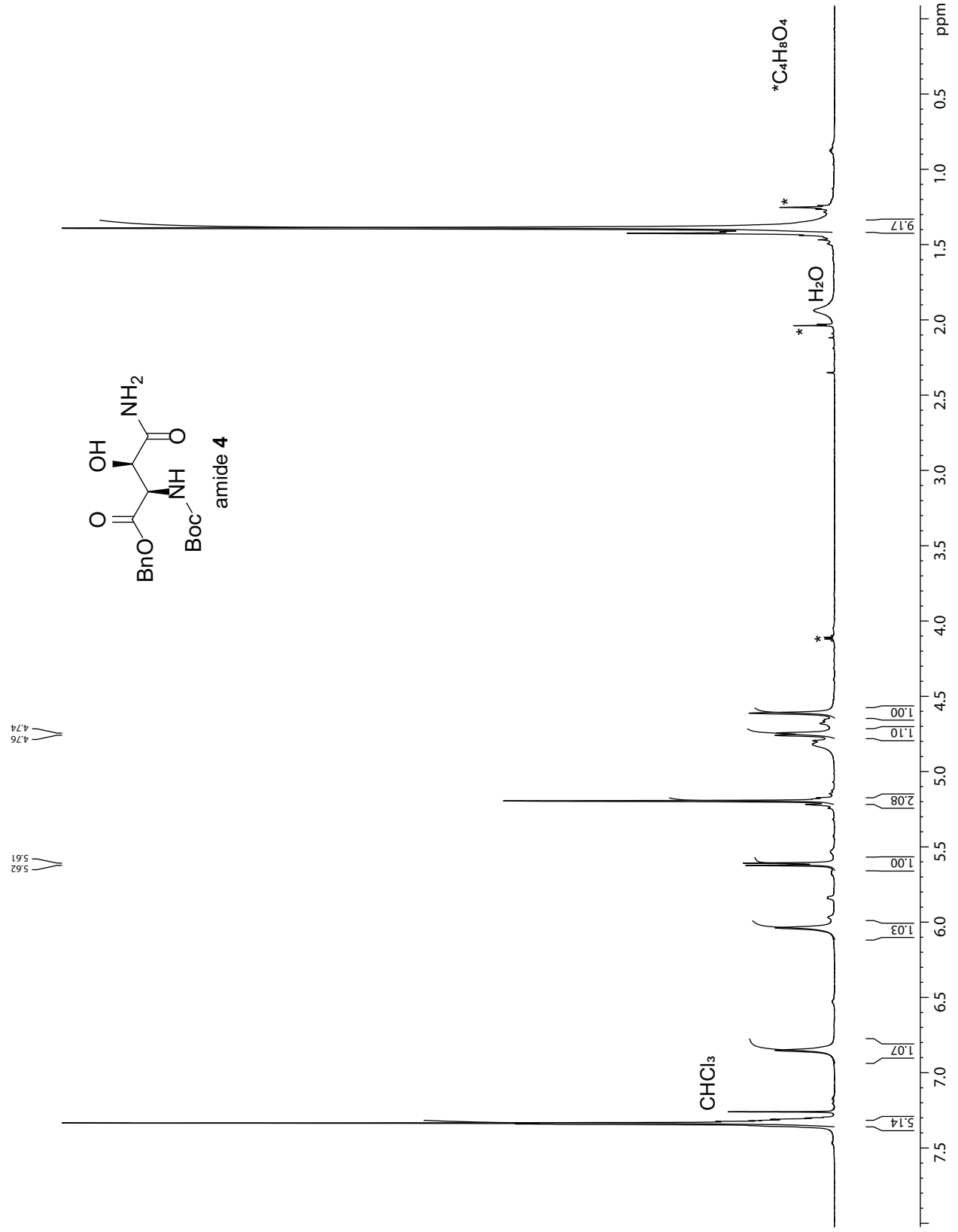
amide 4
CHCl3
H2O
*C4H8O4
ppm

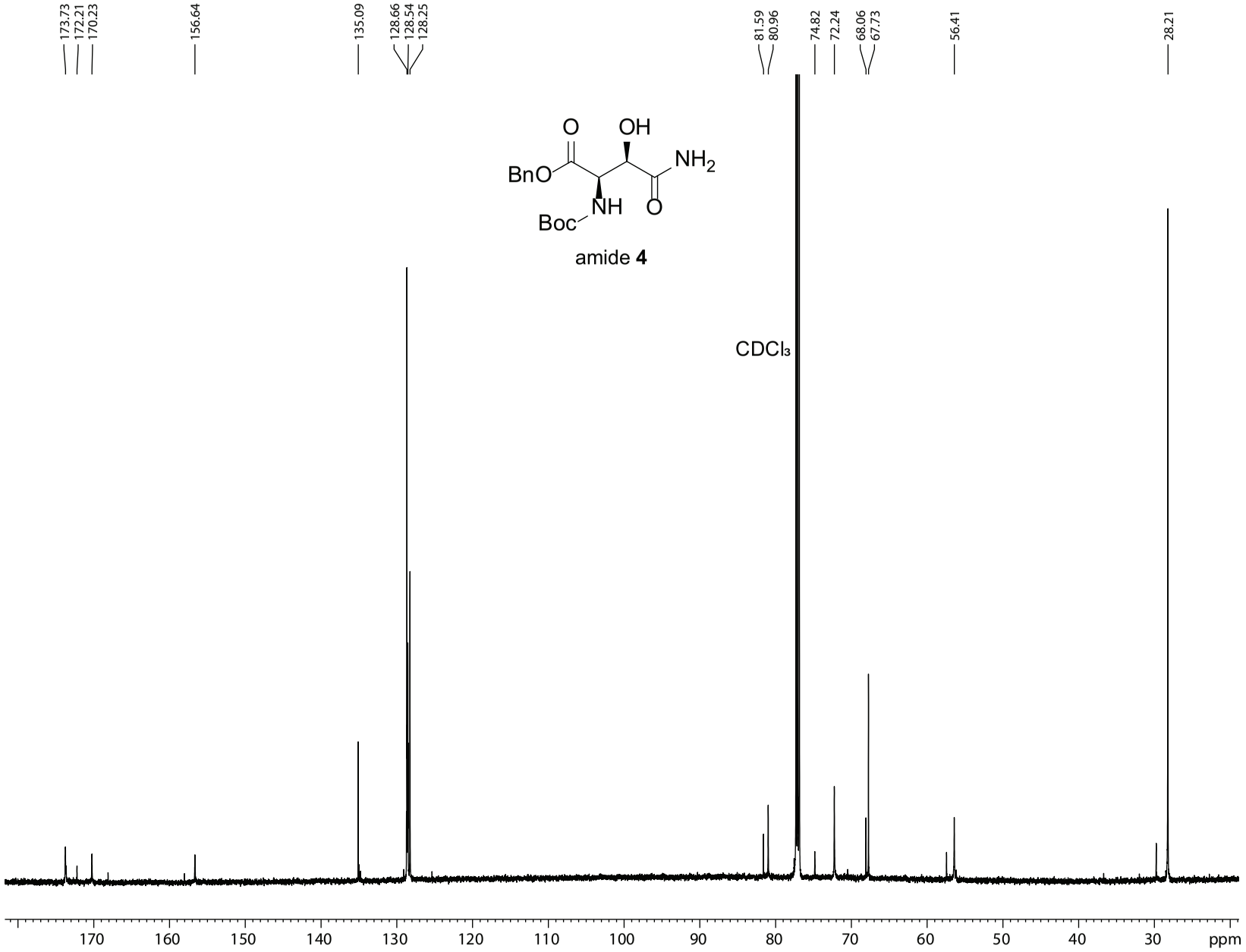
173.73
172.21
170.23
156.64
135.09
128.66
128.54
128.25
81.59
80.96
74.82
72.24
68.06
67.73
56.41
28.21
O
OH
BnO
NH2
NH
O
Boc
amide 4
CDCl3
170
160
150
140
130
120
110
100
90
80
70
60
50
40
30
ppm

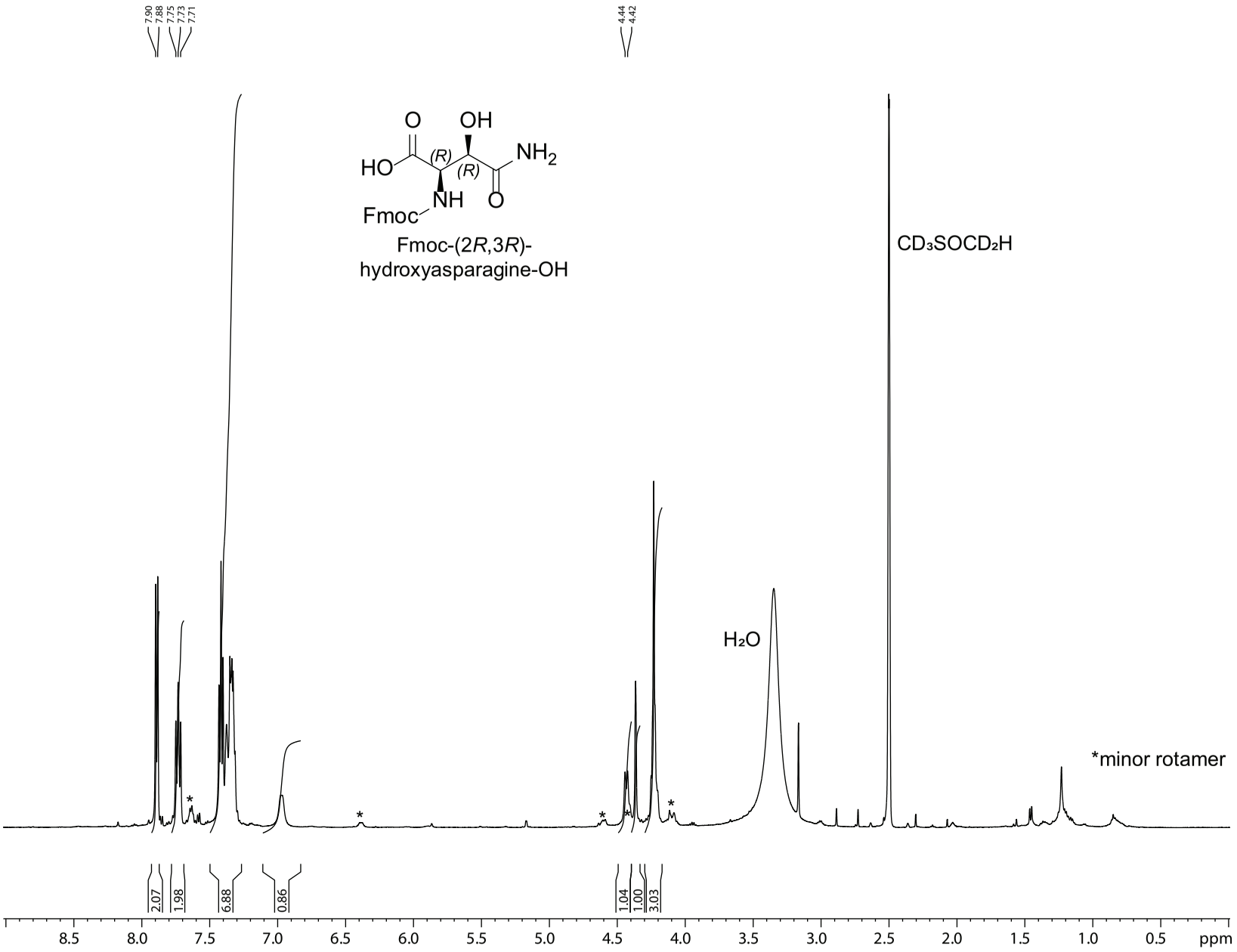
7.90
7.88
7.75
7.73
7.71
4.44
4.42
O
OH
HO
(R)
(R)
NH2
NH
O
Fmoc
Fmoc-(2R,3R)-
hydroxyasparagine-OH
CD3SOCD2H
H2O
*minor rotamer
2.07
1.98
6.88
0.86
1.04
1.00
3.03
8.5
8.0
7.5
7.0
6.5
6.0
5.5
5.0
4.5
4.0
3.5
3.0
2.5
2.0
1.5
1.0
0.5
ppm

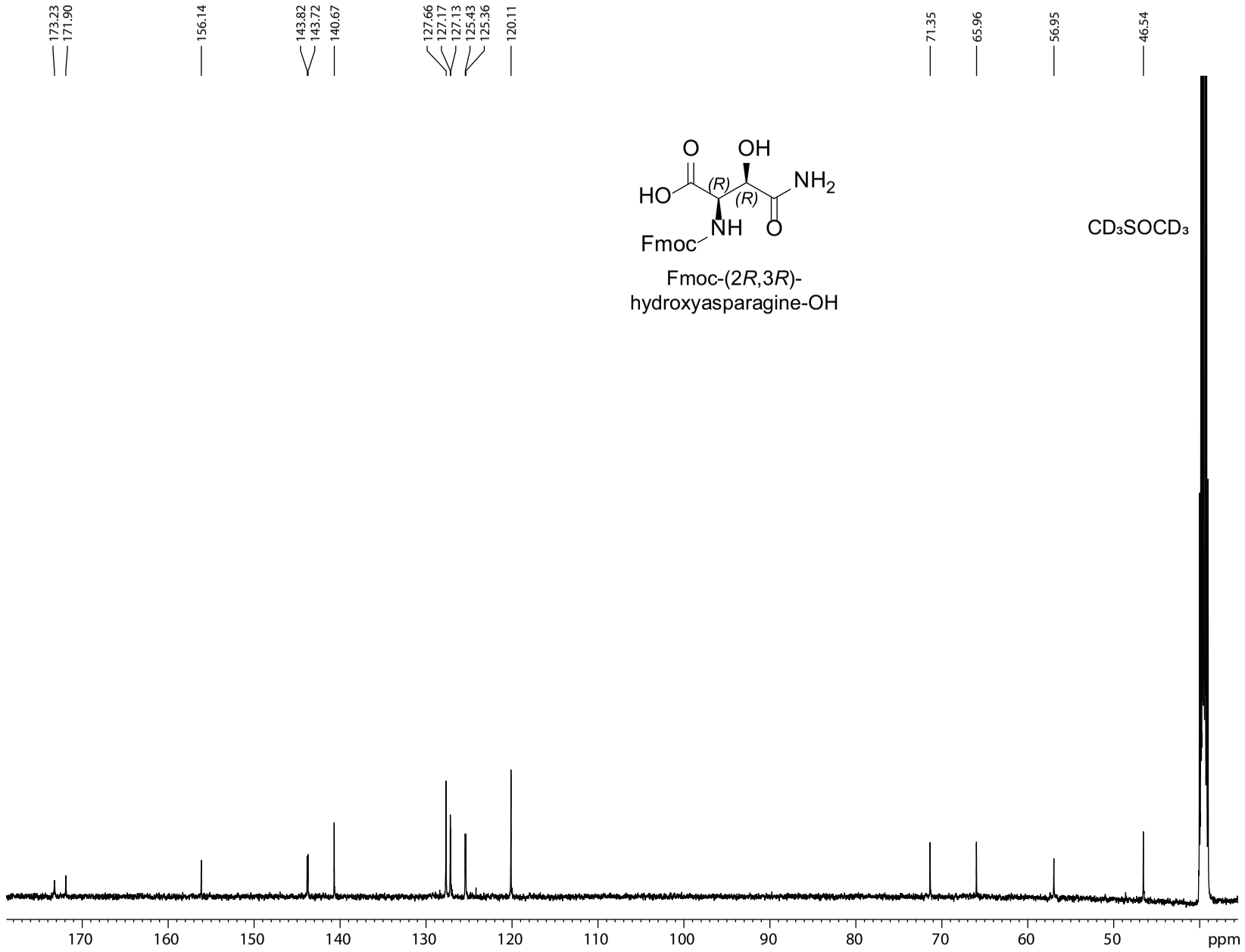
173.23
171.90
156.14
143.82
143.72
140.67
127.66
127.17
127.13
125.43
125.36
120.11
71.35
65.96
56.95
46.54
O
OH
HO
(R)
(R)
NH2
NH
O
Fmoc
Fmoc-(2R,3R)-
hydroxyasparagine-OH
CD3SOCD3
170
160
150
140
130
120
110
100
90
80
70
60
50
ppm

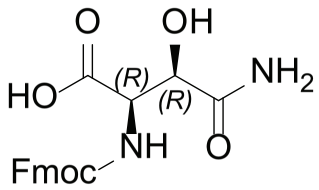

Fmoc-(2*R*,3*R*)-hydroxyAsn-OH

500 MHz EXSY (NOESY) spectrum of Fmoc-(2*R*,3*R*)-hydroxyAsn illustrating the exchange between rotamers.
800-ms mixing time in DMSO-d_6, 298 K.
Cross peaks demonstrating exchange of protons from rotamers are circled in red.
Pairs of resonances associated with major and minor rotamers are designated A and A*, B and B*, etc.

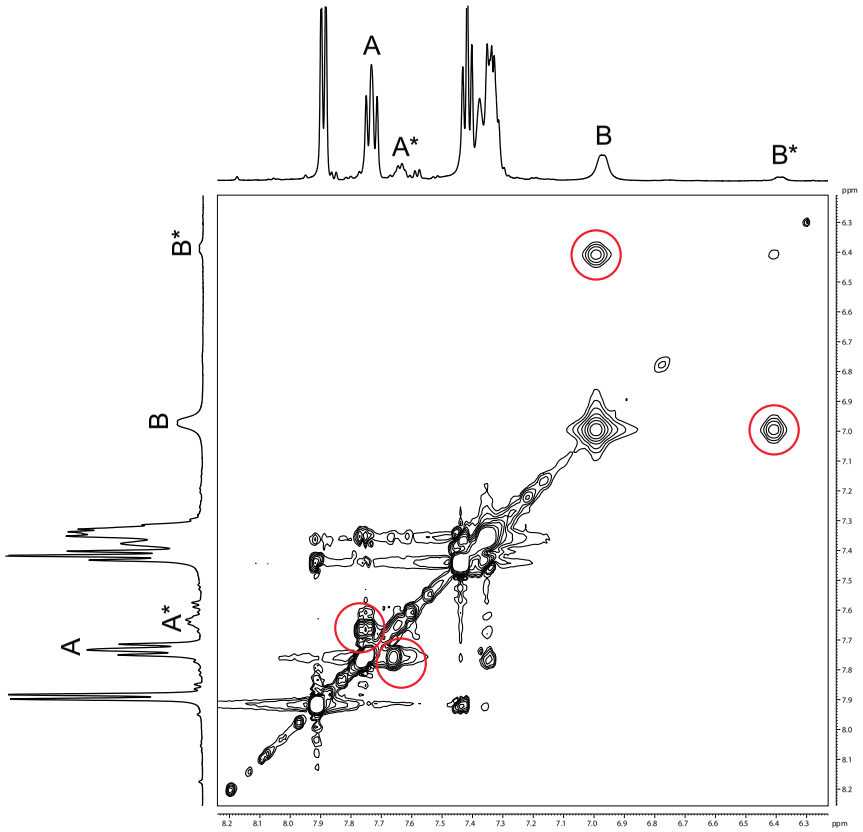

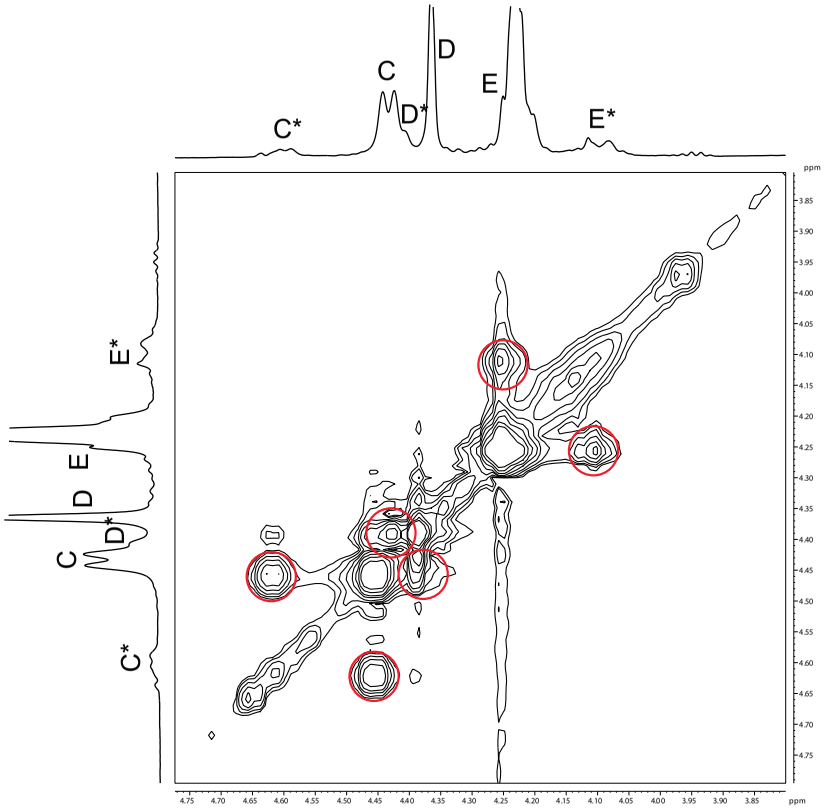

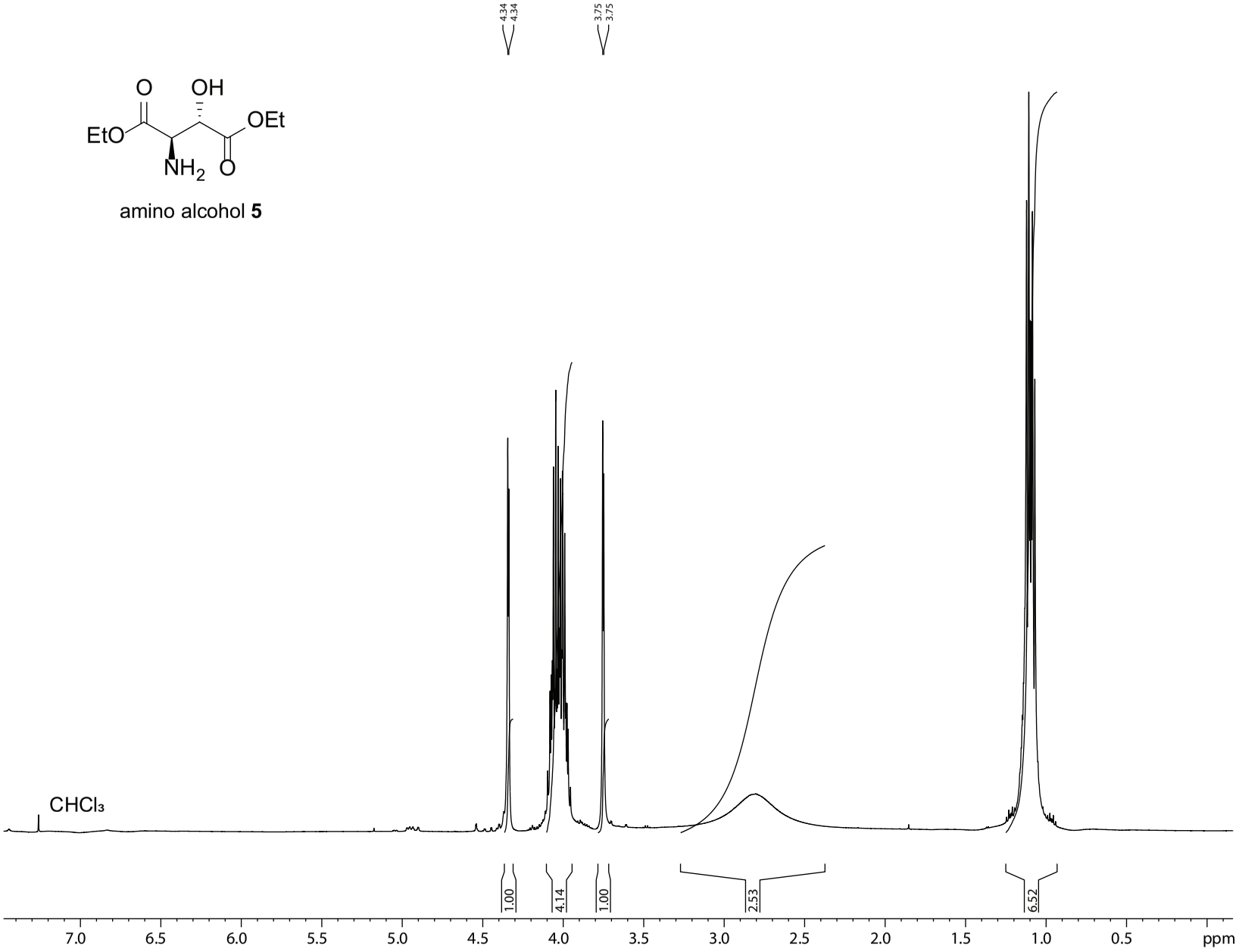
O
OH
EtO
OEt
NH2
O
amino alcohol 5
4.34
4.34
3.75
3.75
CHCl3
1.00
4.14
1.00
2.53
6.52
7.0
6.5
6.0
5.5
5.0
4.5
4.0
3.5
3.0
2.5
2.0
1.5
1.0
0.5
ppm

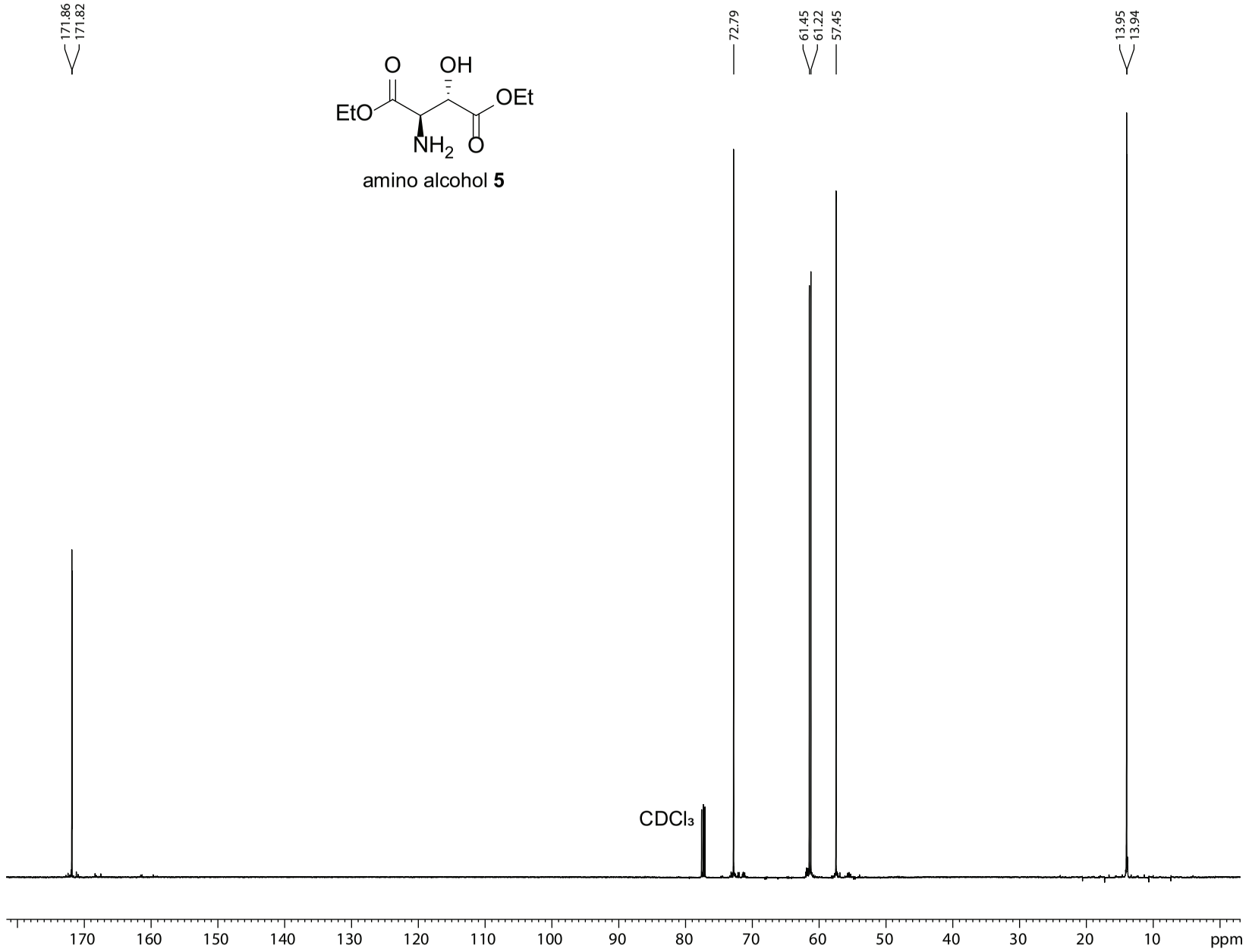

amino alcohol **5**

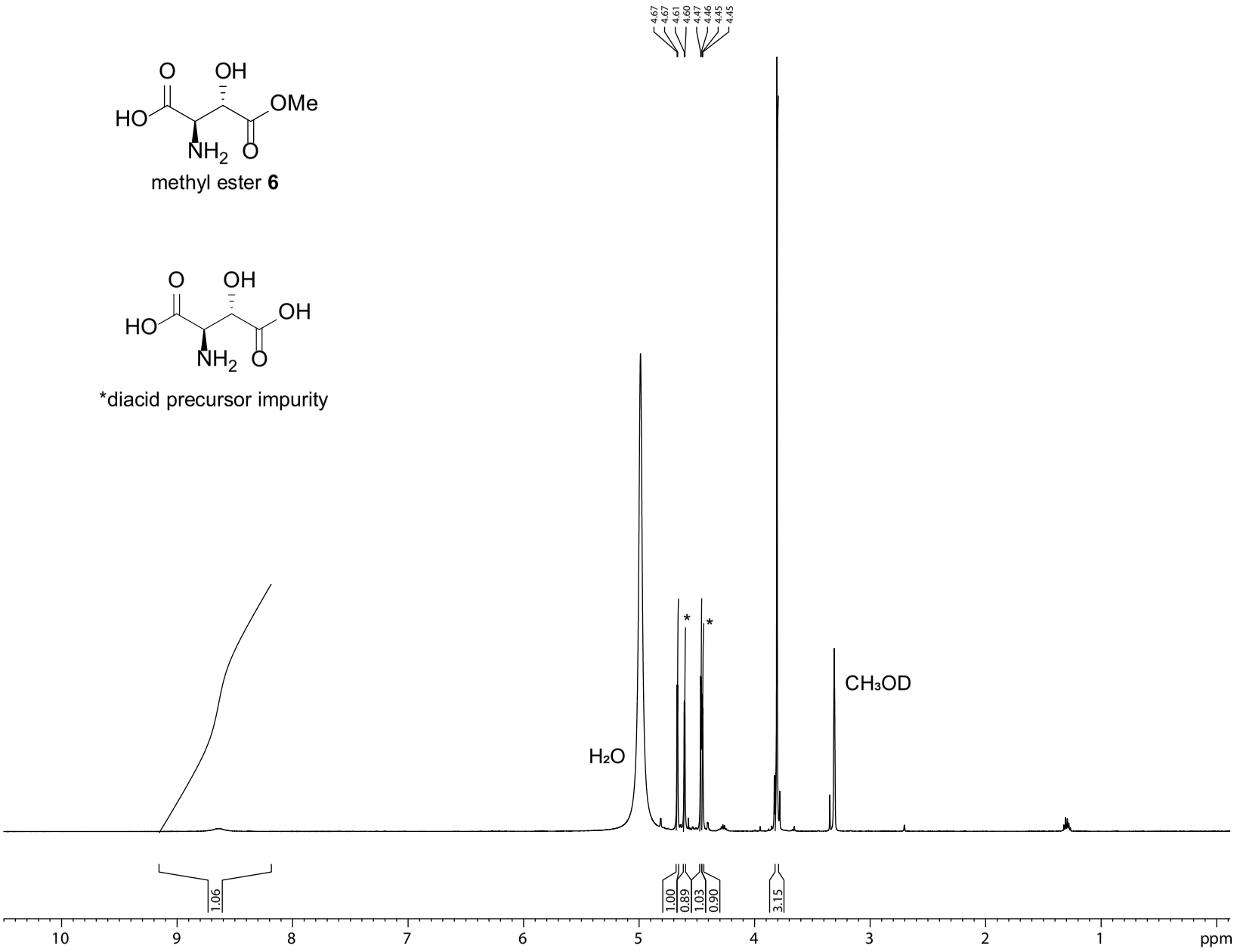
O
OH
HO
OMe
NH2
O
methyl ester 6
O
OH
HO
OH
NH2
O
*diacid precursor impurity
4.67
4.67
4.61
4.60
4.47
4.46
4.45
4.45
H2O
*
*
CH3OD
1.06
1.00
0.89
1.03
0.90
3.15
10
9
8
7
6
5
4
3
2
1
ppm

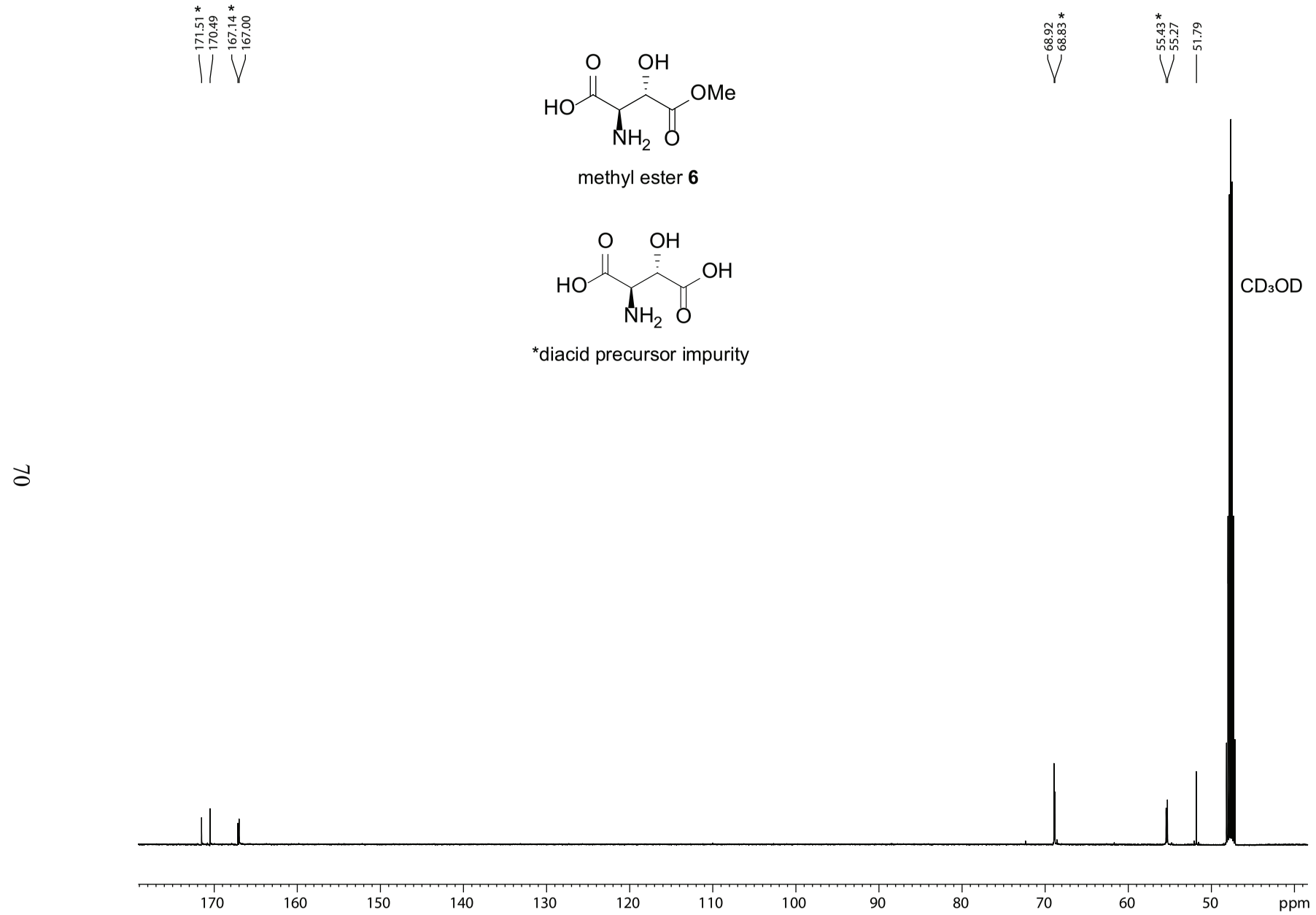
171.51 *
170.49
167.14 *
167.00
68.92
68.83 *
55.43 *
55.27
51.79
CD3OD
methyl ester 6
*diacid precursor impurity
170
160
150
140
130
120
110
100
90
80
70
60
50
ppm

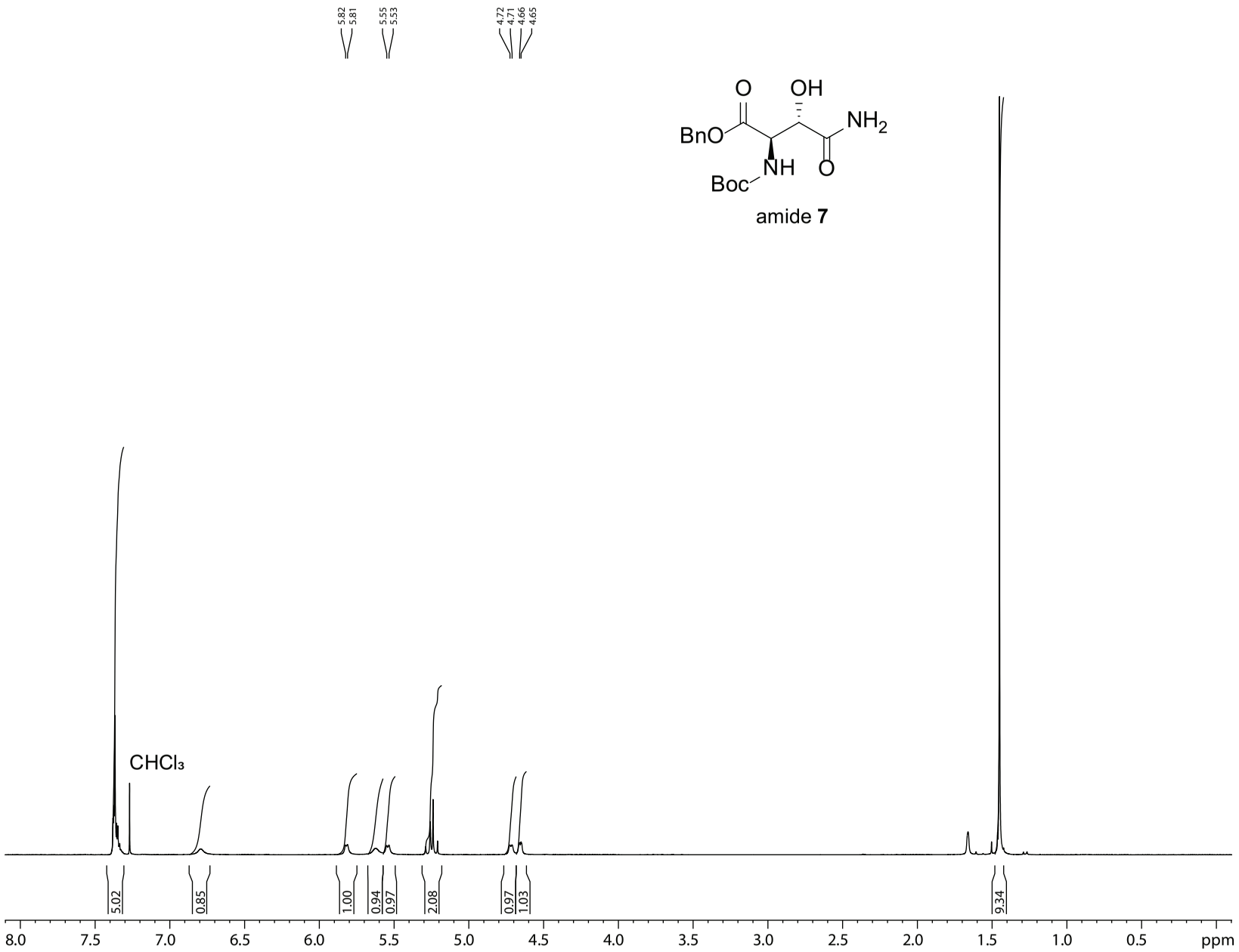
5.82
5.81
5.55
5.53
4.72
4.71
4.66
4.65
O
OH
BnO
NH2
NH
O
Boc
amide 7
CHCl3
5.02
0.85
1.00
0.94
0.97
2.08
0.97
1.03
9.34
8.0
7.5
7.0
6.5
6.0
5.5
5.0
4.5
4.0
3.5
3.0
2.5
2.0
1.5
1.0
0.5
ppm

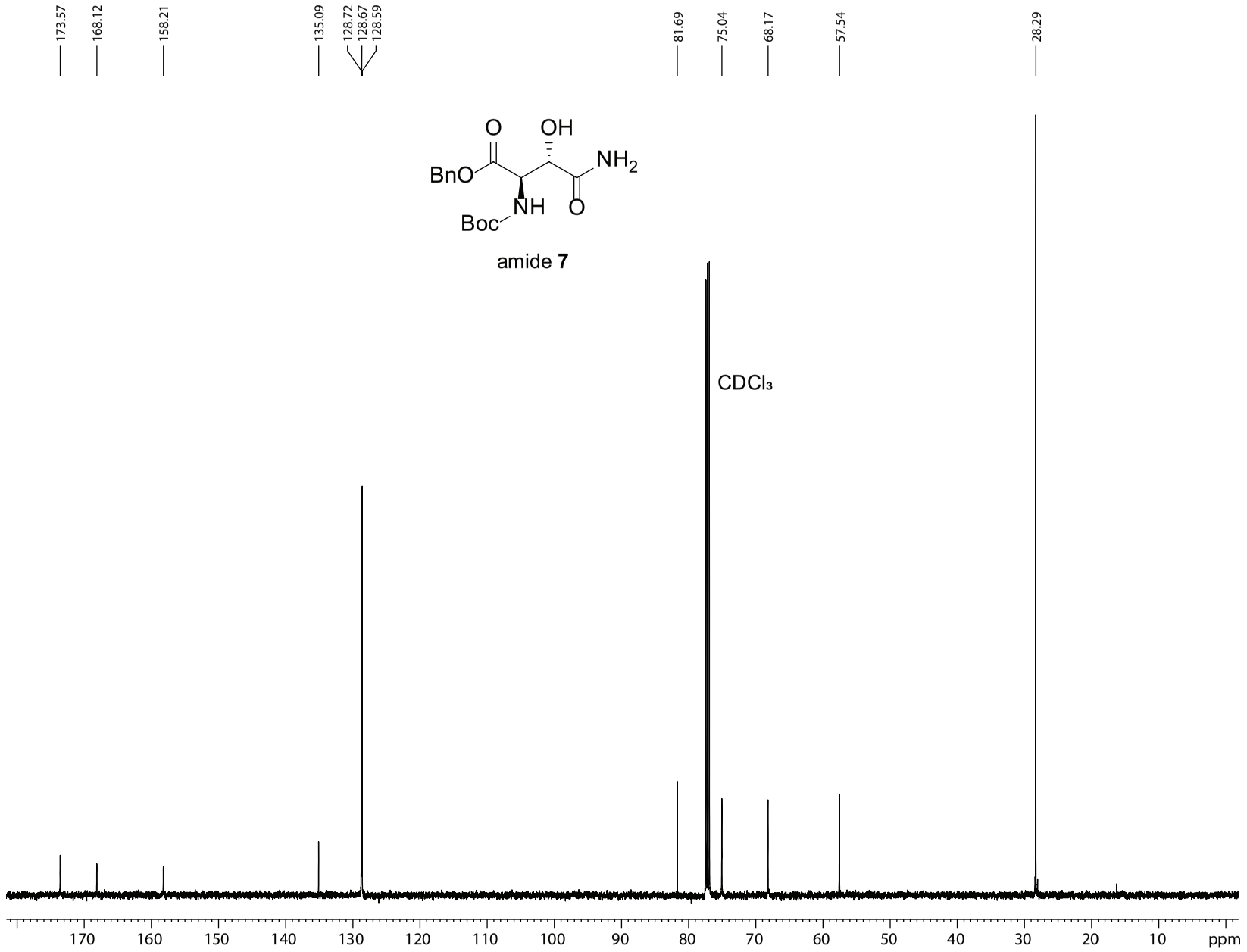
173.57
168.12
158.21
135.09
128.72
128.67
128.59
81.69
75.04
68.17
57.54
28.29
O
OH
BnO
NH2
NH
O
Boc
amide 7
CDCl3
170
160
150
140
130
120
110
100
90
80
70
60
50
40
30
20
10
ppm

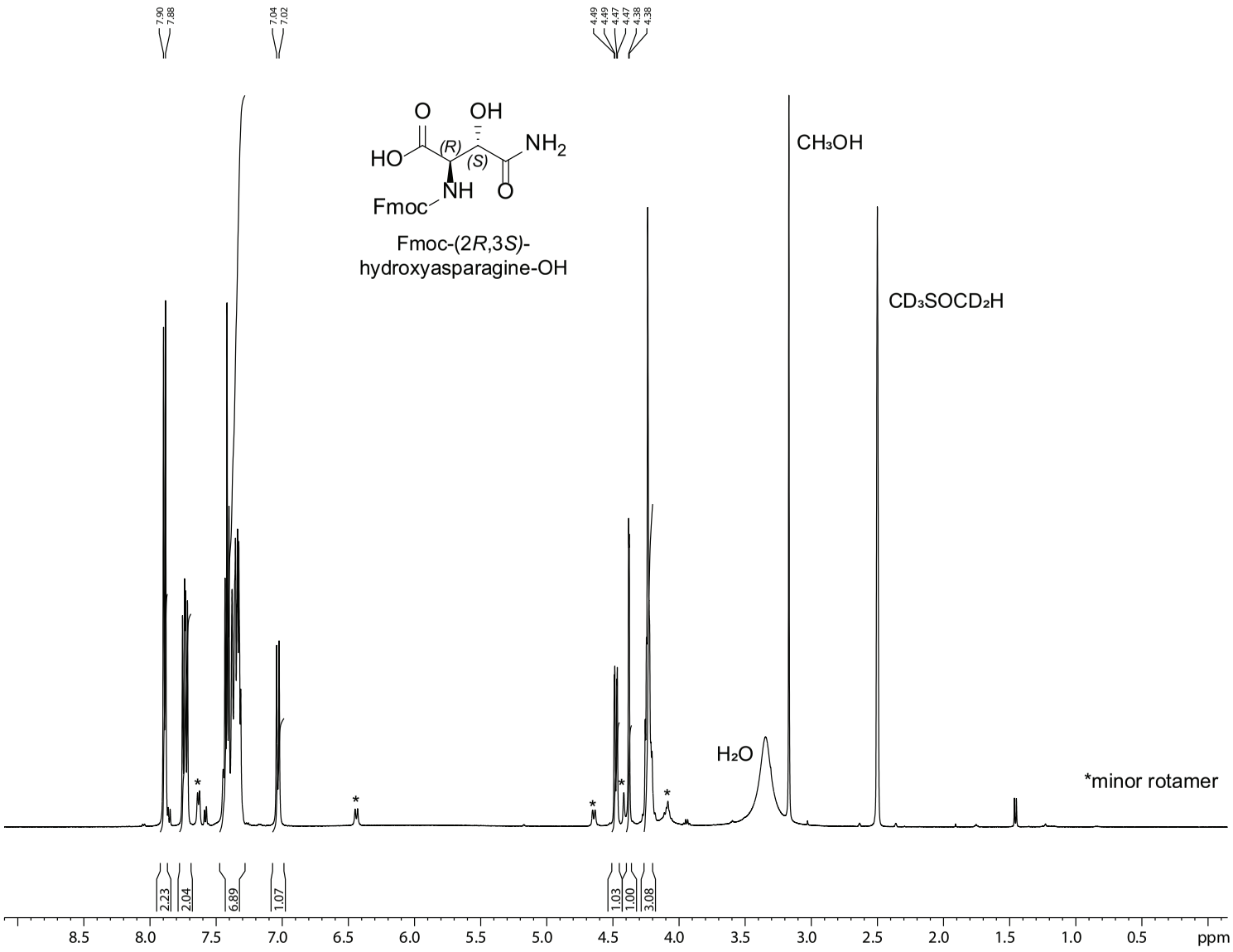
7.90
7.88
7.04
7.02
4.49
4.49
4.47
4.47
4.38
4.38
O
OH
HO
(R)
(S)
NH2
NH
O
Fmoc
Fmoc-(2R,3S)-
hydroxyasparagine-OH
CH3OH
CD3SOCD2H
H2O
*minor rotamer
2.23
2.04
6.89
1.07
1.03
1.00
3.08
8.5
8.0
7.5
7.0
6.5
6.0
5.5
5.0
4.5
4.0
3.5
3.0
2.5
2.0
1.5
1.0
0.5
ppm

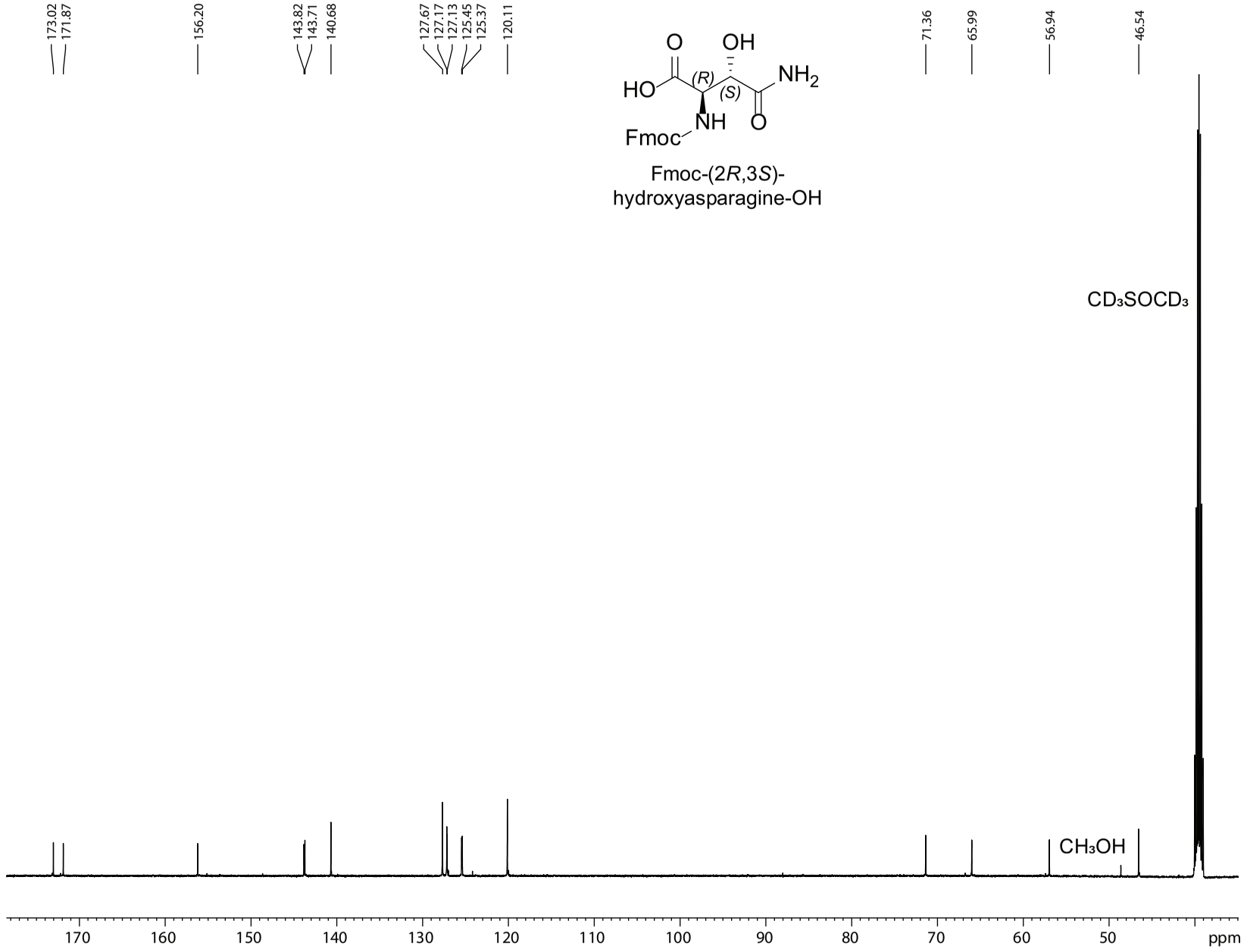
173.02
171.87
156.20
143.82
143.71
140.68
127.67
127.17
127.13
125.45
125.37
120.11
71.36
65.99
56.94
46.54
O
OH
HO
(R)
(S)
NH2
NH
O
Fmoc
Fmoc-(2R,3S)-
hydroxyasparagine-OH
CD3SOCD3
CH3OH
170
160
150
140
130
120
110
100
90
80
70
60
50
ppm

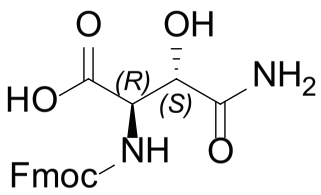

Fmoc-(2*R*,3*S*)-hydroxyAsn-OH

500 MHz EXSY (NOESY) spectrum of Fmoc-(2*R*,3*S*)-hydroxyAsn illustrating the exchange between rotamers.
1000-ms mixing time in DMSO-d_6, 298 K.
Cross peaks demonstrating exchange of protons from rotamers are circled in red.
Pairs of resonances associated with major and minor rotamers are designated A and A*, B and B*, etc.

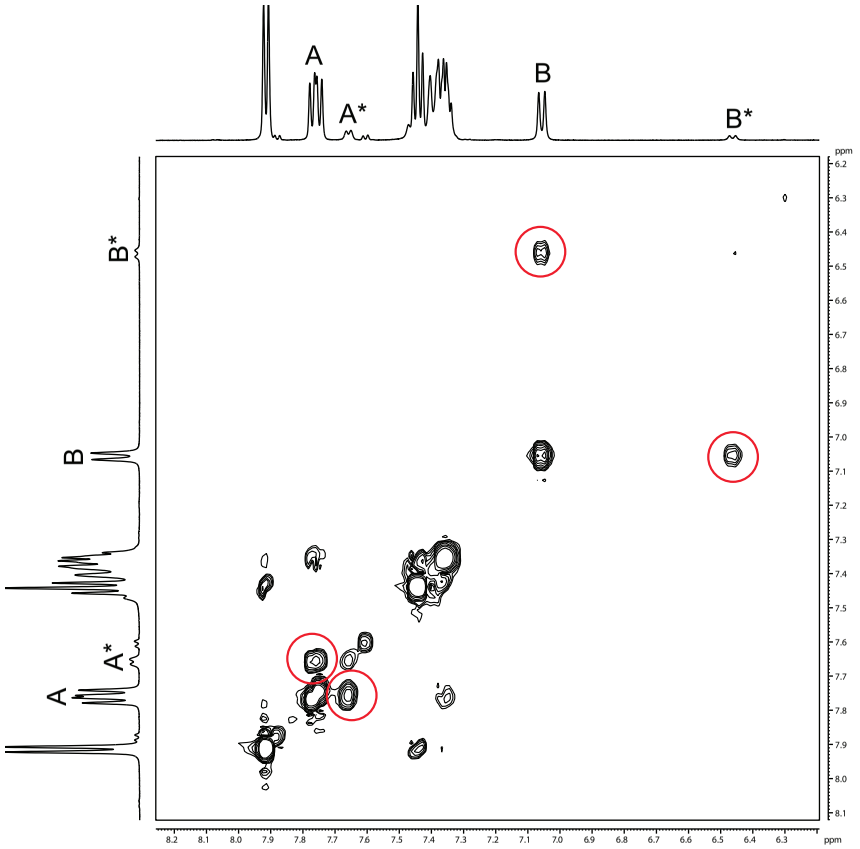

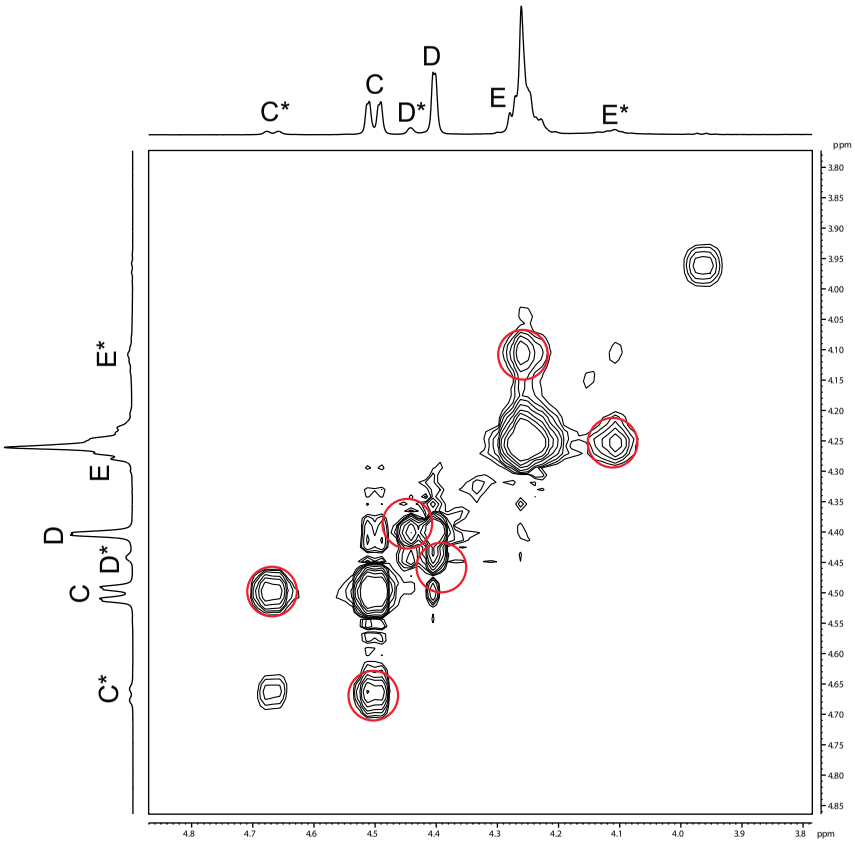

^{1}H NMR of 3 mM natural Novo29 in DMSO-d_6 at 500 MHz and 298 K

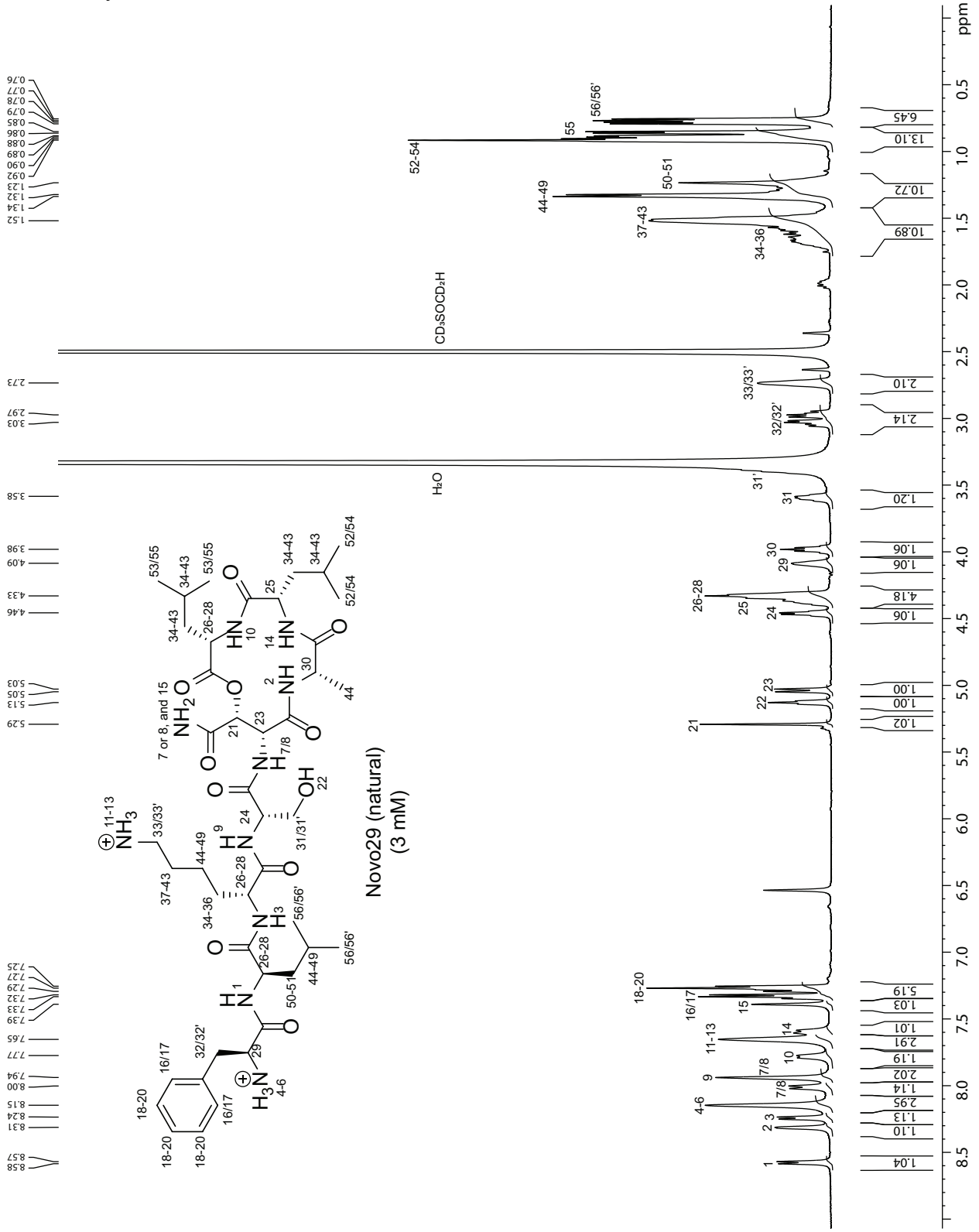

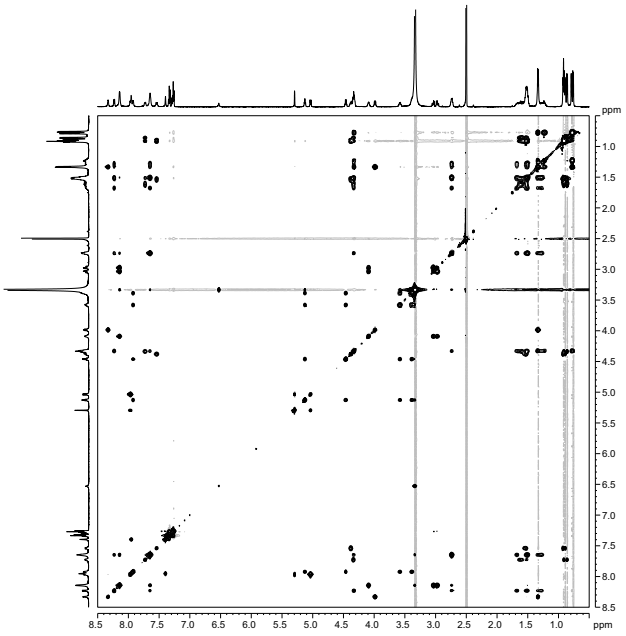

2.0 mM natural Novo29
in DMSO-d_6, 150-ms mixing time, 298 K
600 MHz TOCSY spectrum

Novo29

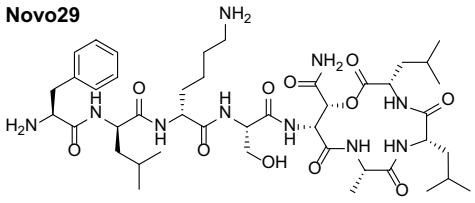

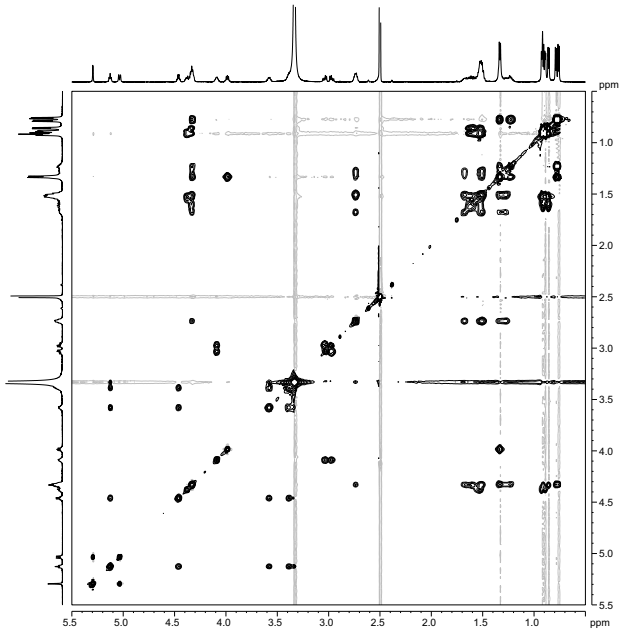

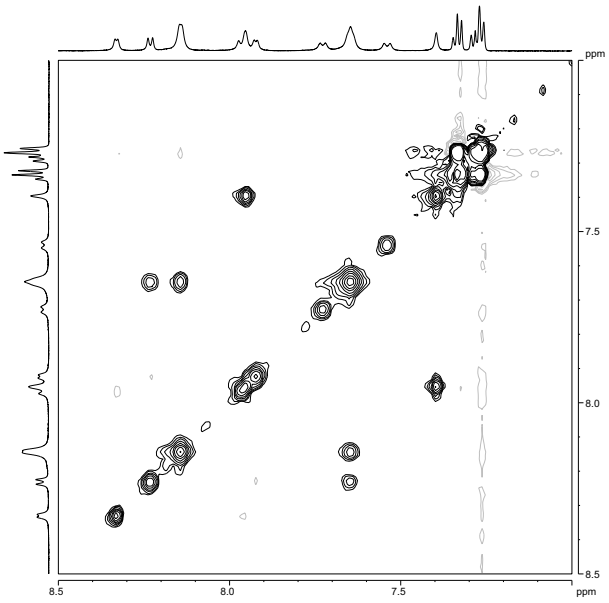

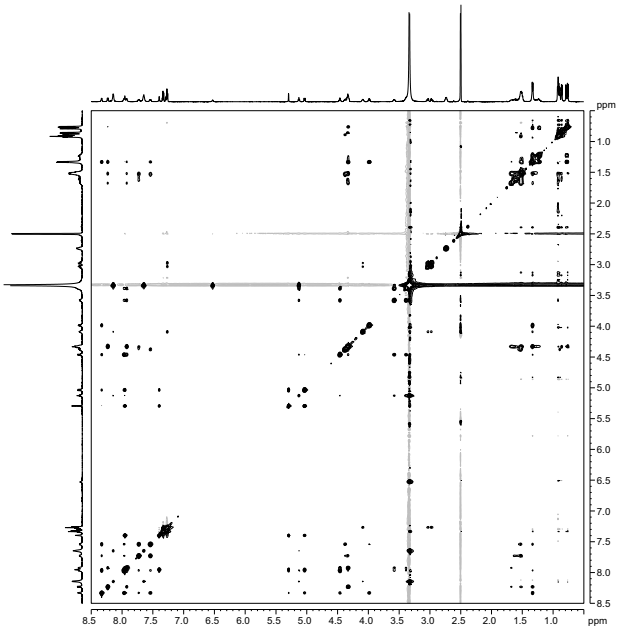

2.0 mM natural Novo29
in DMSO-d_6, 200-ms mixing time, 298 K
600 MHz NOESY spectrum

Novo29

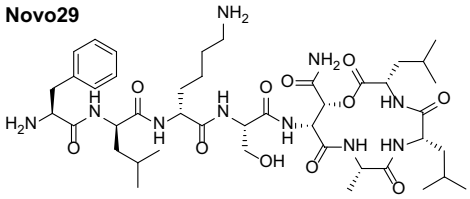

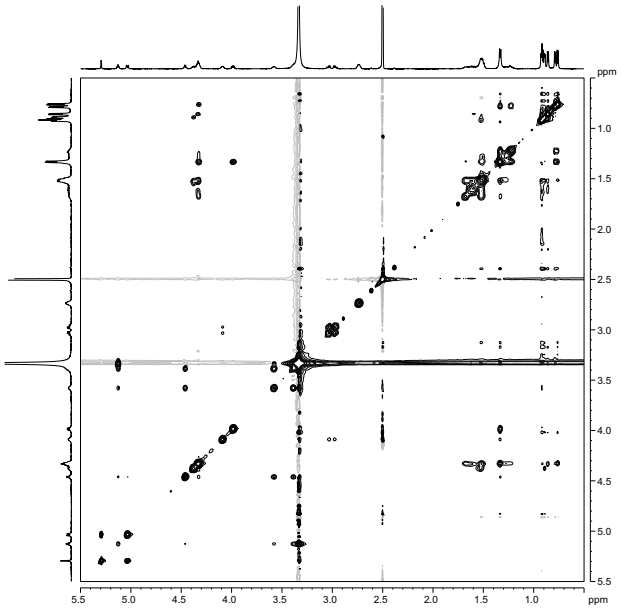

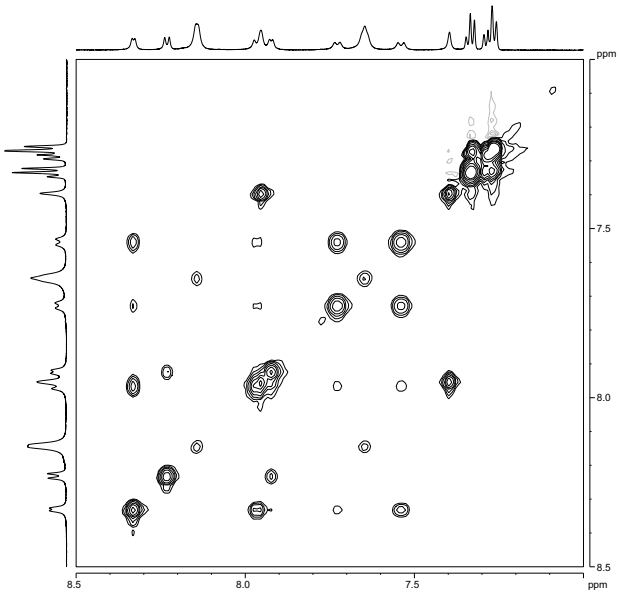

Table S4. Chemical shift assignments for natural Novo29.

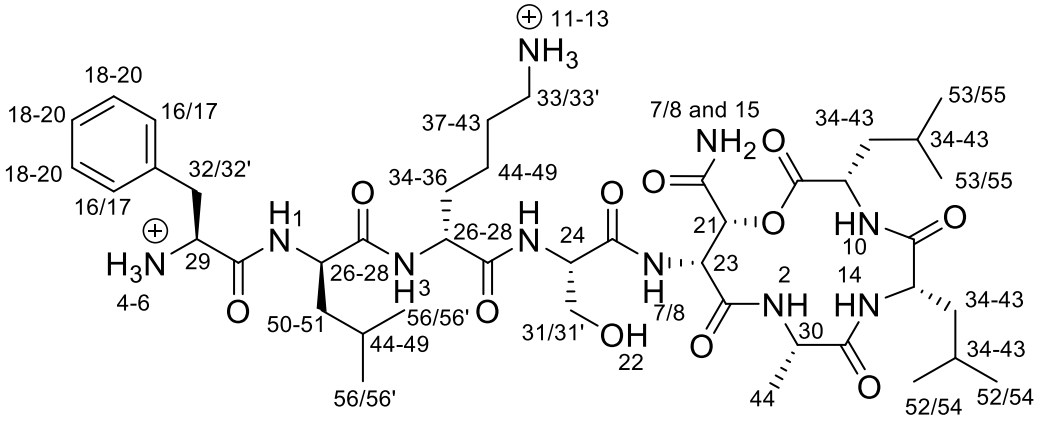

#	Natural Novo29 3 mM (nominal)	#	Natural Novo29 3 mM (nominal)
1	8.57	25	4.38
2	8.31	26-28	4.33
3	8.24	29	4.09
4-6	8.15	30	3.98
7/8	8.01 and 7.95	31/31'	3.59 and 3.91
9	7.94	32/32'	3.00
10	7.78	33/33'	2.74
11-13	7.65	34-36	1.63
14	7.60	37-43	1.52
15	7.39	44-49	1.33
16/17	7.33	50-51	1.23
18-20	7.27	52-54	0.92
21	5.29	55	0.86
22	5.13	56/56'	0.77
23	5.04		
24	4.46		

^{1}H NMR of 2 mM synthetic Novo29 in DMSO-d_6 at 500 MHz and 298 K

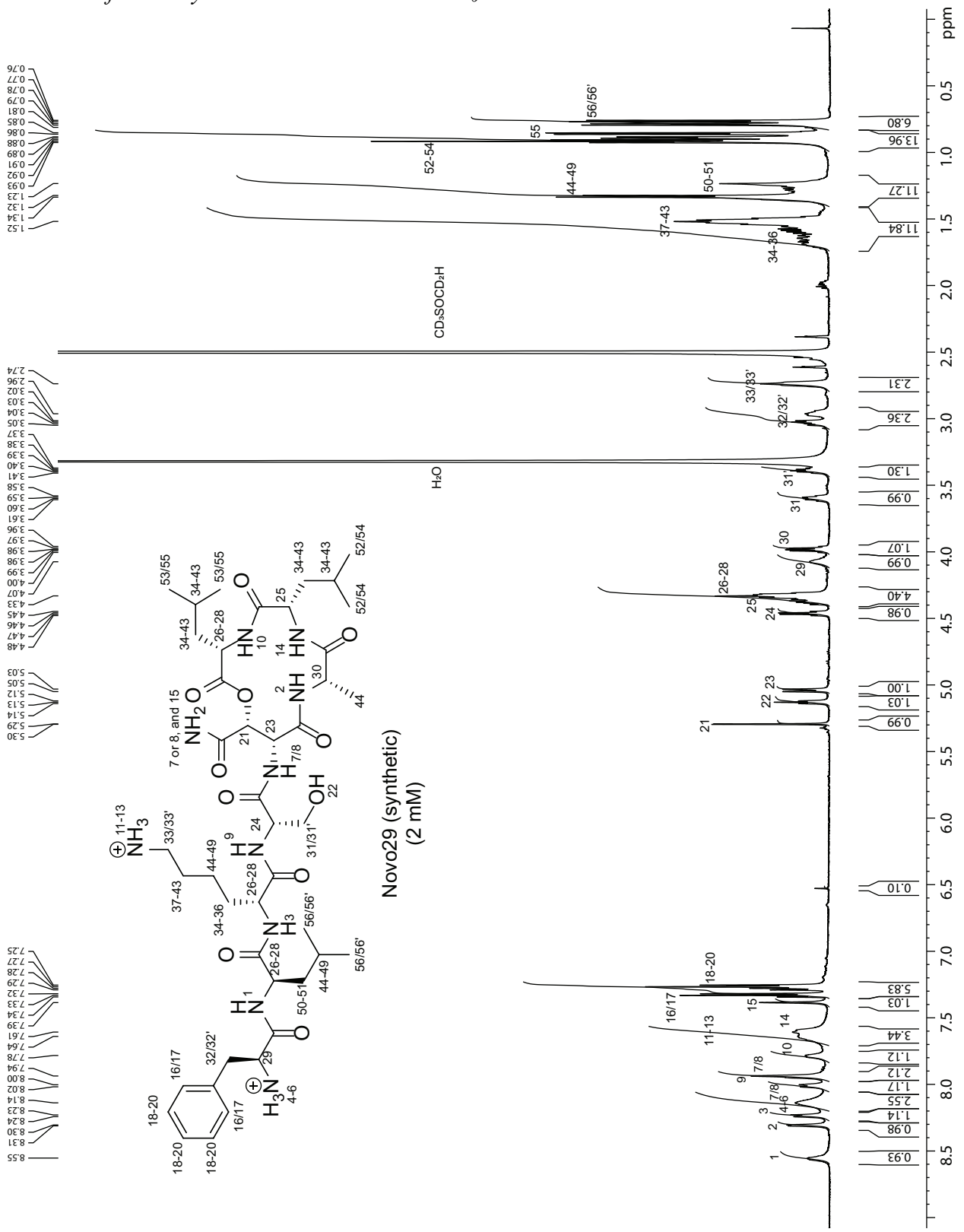

Table S5. Chemical shift comparison between natural Novo29 and synthetic Novo29.

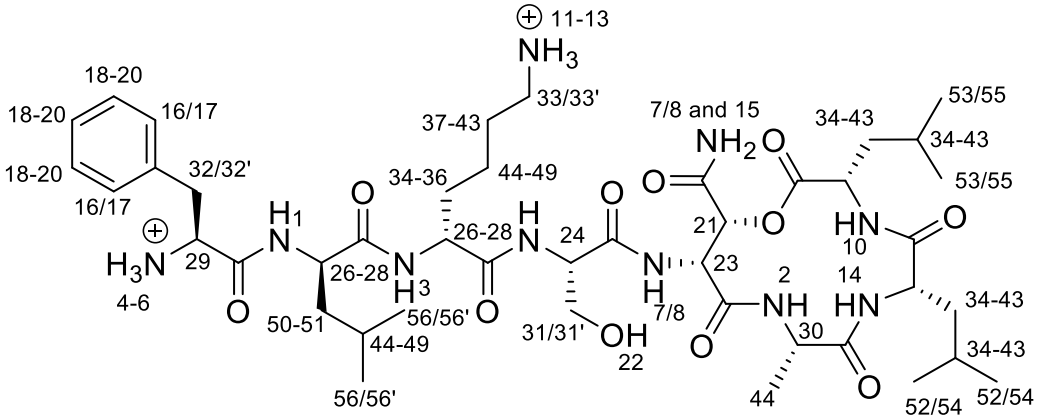

#	natural Novo29 3 mM (nominal)	synthetic Novo29 2 mM (nominal)	Δδ ppm	#	natural Novo29 3 mM (nominal)	synthetic Novo29 2 mM (nominal)	Δδ ppm
1	8.57	8.56	-0.01	25	4.38	4.38	0
2	8.31	8.30	+0.01	26-28	4.33	4.33	0
3	8.24	8.24	0	29	4.09	4.08	-0.01
4-6	8.15	8.14	-0.01	30	3.98	3.98	0
7/8	8.01 and 7.95	8.01 and 7.94	0 and -0.01	31/31’	3.59 and 3.91	3.59 and 3.91	0 and 0
9	7.94	7.94	0	32/32’	3.00	3.00	0
10	7.78	7.78	0	33/33’	2.74	2.74	0
11-13	7.65	7.65	0	34-36	1.63	1.63	0
14	7.60	7.60	0	37-43	1.52	1.52	0
15	7.39	7.39	0	44-49	1.33	1.33	0
16/17	7.33	7.33	0	50-51	1.23	1.23	0
18-20	7.27	7.27	0	52-54	0.92	0.92	0
21	5.29	5.29	0	55	0.86	0.86	0
22	5.13	5.13	0	56/56’	0.77	0.77	0
23	5.04	5.04	0				
24	4.46	4.46	0				

[1]H NMR of 2 mM epi-Novo29 in DMSO-d_6 at 500 MHz and 298 K